



UNIVERSITY
OF SOUTHERN
CALIFORNIA



CALIFORNIA
INSTITUTE OF
TECHNOLOGY



UNIVERSITY OF
CALIFORNIA
LOS ANGELES



UC SAN DIEGO
SCRIPPS INSTITUTION
OF OCEANOGRAPHY



UNIVERSITY OF
CALIFORNIA
SANTA BARBARA



LAMONT-DOHERTY
EARTH OBSERVATORY
OF COLUMBIA
UNIVERSITY



UNIVERSITY OF
NEVADA
RENO



SAN DIEGO
STATE UNIVERSITY



UNITED STATES
GEOLOGICAL
SURVEY

2000 SCEC Annual Meeting

September 17-20, 2000

Proceedings and Abstracts

Embassy Suites Mandalay Bay
Oxnard, California

2000 SCEC Annual Meeting

September 17-20, 2000

Proceedings and Abstracts

**Embassy Suites Mandalay Bay
Oxnard, California**

Table of Contents

SCEC Annual Meeting Agenda	3
2000 Annual Meeting Participants	6
SCEC Organization	10
2000 SCEC Advisory Council	12
SCEC Senior Research Investigators	13
Message from the Directors	17
The Current Status of EarthScope	18
SCEC Outreach Program Overview	20
2000 SCEC Abstracts	39

2000 SCEC ANNUAL MEETING

“The SCEC Transition and Future”

Sunday, September 17

Arrival in Oxnard

2:00 to 5:00 Santa Clara Basin Working Group Meeting - Steve Day

There may be other specialized group meetings this afternoon.

Poster Session Set-Up

7:00 SCEC Steering Committee Meeting

Monday, September 18, 2000

6:00 to 8:30 Breakfast (Surf Room)

SCEC Plenary Session I

8:30 Introduction – John McRaney

8:45 EarthScope Update – Tom Henyey

9:00 NSF Perspective – Jim Whitcomb

9:15 USGS Perspective – John Unger

9:30 SCEC Advisory Council Perspective – Bob Smith

9:45 Education and Outreach Report - Jill Andrews

Intern Introduction

10:20 **Break**

10:45 SCEC Science Report - Highlighting the First Decade – Bernard Minster

The SCEC Highlights (15 minutes each)

11:15 Southern California as a Natural Laboratory – Bernard Minster

11:30 The Landers Story – Duncan Agnew/Tom Rockwell

11:45 The L.A. Basin Story (including the Northridge EQ)– Ralph Archuleta

12:00 Data Collection, Synthesis, and Products – Ken Hudnut

12:15 – 1:30 Lunch

- 1:30 Hazard Estimation – Dave Jackson
 1:45 Fault System Behavior – Steve Day
 2:00 Education and Outreach – Jill Andrews
 2:15 New Master Model – Ned Field
 2:30 SCEC Themes – Tom Henyey
- 2:45 Discussion of SCEC Highlights – What is Missing?
- 3:15 Instructions to Working Groups on 2001/Year 11 Plans– Bernard Minster

Group Meetings (Note: There will be some overlap in the group meetings)

- 3:30 SCIGN Coordinating Board Meeting – Ken Hudnut
- 3:30-5:00 Group A – Dave Jackson
- 4:30-6:00 Group B – Ralph Archuleta
- 5:00 – 7:00 Cocktail Hour and Dinner
 SCEC Advisory Council Executive Session (begins during dinner)
- 7:00 Poster Session I**

Tuesday, September 19, 2000

- 7:30 – 8:30 Continental Breakfast**
- 8:00-9:30 Group C – Tom Rockwell
- 9:00-10:30 Group D – Rob Clayton
- 10:00-11:30 Group E – Duncan Agnew
- 11:00-12:30 Group F – Steve Day
- 12:30 Lunch**
- SCEC Plenary Session II
- 2:00 Introduction to SCEC 2 and Breakout Session– Tom Jordan
- 2:30 – 5:30 Breakouts (Chairs/Co-Chairs to be named later)
 First Session
- 2:30 – 4:00 Rupture Dynamics –
 Microscale Processes –
 Fault Systems –

Second Session

- 4:00 – 5:30 Plate-Boundary Tectonics -
Wave Propagation –
Seismic Hazard Analysis –
- 5:30 – 7:00 Cocktail Hour and Dinner
Outreach Awards
- 7:00 **Poster Session II**
- 8:30 **SCEC Advisory Council Meeting**
WInSAR Meeting - David Sandwell/Chair

Wednesday, September 20, 2000

SCEC Plenary Session III

- 7:30 – 8:30 **Continental Breakfast**
- 8:30 – 10:00 Reports from Breakout Groups
- 10:00 Break
- 10:30 – 11:30 Discussion of Breakouts and Vision for SCEC 2 - Jordan

End of SCEC Meeting

- 1:00 SCIGN Advisory Council Meeting

2000 SCEC ANNUAL MEETING PARTICIPANTS

Robert Abbott	Nevada-Reno
Duncan Agnew	UC-San Diego
Orgil Altangerel	San Diego State
Marie Ammerman	SCEC Intern/UC-Santa Barbara
Greg Anderson	UC-San Diego
John Anderson	Nevada-Reno
Jill Andrews	SCEC Outreach
Rasool Anooshehpour	Nevada-Reno
Ralph Archuleta	UC-Santa Barbara
Ramon Arrowsmith	Arizona State
Aris Aspiotes	USGS-Pasadena
Kenneth Austin	Central Washington
Shirley Baher	UCLA
Teresa Baker	SCEC Intern/MIT
Mark Benthien	SCEC Outreach
Yehuda Ben-Zion	USC
Michael Bevis	Hawaii
Jacobo Bielak	Carnegie-Mellon
Tom Bjorklund	Houston
Jay Blaire	USC
Ann Blythe	USC
Yehuda Bock	UC-San Diego
Margaret Boettcher	MIT
Fabian Bonilla	UC-Santa Barbara
Adrian Borsa	UC-San Diego
Rich Briggs	Nevada-Reno
Emily Brodsky	Caltech
Jim Brune	Nevada-Reno
Doug Burbank	Penn State
Roland Burgmann	UC-Berkeley
Tianqing Cao	CDMG
Ji Chen	Caltech
Liangjun Chen	MIT/USC
Po Chen	USC
Youlin Chen	USC
Yun-tai Chen	UCLA
Shari Christofferson	USC
Rob Clayton	Caltech
Laura Colini	Arizona State
Michele Cooke	Massachusetts
C.B. Crouse	URS Corp
Paul Davis	UC-Los Angeles
Steve Day	San Diego State
Desiree Dier	San Diego State
Bob de Groot	SCEC Outreach
Safaa Dergham	CSU-Long Beach
Jim Dieterich	USGS-Menlo Park
James Dolan	USC
Andrea Donnellan	JPL
Herb Dragert	Geological Survey of Canada
Doug Dreger	UC-Berkeley
Deborah Eason	Caltech

Leo Eisner
Antonio Fernandez
Ned Field
Sheryl Fontaine
Bill Foxall
Jeff Freymueller
Gary Fuis
John Galetzka
Carrie Glavich
Javier Gonzalez
Lisa Grant
Robert Graves
Larry Gurrola
Katrin Hafner
Brad Hager
Robert Hamilton
Jeanne Hardebeck
Ruth Harris
Ross Hartleb
Egill Hauksson
Tom Heaton
Sally Henyey
Tom Henyey
Sue Hough
Yue-qiang Huang
Ken Hudnut
Ken Hurst
Dave Jackson
Allison Jacobs
Lucy Jones
Alexandra Jordan
Tom Jordan
Yan Kagan
Marc Kamerling
Nancy King
Robert King
Monica Kohler
John Labrecque
Daniel Lavallee
Mark Legg
Shoshana Levin
Yong-Gang Li
Eric Libicki
Scott Lindvall
Peng-Cheng Liu
Yun-Feng Liu
John Louie
Bruce Luyendyk
Harold Magistrale
Narbik Manukian
John Marquis
Aaron Martin
Kevin Mass
Sally McGill

Caltech
Carnegie-Mellon
USGS-Pasadena
Nevada-Reno
LLNL
Alaska
USGS-Menlo Park
SCIGN/USC
UC-Santa Barbara
CICESE
UC-Irvine
URS
UC-Santa Barbara
Caltech
MIT
National Academy of Sciences
UC-San Diego
USGS-Menlo Park
USC
Caltech
Caltech
USC
USC
USGS-Pasadena
USC
USGS-Pasadena
JPL
UC-Los Angeles
SCEC Intern/UC-San Diego
USGS-Pasadena
SCEC Intern/USC
USC
UC-Los Angeles
UC-Santa Barbara
USGS-Pasadena
MIT
UC-Los Angeles
NASA
UC-Santa Barbara
Legg Geophysical
USC
USC
USC
William Lettis Assoc.
UC-Santa Barbara
USC
Nevada-Reno
UC-Santa Barbara
San Diego State
USC
SCEC Outreach
UC-Santa Barbara
SCEC Intern/Whittier
Cal State-San Bernardino

John McRaney	SCEC
Bernard Minster	UC-San Diego
Lalliana Mualchin	Caltrans
Janice Murphy	USGS/Menlo Park
Nancy Natek	SCEC Intern/New Mexico
Laura Nett-Carrington	UC-San Diego
Craig Nicholson	UC-Santa Barbara
David Oglesby	UC-Riverside
David Okaya	USC
Kim Olsen	UC-Santa Barbara
John Orcutt	UC-San Diego
Mike Oskin	Caltech
Sue Owen	USC
Tracy Pattelena	SCEC Intern/UC-Santa Cruz
Zhi-Gang Peng	USC
Sue Perry	ECI
Andreas Plesch	Harvard
Will Prescott	USGS-Menlo Park
Evelyn Price	UC-Berkeley
Kenton Prindle	UC-Santa Barbara
Daniel Ragona	San Diego State
Daniel Raymond	SCEC Intern/UC-Irvine
Mike Reichle	CDMG
Jim Rice	Harvard
Tom Rockwell	San Diego State
Yufong Rong	UCLA
Paul Rosenbloom	USC
Charlie Sammis	USC
Dave Sandwell	UC-San Diego
Jim Savage	USGS-Menlo Park
Michael Scharber	UC-San Diego
Jon Schuller	UC-Santa Barbara
Nano Seeber	Lamont
Paul Segall	Stanford
Gordon Seitz	LLNL
Amy Selting	UC-Santa Barbara
Enrico Serpelloni	UCLA
Bruce Shaw	Lamont
Kaye Shedlock	USGS/Golden
Zheng-Kang Shen	UCLA
Gerry Simila	Cal State-Northridge
Mark Simons	Caltech
Bob Smith	Utah
Michelle Smith	SCEC/USC
Stewart Smith	Washington
Chris Sorlien	Lamont
Keith Stark	USGS-Pasadena
Jamie Steidl	UC-Santa Barbara
Ross Stein	USGS/Menlo Park
Clay Stevens	SCEC Intern/Cal State-Northridge
Toshiro Tanimoto	UC-Santa Barbara
Jerry Treiman	CDMG
Susan Tubbesing	EERI
John Unger	USGS-Reston

Matt van Domselaar
Kathryn van Roosendaal
Shannon VanWyk
Jan Vermilye
John Vidale
Antonio Vidal-Villegas
Dave Wald
Steve Ward
Kris Weaver
Frank Webb
Joel Wedberg
Shelly Werner
Steve Wesnousky
Rob Wesson
Jim Whitcomb
Frank Wyatt
Zhimei Yan
Bob Yeats
Bill Young
Jeri Young
Doug Yule
Howar Zebker
Yuehua Zeng
Li Zhao
Lupei Zhu

UCSD
SCEC Intern/Cal State-Northridge
SCIGN/USC
Whittier
UCLA
CICESE
USGS-Pasadena
UC-Santa Cruz
Lettis and Associates
JPL
USC
SCEC
Nevada-Reno
USGS/Golden
NSF
UC-San Diego
Caltech
Oregon State
SCIGN
Arizona State
CSU-Northridge
Stanford
Nevada-Reno
USC
USC

SCEC ORGANIZATION - 2000

Management

Center Director: Thomas L. Henyey
University of Southern California

Science Director: J. Bernard Minster
University of California, San Diego

Director for Administration: John K. McRaney
University of Southern California

Director for Outreach: Jill H. Andrews
University of Southern California

Board of Directors

Chair: J. Bernard Minster
University of California, San Diego

Vice-Chair: Ralph Archuleta
University of California, Santa Barbara

Members: John Anderson
University of Nevada, Reno

Robert Clayton
California Institute of Technology

Thomas H. Jordan
University of Southern California

Kenneth Hudnut*
United States Geological Survey

David D. Jackson
University of California, Los Angeles

Thomas Rockwell
San Diego State University

Leonardo Seeber
Columbia University

Ex-officio: Thomas Henyey
University of Southern California

- represents Lucy Jones on Board.

Research Group Leaders

A: Master Model:	David D. Jackson University of California, Los Angeles
B: Strong Motion Prediction:	Ralph Archuleta University of California, Santa Barbara
C: Earthquake Geology:	Thomas Rockwell San Diego State University
D/F: Subsurface Imaging and Tectonics and Seismicity and Source Parameters:	Robert Clayton California Institute of Technology
E: Crustal Deformation:	Duncan Agnew University of California, San Diego
G: Earthquake Source Physics:	Steve Day San Diego State University

Steering Committee Members (ex-officio)

Director Emeritus	Keiiti Aki University of Southern California
State of California Representative	James Davis California State Geologist
SCIGN Board Chairman	Ken Hudnut United States Geological Survey

2000 SCEC ADVISORY COUNCIL

Robert SMITH (Chair), University of Utah, Department of Geology and Geophysics, Salt Lake City, UT 84112-1183

Lloyd S. CLUFF, Pacific Gas and Electric Co., Geosciences Department, P.O. Box 770000, Mail Code N4C, San Francisco, CA 94177

C. B. CROUSE, URS Corporation, 2025 First Avenue, Suite 500, Seattle, WA 98121

George DAVIS, Department of Geosciences, University of Arizona, Tucson, AZ 85721

James DIETERICH, United States Geological Survey, 345 Middlefield Road, MS 977, Menlo Park, CA 94025

Robert HAMILTON, NRC/National Academy of Sciences, 2101 Constitution Ave., NW, Washington, DC 20418

Dennis MILETI, University of Colorado, Natural Hazards Research and Applications Information Center, Campus Box 482, Boulder, CO 80309-0482

Jack MOEHLE, Pacific Earthquake Engineering Center, University of California, 1301 South 46th Street, Richmond, CA 94804-4698

Barbara ROMANOWICZ, University of California, Berkeley, Department of Geology and Geophysics, Berkeley, CA 94720

Kaye SHEDLOCK, United States Geological Survey, Denver Federal Center, MS 966, Denver, CO 80225

Susan TUBBESING, EERI, 499 14th St., Suite 320, Oakland, CA 94612-1902

Mary Lou ZOBACK, United States Geological Survey, 345 Middlefield Road, MS 977, Menlo Park, CA 94025

Southern California Earthquake Center
Senior Research Investigators (2000)

Center Director:

Thomas L. Henyey
Department of Earth Sciences
University of Southern California
Los Angeles, California 90089

Science Director:

J. Bernard Minster
Scripps Institution of Oceanography
University of California
San Diego, California 92093

Principal Institutions

University of Southern California
Department of Earth Sciences
Los Angeles, California 90089

Scientists

Yehuda Ben-Zion
James F. Dolan
Yong-Gang Li
David Okaya
Susan Owen
Charles G. Sammis
Leon Teng
Lupei Zhu

California Institute of Technology
Seismological Laboratory
Pasadena, California 91125

Robert Clayton
Michael Gurnis
Egill Hauksson
Thomas Heaton
Donald Helmberger
Martha House
Hiroo Kanamori
Kerry Sieh
Mark Simons
Joann Stock

Columbia University
Lamont-Doherty Earth Observatory
Palisades, New York 10964

John Armbruster
Leonardo Seeber
Bruce Shaw
Lynn Sykes

University of California
Department of Earth and Space Sciences
Los Angeles, California 90024

Paul Davis
Yan Kagan
Monica Kohler
Zheng-kang Shen
John Vidale

University of California
Scripps Institution of Oceanography
LaJolla, California 92093

Duncan Agnew
Yehuda Bock
David Sandwell
Peter Shearer
Frank Vernon
Nadya Williams
Frank Wyatt

University of California
Department of Geological Sciences
Santa Barbara, California 93106

Ralph Archuleta
Marc Kamerling
Edward Keller
Daniel Lavallee
Peng-Cheng Liu
Bruce Luyendyk
Craig Nicholson
Kim Olsen
Chris Sorlien
Jamie Steidl

University of Nevada
Department of Geological Sciences
Reno, Nevada 89557

John Anderson
Rasool Anooshepoor
James Brune
John Louie
Raj Siddharthan
Feng Su
Steven Wesnousky
Yue-hua Zeng

San Diego State University
Department of Geological Sciences
San Diego, California 92182

Steven Day
Harold Magistrale
Thomas Rockwell

United States Geological Survey

Edward Field
Gary Fuis
Tom Hanks
Ruth Harris
Susan Hough
Ken Hudnut
Peggy Johnson
Lucy Jones
Nancy King
Daniel Ponti
Ross Stein
David Wald
Lisa Wald

Member Institutions
Arizona State University
Tempe, Arizona

Scientists
Ramon Arrowsmith

University of California
Berkeley, California

Roland Burgmann
Evelyn Price

University of California
Davis, California

Louise Kellogg

University of California
Irvine, California

Lisa Grant

University of California
Earth Sciences Board of Studies
Santa Cruz, California 95064
California Division of Mines and Geology

Steven Ward

James Davis
Michael Reichle

California State University
Northridge, California

Gerry Simila
Doug Yule

California State University
Department of Geology
San Bernardino, California 92407

Sally McGill

Carnegie Mellon University
Pittsburgh, Pennsylvania

Jacobo Bielak

Central Washington University
Department of Geology
Ellensburg, Washington 98926

Charles Rubin

University of Colorado
Department of Geological Sciences
Boulder, CO 80309

Karl Mueller
John Rundle

Harvard University
Department of Earth and Planetary Sciences
Cambridge, Massachusetts 02138

James Rice
John Shaw

Jet Propulsion Laboratory
Pasadena, California

Danan Dong
Andrea Donnellan
Mike Heflin
Ken Hurst
Michael Watkins
Frank Webb

Lawrence Livermore National Lab
Livermore, California

Bill Foxall
Gordon Seitz

University of Massachusetts

Michelle Cooke

Massachusetts Institute of Technology
Department of Earth, Atmospheric, and
Planetary Sciences
Cambridge, Massachusetts 02139

Brad Hager
Tom Herring
Robert King
Simon McClusky
Robert Reilinger

University of New Mexico
Albuquerque, New Mexico

Mousumi Roy

University of Oregon
Department of Geological Sciences
Eugene, Oregon 97403

Gene Humphreys
Ray Weldon

Oregon State University
Department of Geosciences
Corvallis, Oregon 97331

Whittier College
Whittier, California

Industry Participants
Earth Consultants International
Orange, California

Maxwell Labs
La Jolla, California

William Lettis and Associates
Walnut Creek

Pacific Engineering

Pacific Gas and Electric
San Francisco, California

Woodward-Clyde Associates
Pasadena, California

Robert Yeats

Jan Vermilye

Scientists
Eldon Gath
Chris Walls

Jeffry Stevens

Scott Lindvall

Walt Silva

Norman Abrahamson

Robert Graves
Arben Pitarka
Chandon Saikia
Paul Somerville

Message from the Directors

To: SCEC Group Leaders and the SCEC Community

From: Bernard Minster and Tom Henyey

Date: August 28, 2000

As all of you know, the upcoming annual meeting will be making plans for the current Center's final (11th) year. Our budget for that year will be significantly less (15-20%) than for the current one. In addition, we will begin planning for the renewal of SCEC at the annual meeting as you will see on the agenda that John McRaney will be circulating. While there is considerable interest at both the scientific and agency levels in seeing the center continue, it is by no means a certainty. For that reason, we feel that it is necessary to devote a portion of our 11th year funding to what might be termed "transitional science" – scientific activities carrying us toward the next generation of SCEC. This will further impact the dwindling budget.

For these reasons, we have decided that we will not engage in the usual proposal process for this final year. Also, as you recall, we asked last year that proposals address the needs of SCEC's "legacy", but got very little return. Most proposals simply reflected business as usual. Thus, for the 11th year, decisions on funding priorities will be made by the SCEC Steering Committee and Board of Directors. (This recommendation was made by the Board at their meeting of February, 2000)

However, these decisions will not be made without input from the SCEC scientific community. While the annual meeting will be an important forum for gathering input, we urge the Group Leaders to contact their group members, before the meeting if possible, to begin the dialogue of how to wrap things up. The annual meeting can then serve to summarize the input so that the Group Leaders can present their plans to the full Steering Committee for discussion and coordination. Groups will not be given budget targets, but instead should prioritize their funding needs, remembering that the budgets will be significantly reduced and that we must bring research activities to a logical conclusion even if the center is to continue.

We also want to gather input on the future of SCEC and what activities we might begin this transitional year. This part of the meeting will be led by Tom Jordan, who has been asked by the Board to lead the efforts to renew the center. He will work with the Steering Committee on a transitional plan.

The Current Status of EarthScope

EarthScope Working Group

As most of you know, a Working Group consisting of representatives from the major consortia funded by the National Science Foundation has been assisting NSF in developing the rationale for the proposed EarthScope facilities (USArray, SAFOD, PBO, and an InSAR mission). Activities of this group (members are listed on the EarthScope Web site at www.earthscope.org) have included organizing workshops to help define the major components of EarthScope, providing documentation and resource materials to NSF EAR staff as needed for their presentations to senior NSF management and the National Science Board, devising a management plan for implementation of EarthScope, and informing House and Senate members and their staff about EarthScope and its value to the country.

Status at NSF

As you no doubt are aware, EarthScope Phase I (USArray and SAFOD) has been approved by the National Science Board and was included in NSF's FY01 request to Congress as an item in the Foundation's MRE (Major Research Equipment) account. The Working Group is now assisting NSF, NASA and USGS with Phase II (PBO) and Phase III (InSAR). Preliminary indications are that these next phases have been well received by the agencies, and work has begun on developing them into EarthScope/MRE initiatives.

Status in Congress

During the initial FY01 Congressional budget negotiations earlier this year, the House Appropriations Subcommittee that deals with NSF was unable to support the full MRE request that included EarthScope "because of budget restrictions" and thus EarthScope was not included in the initial budget report. The corresponding Senate Subcommittee and the full Committee have yet to act. There is still the possibility that during the House-Senate conference, NSF's budget could be increased, including additional support for the MRE account and EarthScope. Contacts with your Congressional delegations can only help. But time is of the essence since decisions will be made later this month.

MRE Phase I Facilities Proposal

In anticipation of the possibility that MRE funding for EarthScope may eventually be approved for the FY01 budget, NSF has encouraged the EarthScope Working Group to submit an implementation proposal for the construction, operation, and maintenance of the facilities included in the Phase I MRE request. This would be for USArray and SAFOD as described in the EarthScope planning document (see EarthScope Web site). The EarthScope Working Group is assisting SAFOD and IRIS in the preparation of this proposal for submission on October 1.

EarthScope Science Support

Assuming favorable action on the facilities funding, NSF intends to have a yearly competition to fund science proposals that utilize the EarthScope facilities. Science research projects related to EarthScope will be supported through the EAR Division at NSF, separate from the facilities. NSF is working on an announcement for this science support and expects to have it issued by early next year. With the uncertainty in funding for FY01, it is likely that the initial request for science proposals will focus on planning and exploratory grants, with requests for more specific proposals as the facilities develop over the next few years.

Future Planning

Just a reminder that the next planning meeting for PBO will be October 30 to November 1 in Palm Springs, California. Also to be scheduled is a briefing of Dan Goldin, Rita Colwell and Chip Groat on InSAR by the Working Group Executive Committee in early October. The evolution of EarthScope facilities and science plans will be an on-going process and your support is both welcome and encouraged. The progress to date has been spectacular, and the support from many areas has been encouraging. To continue on the road to success will require your on-going involvement in planning workshops and your vocal and written support of the EarthScope concept in interactions with NSF, other federal agencies, Congress, and the public.

The FY 2000 Southern California Earthquake Center (SCEC) Communication, Education and Outreach (CEO) Program: Overview, Method, Projects, Objectives, Tasks

By Jill Andrews

In collaboration with Mark Benthien, John Marquis, and Bob de Groot

Introduction

SCEC, an interdisciplinary consortium of scientists and engineers who conduct earthquake research using southern California as a natural laboratory, was established in 1991 as a **National Science Foundation (NSF) Science and Technology Center**. From the beginning, SCEC scientific activities were strongly influenced by a series of timely, moderate earthquakes – in most cases damaging – that occurred from 1987 - 1999¹. Center leaders recognized the urgent need to communicate the results of their research with the multiple millions of citizens who live and work in this seismically active region (and other populous regions affected by earthquakes), and established in 1992 the **SCEC Communication, Education and Outreach (CEO) program**. Today we represent over **150 leading earthquake scientists** from more than **30 academic institutions** (a total of 423 people make up today's SCEC community of researchers, including principal investigators, post-doctorals, graduate and undergraduate students). We enjoy working **partnerships** with more than 50 other earthquake science, engineering, education, and government organizations worldwide.

CEO Mission and Programs

With ongoing expert advice from constituents and partners, SCEC leaders formed a **CEO program mission** that has evolved as Center activities matured: **to increase earthquake awareness and knowledge so that people take actions that improve safety and reduce loss**.

To fulfill this mission, SCEC leaders and CEO professionals emphasize the importance of **programmatic flexibility** as new communications tools, technologies and methods arise. We recognize that we must be **responsive to change** as research results emerge and understanding of earthquakes increases. Although we strive to maintain a cutting-edge approach, the basic program components remain constant: **public awareness** programs and products for media reporters and writers, civic groups and the general public; **education** programs and products for students, educators, and working professionals; and **knowledge transfer** programs and products for technical professionals, scientists and engineers. We manage an array of activities based on the Center's scientific research results and processes. **Products** such as fact sheets, maps, posters, videos, working group reports, news briefs, public awareness brochures, educational modules and curricula,

¹ 1987 5.8 Whittier Narrows, 1992 6.1 Joshua Tree, 1992 7.3 Landers, 1992 6.2 Big Bear, 1994 6.7 Northridge, 1995 5.5 Ridgecrest, 1999 7.1 Hector Mine.

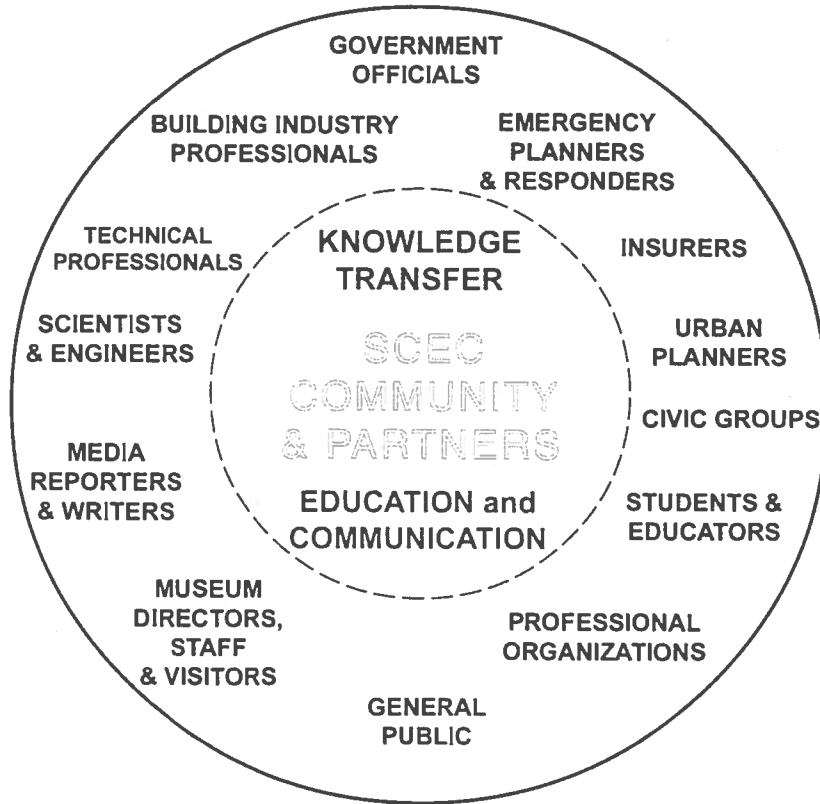
proceedings, consensus documents and databases are disseminated through mechanisms such as **workshops, seminars, short courses, field trips, a web service, email list-services, print and electronic newsletters, museum exhibits, and media briefings and interviews.**

Partnerships

We recognized early on that **partnerships** could greatly enhance our efforts. **Our partners are individuals and organizations who co-sponsor, support, or otherwise aid in development and implementation of CEO activities and products.** They are often users of our products as well. (Figure 1, Page 3.) They have helped us bring together disparate groups (scientists – engineers – government officials – educators – the general public) to attempt to solve the very complex problems posed by our active faults. (A distinction should be made here – through our partnerships for knowledge transfer with agencies charged with producing official products that feature our scientific results, we conduct workshops that promote understanding and support of these items, such as official maps, databases, technical reports and documents.)

Our partners in academia, government, industry and education aid us in assessment, evaluation and follow through by participating in our **advisory groups** and providing **cost-sharing** and **matching funds**. They also provide us with the ability to **reach larger audiences far beyond the borders of our study region**. Since 1995, SCEC CEO professionals have been invited to conduct workshops and make presentations at earthquake science and engineering meetings throughout the United States as well as other countries such as Canada, Italy, New Zealand, China, Greece, and Japan. Earthquake researchers and CEO experts in many of these countries have based their public awareness, education and knowledge transfer programs on the SCEC CEO model. We recently learned that Istanbul, Turkey, with an at-risk population of more than 11 million, is creating an earthquake public awareness and education program that will be modeled on the SCEC CEO program.

**The FY 2000 Southern California Earthquake Center (SCEC)
Communication, Education and Outreach (CEO) Program**



**The SCEC CEO Mission is
to increase earthquake awareness and knowledge
so that people take actions that improve safety and reduce loss.**

Figure 1.

CEO Method

Each SCEC CEO project is planned and executed in the context of our overall mission. **Each has its own set of objectives and tasks related to products, dissemination mechanisms, and evaluation and/or follow-through mechanisms.** The flow chart in below (Figure 2) illustrates the process, and the following pages describe current projects.

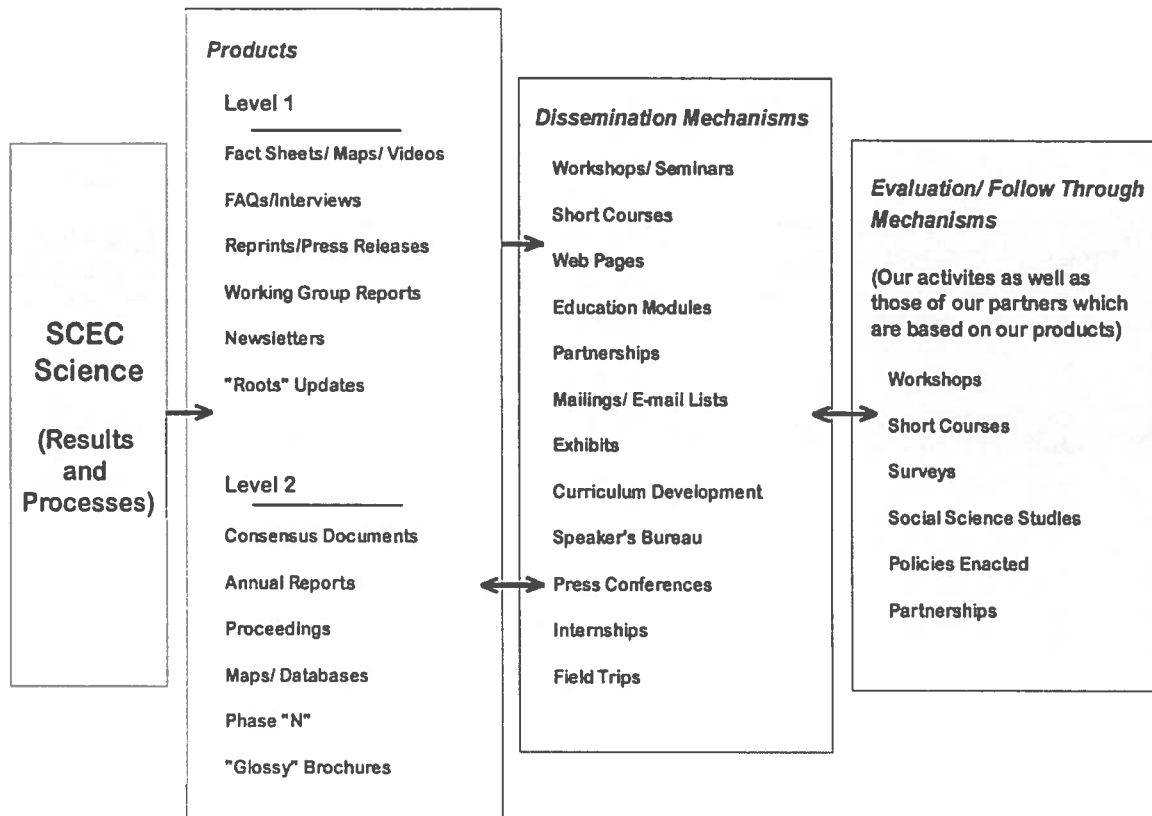


Figure 2.

Project	Objective(s)	Description / Tasks
<p>#100 SCEC Legacy</p>	<p>The legacy objective is to tell the stories of SCEC's scientific and CEO activities conducted during the first decade, with the goal of securing future support from a variety of sponsors.</p> <p><u>Stories to be told:</u></p> <ul style="list-style-type: none"> • Landers • LA Basin • Hypothesis testing • Data collection • Fault system behavior • SCEC as a natural lab • Master Model <p><u>General Topics</u></p> <ul style="list-style-type: none"> • Integration / community building • Open data / data archiving • Model-based inference/system-level science • E&O • Rapid, coordinated response / cyberquakes • Problem identification / consensus building • Sustained scientific effort • Interdisciplinary training • Shared facilities • Seed funding for "risky" projects • Infrastructure • Successful Center (Center as a paradigm) • Science-Engineering interface 	<p>The first workshop to plan the SCEC Legacy Document was conducted in July 2000 by members of SCEC's Steering Committee and Advisory Council. The group agreed that the most urgent next step is to write a polished, full-blown proposal, with figures, that can be circulated and discussed at the SCEC annual meeting.</p> <p>A session at the SCEC annual meeting will feature a series of 10-15 minute talks that will serve as the basis for the NSF proposal, which is due December 1, 2000.</p> <p>CEO's participation will include short vignettes on how SCEC has turned its science into products – across all topics addressed in the proposal – and suggestions as to how it will continue with those effective efforts. (Andrews to check list, make presentation based on these stories).</p> <p>Each presenter will write a narrative / speech (progress report) to go along with their presentation on PPT. This is due by October 1, 2000.</p> <p><u>CEO issues to address at the Annual Meeting:</u></p> <ul style="list-style-type: none"> • How to allocate funds in our final STC year (CEO objectives: wrap up current projects; during "transition years," focus on legacy document; fundraising from new sources; reorganization according to funding levels). • Weave the CEO story into the science stories
<p>Project</p>	<p>Objective(s)</p>	<p>Description / Tasks</p>
<p>#105 Electronic Encyclopedia of Earthquakes (E3)</p>	<p>This project will produce a pilot version of the Electronic Encyclopedia of Earthquakes, E³, which will synthesize a large and varied amount of data and explanatory information and provide broad access via the World Wide Web in the context of</p>	<p>The subject matter will feature Earth science and also include engineering, physics and mathematics areas of knowledge and inquiry. The collection is aimed at supporting high-quality high school and undergraduate education by providing educators and students with the tools and resources for instruction and research. Primary users would include investigators who employ inquiry-based techniques to explore specific topics. Archived and/or real time data</p>

	<p>the NSF-funded Digital Library for Earth System Education (DLESE). E³ would constitute a Collection within Element 2, Application of Digital Libraries to Undergraduate Earth Systems Education, as defined in NSF Program Solicitation 00-38, Geoscience Education.</p>	<p>sets and links to teaching materials would be available via the site, coupled with curricula that aid users in computing answers. Thus the site will promote the use of large data sets to help students simulate research.</p> <p>The three terms in the project name have been selected to accurately reflect the aim of this project, as explained below. The wide field of knowledge to be eventually included within the scope of E³ (2,000 entries are planned) renders the long range project ambitious, but the qualifications and resources of the three partners in the project, the Southern California Earthquake Center (SCEC), California Universities for Research in Earthquake Engineering (CUREE), and the Incorporated Research Institutions for Seismology (IRIS) make this scope feasible. A large amount of content already exists within other collections that can be adapted for use, such as those that will be provided by the three principal organizations, including innovative Earth systems curricula, associated archive data sets, and tools for handling real-time data. The pilot phase proposed here will develop the entire framework and include approximately 15-20 high-quality entries in an operational Webservice. Because of the extensive cross-referencing, linking, and tagging capability of a state-of-the-art Webservice, it will be possible to provide threads of continuity through layers of different articles or entries.</p>
--	--	--

Project	Objective(s)	Description / Tasks
<p>#110 Earthquake Studies and the Civic Scientist</p>	<p>The objectives of the Earthquake Studies and the Civic Scientist project are to</p> <ul style="list-style-type: none"> • provide information and resources to the media so that they are well-prepared to report about earthquakes, • conduct workshops for the media to explain the information (purpose and how to use); and • educate earth scientists, earthquake engineers and Public Information Officers on how to better communicate with reporters, writers, and the public. 	<p>1. Create reporters', writers', public information officers' information packets (printed and online)</p> <p>Description: Fact sheets and other products to be provided to reporters in advance of earthquakes and "on the spot." Selected materials will also be distributed to the general public. A small committee will periodically review and update information represented in fact sheets, especially the scenarios presented. The materials will be assembled in a binder and also mounted on the WWW for use by scientists and engineers in a post-earthquake (or interview) setting. NOTE: this project is to be combined with USGS products during FY 2000 and 2001.</p> <p>Fact sheets:</p> <ul style="list-style-type: none"> 1.1) Basic earthquake information (faults, why earthquakes happen, etc.) 1.1) Relative Scales (magnitude, moment magnitude, Modified Mercalli Intensity...) • Past earthquakes- concise list (magnitude, location, damage estimates) • Past earthquakes- detailed information for each

		<p>earthquake (magnitude, location, damage estimates, maps, conclusions of earth science and engineering studies (code improvements?), etc.)</p> <ul style="list-style-type: none"> • Possible future earthquakes (may include simplified scenarios; and preparation information) • Faults map (southern California active faults with probable magnitudes) • Fault maps (individual faults with synopsis of past earthquakes, probable future earthquakes recurrence intervals, slip rate, adjacent cities, etc.) • Preprinted fault map templates with a blank reverse side -- ready to be printed with info on the earthquake that just happened" <ul style="list-style-type: none"> • Short summaries (one for broadcast reporters; one for writers; one for general public) of the earthquake that just happened • Source characterizations • Aftershock sequences (measured and expected) • Shake Map from TriNet (intensity, magnitude, explanatory text) • Links to supplementary information (if on Web). <p>4) The most important things to report about the earthquake that just happened:</p> <ul style="list-style-type: none"> • What happened? • What does it mean? • What can we do about it? • Things people should do to respond to the earthquake that just happened <p>5) Earthquake Information Sources Brochure. Updated version of EERI's "Earthquake Basics"</p> <p>Other products (?):</p> <ul style="list-style-type: none"> • Maps and other graphics on CD-ROM • Videos <p>Suggested Reviewers: Jack Popejoy, Alison Horn, Lucy Jones, Bay Area Media person, Tom Henyey, Tom Rockwell</p>
Project	Objective(s)	Description / Tasks
#110 Earthquake Studies and the Civic Scientist (continued)	See above	<p>2. Conduct workshops to provide information and resources to the media so that they are well prepared to report about earthquakes. (In partnership with USGS Pasadena)</p> <p>Description Existing course curricula may be used.</p>
Project	Objective(s)	Description / Tasks
#110 Earthquake Studies and the Civic Scientist (continued)	See above	<p>3. Conduct workshops to educate earth scientists how to better communicate with reporters, writers, and the public. (In partnership with USGS Pasadena)</p> <p>Description Existing course curricula may be used.</p>

Project	Objective(s)	Description / Tasks
#120 INSTANeT News Service	To provide a reliable source of information in all matters relevant to the SCEC community; to disseminate news, announcements, earthquake information, and in-depth coverage of earthquake research, in a timely manner via the world wide web.	<p>Description "SCEC INSTANeT Newsservice" is produced by Jill Andrews (writer, editor), who recruits other writers from the SCEC community and edits copy; SCEC Staff Benthien, de Groot & Andrews contribute copy; and Mark Benthien prepares all articles for uploading to SCEC's Webservice and distributes newsbytes.</p> <p>SCEC INSTANeT is prominently featured on the SCEC Webservice Home Page; articles relating to research will be located on both the research pages and in the "News Service" section of the site. Links to resources, related information, and other sites will be added where appropriate.</p> <p>A brief news "byte" is written for each article added to the INSTANeT web pages. These bytes are e-mailed to subscribers of the scecinstanet-l@usc.edu listserv. After each "byte:" a link to the complete articles is listed. The intention is to produce new articles each week.</p> <p>NB: News Brief (goal: 1-2 each week) FS: Feature Story (goal: every 2 weeks, alternate with SL) FTC: From the Center (goal: every 4 weeks) SL: Spotlight (goal: every 2 weeks, alternate with FS)</p>
#130 Insurance Workshops	To provide a forum for insurance industry representatives, earth scientists, engineers, and policy officials to discuss key issues of earthquake insurance.	<p>Description Following the lead of WSSPC and others, SCEC will restart its Insurance Workshop Series, in partnership with WSSPC. Issues to be covered will include: how to use public maps; interpretation of maps and software for damage/loss estimation; how and why the maps came into existence; how are ZODs depicted; collection of input on usefulness of these tools; CEA update; update from WSSPC on outcomes from its policy making workshop; and updates on SCEC research (i.e., Phase 3).</p> <p>Planning for these workshops will resume in October, 2000 (WSSPC is not available until then)</p>
#140 SCEC Webservice	To present the ongoing research and results of SCEC scientists; provide links to SCECs member institutions, research facilities, and SCEC-supported databases; distribute information ranging from new briefs to	<p>Description: A reorganization of staff responsibilities will be conducted over the remainder of the summer and into the fall, 2000. The site will be reviewed (internally and externally); suggestions for improvement will be solicited from the SCEC community and its audiences. Basic areas of responsibility will be assessed and assigned:</p>

	in-depth articles; and serve as a resource for earthquake information, educational products and experiences, and links to other earthquake organizations.	<ul style="list-style-type: none"> • Andrews: General guidance on design, content, copy editing • Marquis: Architecture; overall design; graphics creation / enhancements • Benthien: Content (procurement and accuracy); maintenance / maintenance oversight • Benthien, Office Staff: Maintenance: (links checks; adding pages; content changes, updates) • Internal and External Groups (TBD): Review
--	---	---

Project	Objective(s)	Description / Tasks
#145 HAZUS	<ul style="list-style-type: none"> • To improve the earth science inputs (attenuation functions, soil maps, etc.) used by HAZUS to calculate ground shaking by forming a committee of scientists, engineers, and HAZUS programmers to recommend needed revisions. • To foster implementation of HAZUS by governments, corporations, and consultants by forming a So. California HAZUS users group. • To assist citizens, through a user group in southern California, to develop natural hazard preparedness, response, damage prevention and recovery programs; to promote a world class, user-friendly software. 	SCEC scientists and CEO staff are moving toward greater use and understanding of Hazards US (HAZUS), FEMA's earthquake loss estimation software program. SCEC is now considering launching activities to improve the scientific data and models that HAZUS uses in its calculations, and to promote the use of the tool to governments, corporations, and consultants by forming a southern California HAZUS users group. See appendix for more information on development of a southern California HAZUS users' group.

Project	Objective(s)	Description / Tasks
#150 SCEC Published Research Database and Reprint Collection	To maintain the scientific legacy of papers published as the result of SCEC-funded research	The database currently has 471 records. Of these records, 132 are represented by reprints stored in the SCEC CEO office (1 copy: 54, 2 copies: 26, 3 copies: 13, 4 copies: 5, >6 copies: 33). The first goal is to add more papers to the database so that ALL SCEC-funded papers are included. Another goal is to collect at least 1 copy of every paper listed in the database. In addition, 138 of the 471 records include the paper's abstract. A third goal is to have the abstract for every paper as well.

Project	Objective(s)	Description / Tasks
#190 The Real Meaning of Seismic Risk	The objective of the "Real Meaning of Seismic Risk" project is to increase public	We will continue to conduct a series of symposia and workshops that focus on urban seismic risk issues. These feature experts who are earth scientists,

Workshops	awareness and understanding of urban seismic risk and related social and public policy issues.	<p>earthquake engineers, building officials, public policymakers, architects, insurers, developers, educators and the media. During FY 1999 and FY 2000, 2 workshops were conducted for emergency responders, planners, and educators.</p> <p>Topics may include:</p> <ul style="list-style-type: none"> • methods used to interpret the earthquake threat; • vulnerability of tall buildings and other structures located near faults; • design codes; • perceived socio-economic impacts of earthquakes and secondary hazards in California vs. other natural hazards outside the State • others? <p>Funding is provided through registration fees of participants and/or from other donors, such as the LA County Emergency Preparedness Commission.</p>
Project	Objective(s)	Description / Tasks
#230 Summer Undergrad Internship Program	The objective of the Summer Undergraduate Internship Program is to provide hands-on experiences in the earth sciences or science outreach, to provide insights into career opportunities, and to interest, train, and retain underrepresented minority undergraduate students and women in earth science-related careers.	<p>We are continuing career oriented programs for undergraduates by supporting eight earth science undergraduate student research projects through the <u>SCEC Summer Internship Program</u>. All interns present posters at SCEC's Annual Meeting. A special Colloquium (where progress is shared via powerpoint presentations) and a field trip to southern California geologic points-of-interest will be conducted. To enhance the program this year, we have added two "CEO" internships.</p> <p>Statistics on Internships to date: 69 Internships total since 1994 36 Interns were women (33 were men) 10 were minorities (black, Hispanic) Students from 25 colleges or universities 22 interns still actively involved with SCEC 47 SCEC Scientists have been Research Mentors</p>
Project	Objective(s)	Description / Tasks
#235 Interpretive Trail along SAF and Wallace Creek	To provide a first-rate interpretive trail at a geologically significant site along the San Andreas Fault in California; to facilitate students, scientists and the general public with accurate and up-to-date information about the fault zone; to encourage investigation of this site by providing images, activities, a self-guided tour, and other information through an interactive Wallace Creek website.	<p>In cooperation with the Bureau of Land Management, Prof. Kerry Sieh and Aron Meltzner (Caltech undergraduate student) proposed an interpretive trail along a particularly spectacular and accessible 2-km-long stretch of the San Andreas fault near Wallace Creek, in the Carrizo Plain. The objective is to create a first-rate educational field site where students, scientists and the general public can investigate, in detail, the basic nature of strike-slip faulting. SCEC will create the infrastructure and interpretive materials (durable signage, brochure content and a website). BLM has agreed to maintain the site and print and distribute the educational materials, into the foreseeable future.</p>

Project	Objective(s)	Description / Tasks
#241 School District Partners	Curriculum enhancement, teacher training, resources for K-12 earth science education.	In 1999, we continued the three School District Partnerships with Palos Verdes, La Cañada and Rialto Unified School Districts in a limited way, providing them with SCEC CEO expertise and resources. Through February 2002, we will continue limited provision, based on available time and resources. Form a partnership with USGS Pasadena.
Project	Objective(s)	Description / Tasks
#260 Middle School level online Earth Science Education Module, Version "Earth Works"	<ul style="list-style-type: none"> Promote Center development and distribution of original educational products that feature SCEC scientific research. To develop and distribute, in partnership with others, original educational products that feature SCEC scientific research. 	SCEC's DESC Online Advisory Group, led by Jill Andrews and Meridith Osterfeld (K12 Alliance) has conducted five meetings and completed the overall design, story line and accompanying lessons and activities for a Middle School level module. The lessons are now in the hands of Web author John Marquis. Web author John Marquis, now an employee of USC SCEC CEO, will continue development and complete the middle school version of the SCEC web-based education module, with partial support (3 months salary) from IRIS. Modules to be reviewed and distributed with the aid of the DESC Online group. Budget includes Marquis' salary for 6 months. Estimated time to completion of the Middle School modules is mid- to late 2001.
Project	Objective(s)	Description / Tasks
#270 Museum Partners	General: Encourage public participation in and understanding of earthquake science through interactivity with SCEC.	<p>1. California Science Center: SCEC influenced development of its earthquake exhibit. They requested our assistance with compiling earthquake data and graphics for a new Technopolis interactive exhibit, "Track the Quake". SCEC formed an advisory group to aid in display/exhibit/program development. A class based on the resulting product is now taught three times a week, to grades 9-12, at the California Science Center. SCEC's CEO staff (Andrews, de Groot) will periodically visit the Friday afternoon "Track the Quake" course to provide feedback for enhancement / improvement of the course. We furnished speakers and trainers for children's programs and the grand opening of the Powers of Nature exhibit.</p> <p>2. San Francisco Exploratorium: Andrews acted as chief consultant to the producers of "Faultline," a multi-media, interactive exhibit that aired on local TV and the Web in October, 1999 to commemorate the 10th anniversary of the 1989 Loma Prieta earthquake. See http://www.exploratorium.org/faultline/ for an interesting tour of SCEC-related research on the SAF. In December 1999, Andrews, Marquis and Hafner led teachers' workshop, hosted by the Exploratorium as part of AGU's Fall Meeting education workshop</p>

		series. 3. Santa Barbara Museum of Natural History: Since 1998, we have been working with museum education staff and curators to help them plan a new earth sciences exhibit, with features such as a tour of the Mission Ridge fault, which runs through museum grounds; a walking tour of the surrounding area, which includes the fault scarp, an ancient landslide, and a paleo channel; and a CUBE/REDI computer display. Museum staff visited Caltech's Seismo Lab, the California Science Center, and USC in late 1999. They will be raising funds over the next year in order to begin work on this project. Prof. Ed Keller, UCSB and SCEC, is preparing support materials and delivers frequent lectures at the museum.
--	--	--

Project	Objective(s)	Description / Tasks
#270 Museum Partners (continued)	ShakeZone Objectives To reach the local community, particularly elementary and secondary school children, with positive messages about studying the Earth and preparing for earthquakes; to provide a global to local perspective of how the Earth changes; to promote empowerment of citizens by providing information and instruction regarding safety and mitigation; to motivate individuals to be active in hazard preparedness in their local communities.	4. Riverside County Children's Museum ("KidZone") Andrews and de Groot are working with museum executive director Patricia Korzac and Board of Trustees, in collaboration with engineering professors from UC Riverside and the CUREe Woodframe Project, to create an educational, family-oriented exhibit on earthquakes in their region. The display, to be completed mid-2001, will occupy fully half the space at "KidZone." Big Idea: I can prepare for earthquakes by learning about how the Earth changes, what happens to my house and other buildings during earthquakes and how I can help my family make a safety plan. -Stress on personal responsibility and empowerment -Global to local / local to global -Earth to my family Voice: A Child – The visitor is on a mission to discover and learn as much as possible to assist her/his family in the preparation for an earthquake. Child takes on the role of scientist, sleuth, engineer and emergency planner. Role reversal – young person assures adults that earthquake risk is manageable.

Project	Objective(s)	Description / Tasks
#280 Seismic Sleuths Update: Video Production and Curriculum	To promote and improve natural hazard education for students; to foster preparedness for natural hazards through	NSF provided a \$25,000 supplemental grant (thanks to Jim Whitcomb) to support USC science education graduate student Bob de Groot to launch a project to partner with AGU and FEMA on updating Seismic Sleuths, a middle school/high school curriculum on

Revision	empowerment and encouraging personal responsibility; to provide an updated and redesigned learning tool that can be easily integrated into a curriculum based on national standards; to provide constant updates in science content, pedagogy, and resource information through an interactive website.	<p>earth sciences. De Groot started the project late spring 1999, and is developing activities to accompany the Seismic Sleuths teacher's package, as well as working as consultant to a Discovery Channel producer who is creating a television pilot based on the series. We received \$130,000 from IBHS and CEA to fund the video, which we plan to market worldwide. An hour-long video is completed and will be aired on "Assignment Discovery" in Spring, 2001.</p> <p>Materials for curriculum update are under construction by Bob de Groot and Kathryn Van Roosendaal.</p> <p>We are exploring possibilities for "Phase 2" - the original plan to package Seismic Sleuths as part of an all-hazards series has been put into a proposal, a product of collaboration between SCEC Outreach and Summer Productions. The product, if funded, will be a series of five hour-long programs that will be coupled to an interactive website, with activities, live TV broadcasts, webcasts, links to curricula, and streaming video. "The Earth Works," a working title, will capitalize on the convergence of television and the web; it will cover earthquakes, hurricanes and tornadoes, volcanoes, floods and tsunamis, and wildfires.</p>
-----------------	---	---

Project	Objective(s)	Description / Tasks
#310 Earthquake Information Providers Groups (EqIP)	The objective of the Earthquake Information Providers group is to provide and promote efficient access to quality earthquake information through active collaboration.	EqIP's MISSION is to facilitate and improve access to earthquake information through collaboration; and minimize duplication of effort by sharing information through individual personal contact, joint activities and projects, group annual meetings and biennial forums, and electronic communication. This Earthquake Information Providers' (EqIP) Web site can be found at www.eqnet.org . MCEER manages the site, with a graduate student working 15 hours a week. Jill Andrews chairs the steering committee for the group that oversees continued development of the website and other EqIP activities. Mark Benthien is the editor of the Seismology/Geophysics pages, and has already done an extensive revision to the ordering and listing of the Seismology/Geophysics section. Benthien also designed an EQIP/EQNET flyer for distribution and co-chaired the EqIP annual meeting at the Natural Hazards Workshop in July 2000. Benthien presented ideas for a survey of current collaboration and communication methods, which will be distributed during summer 2000, and also presented other new ideas for increased communication and collaboration.
Project	Objective(s)	Description / Tasks
#320 Science Seminars	The objective of SCEC Science Seminars is to facilitate the ongoing	SCEC CEO staff proposes organizing SCEC science seminars, which will be held at various SCEC host institutions and will be open to scientists, engineers,

	dialogue between SCEC scientists.	<p>other practicing professionals as appropriate, and students. We plan to give scientists/engineers criteria for giving talks that can be understood by non-scientists/non-engineers, without lessening the scientific content of the discussion.</p> <p>Topics for Seminars will be determined by SCEC Science Director with approval / input from BOD and STC. The following topics were suggested in 1999:</p> <ul style="list-style-type: none"> • Crustal Deformation map workshop for end users (Task E:5, RFP) • 3-D Seismic Velocity Model (for a broader audience; and update) • End users' SCEC-DC workshop • Phase 3 / Master Model workshop (for scientists and end users) • Group C Science Seminar or Field Trip to open trenches on SAF • Joint SCEC/PEER workshop – compile ref. Ground motions/time histories (G. Martin)
Project	Objective(s)	Description / Tasks
#330 Pre- and Post-Earthquake Planning	The objective of the Post Earthquake Planning project is to have pre-determined protocols in place before damaging earthquakes, both for the SCEC community as well as with our partners throughout the state.	<p>1. Preplanning a Post-Earthquake Response To consider the scientific questions that SCEC researchers want to address through post-earthquake investigations, we conducted a seminar led by US Geological Survey Pasadena Office Chief Scientist and seismologist Lucile M. Jones. The seminar was an interactive discussion about why we do what we do after an earthquake. We examined what we are trying to achieve and which of the traditional investigations are obsolete in the era of broadband seismic networks and geodesy. Our objective from this seminar was to form a new plan organized around the scientific objectives of a post-earthquake investigation and how those objectives could be achieved. We also agreed that interactions should be identified and more accurately defined with the already-established "California Post-Earthquake Information Clearinghouse."</p> <p>The goal was to set objectives so that after the next earthquake we can look at the list, pick the three or four objectives most relevant to this event (urban near-field damage? San Andreas rupture? Strike-slip along the side of a basin? etc.), and deploy our resources accordingly. Scientists with field experience following large events brought to the meeting a transparency with important scientific questions they wanted to see answered by the next big earthquake. These were generic, applicable to all events, or specific to a plate boundary event, urban earthquake, etc.</p> <p>The outcome of this seminar contributes to how research money will be spent after the next event.</p>

		<ul style="list-style-type: none"> • Questions presented were assigned to one or more of three disciplinary groupings: Geology, Geodetics, and Seismology. Participants divided into these three disciplinary groupings and discussed and rank the questions presented in the morning session. They then formulated field experiments that would be done after an earthquake to address each question. The results of the discussions were presented to the group as a whole, and the group discussed possible implementation methods. The results of the workshop can be synthesized into an official SCEC Response Plan.
Project	Objective(s)	Description / Tasks
#330 Post Earthquake Planning (continued)		<p>2. California Post-Earthquake Technical Clearinghouse (CPEIC)</p> <p>Clearinghouse collaborators have been meeting quarterly since March 1996 to plan for the needs of all the involved organizations. In summary, the plan calls for the clearinghouse to: 1) be the check-in and check-out point for all investigators and officials who arrive at the scene; 2) collect and verify perishable reconnaissance information; 3) convey that information to the planning/intelligence function of the OES Regional Emergency Operations Center; 4) provide updated damage information through daily briefings and reports; 5) track investigators in the field; and 6) perhaps even direct their movements for maximum coverage with minimal disruption to residents. In the few years since Northridge, the technology for capturing data has been vastly improved, and what was a comparatively primitive system in 1994 is now a networked geographic information system capable of tracking the investigators as well as their findings. Within the clearinghouse management group, CDMG and USGS are responsible for conducting seismologic and geologic assessments of earthquakes. EERI has a charter from the National Science Foundation to investigate the structural and social effects of all major earthquakes in the U.S. and abroad. The CSSC is the main seismic policy body in the state, recommending new legislation and regulations to minimize earthquake losses. OES coordinates all the emergency planning and response activities in the state. Besides the members of the management group, ten other organizations have signed on as participants in the clearinghouse plan:</p> <ul style="list-style-type: none"> • Applied Technology Council • California Institute of Technology • California Universities for Research in Earthquake Engineering • Federal Emergency Management Agency, Region IX • National Aeronautics and Space Administration • Pacific Earthquake Engineering Research Center

		<ul style="list-style-type: none"> • Southern California Earthquake Center • Structural Engineers Association of California • Technical Council on Lifeline Earthquake Engineering • UC Berkeley Seismological Laboratory
Project	Objective(s)	Description / Tasks
#340 Publications Sales	The objective of SCEC's publication sales is to provide quality earthquake information at very reasonable prices and to as many people as possible.	
Project	Objective(s)	Description / Tasks
#350 SCEC Fault Guides	To reach students, the general public and scientists with reliable and up-to-date information about several notable faults in the Los Angeles region; to produce a field guide that will be utilized in several venues by the target audiences; to promote self-motivated preparedness through practical and relevant earth science education experiences.	<p>Since 1995, SCEC has produced several fault guides that should be reviewed for accuracy, converted to html, and mounted on the WWW. These include:</p> <ul style="list-style-type: none"> • Palos Verdes Fault Guide (I and II) (Michael Forrest, Tom Henyey) • Newport-Inglewood / Whittier-Elsinore Fault Guide (Michael Forrest, Tom Henyey) • San Andreas Fault (portions of) – a field trip led by M. Forrest / T. Henyey • Sierra Madre Fault – a field trip led by ... • Faults of Los Angeles (Based on research conducted by SCEC scientists; Ann Blythe, principal author)
Project	Objective(s)	Description / Tasks
#400 ANNA-SCEC Community Earthquake Preparedness Project	Encourage public participation in and understanding of earthquake science through interactivity with SCEC.	The ANNA-SCEC Neighborhood Earthquake Watch program was funded by the USC Neighborhood Outreach Grant and SCEC Education in 1997. USC's School of Psychology recently delivered its final reports on pre-, post- and earthquake fair surveys. Andrews is documenting the activity with a lengthy article scheduled to appear in Natural Hazards Review in the Winter of 2000.
Project	Objective(s)	Description / Tasks
#500 Joint Task Force on Ground Motion	<ul style="list-style-type: none"> • To make recommendations regarding earthquake ground motion hazards to the Los Angeles City Department of Building and Safety for determining public policy related to design of new buildings and seismic retrofit of existing structures. • Conduct monthly workshops, production of technical reports to City of LA, production of 2 public booklets. • Base future efforts with 	<p>The Los Angeles City / SCEC / SEAOSC Ground Motion Joint Task Force monthly workshops began in the winter of 1996 and concluded in the spring of 1999. Four topics were to be addressed: Liquefaction hazards; ground motion; and two vulnerable building types, so-called "tuck-under" parking structures, and non-ductile concrete structures.</p> <p>Two reports, one on liquefaction hazards and the other on "tuck-under" structures vulnerability, were produced. The studies conducted by the JTF produced one technical report on liquefaction hazards and one technical report on tuck-under structures recommending further study; the non-ductile study group disbanded in lieu of work on the same topic now underway by a separate panel funded by the City of Los Angeles. The ground motion group awaits final outcomes of the Phase III report, which has not been</p>

	HAZUS on output / experiences of the task force	<p>published at this writing. All groups called for more work to be done.</p> <p>FEMA provided \$25,000 in 1998 to a public awareness booklet aimed at owners and occupants of the two types of vulnerable buildings (tuck-under and non-ductile). We are partnering with the USGS Pasadena Office (Lucy Jones and Sue Hough) to finish the project. Sue Hough has completed the booklet and it is now under review, scheduled to be published in the fall of 2000.</p>
Project	Objective(s)	Description / Tasks
#510 Liquefaction Technical Report and CD ROM	The objective of the Liquefaction Technical Report CD-ROM project is to increase knowledge of liquefaction evaluation and mitigation methods by creating a CD-ROM based on the popular liquefaction report and explanatory workshops that were held in 1999 such that the information can be available to those who did not attend the workshops.	<p>In 1999 SCEC produced a technical report on how to implement guidelines established by the CDMG for evaluating and implementing effective mitigation measures for liquefaction hazards. This document was then explained at two identical workshops attended by a total of 260 people. Approximately 1500 copies of the document have been distributed (freely or for replacement costs). Both workshops were very popular and it is believed that many more geotechnical engineers and building officials would welcome the information that was presented. Therefore the concept of producing a CD-ROM based on the document and the workshops was conceived in order to make this information widely available. The presentations at the workshops were in a common powerpoint format, which allows for easy translation onto a CD-ROM. The first workshop was recorded on audio and video tape, and these recordings have been transcribed. The plan is to include audio and video clips from the workshops where appropriate, and the complete transcription. The workshop content will be created with the software package "Director" which we purchased in 1999. The original document, CDMG documents if possible, and possibly CDMG maps will also be included in the final product in PDF. We will sell the CD-Rom for the production cost, so there will be upfront costs that will be recovered.</p>
Project	Objective(s)	Description / Tasks
##999 Contacts master updates		<p>Send out flyer for people to update their contact information and codes. Enter the changes into Contactsmaster when flyers are returned.</p> <p>We will ait to send flyers until just prior to the Annual Meeting, so that when they are returned they don't overload the office staff who will be busy preparing for the Annual Meeting.</p>

Appendix

HAZUS: A NEW OPPORTUNITY TO APPLY NEW MODELING TOOLS TO BENEFIT EARTHQUAKE RESEARCH

The Southern California Earthquake Center is a National Science Foundation Science and Technology Center created in 1991. Its 50+ principal investigators at more than 25 institutions have conducted interdisciplinary research on earthquake probabilities in the region, handing off to appropriate government agencies the calculation of estimated economic and social impacts. Now, with the introduction of a new Geographic Information Systems (GIS) based loss estimation tool created by the US Government, earth scientists' research results can be automatically combined with building inventories and demographic information, enabling researchers across disciplines to produce earthquake loss estimation models and calculate probable loss.

HAZUS, or "Hazards US," was developed by the Federal Emergency Management Agency (FEMA) through a cooperative agreement with the National Institution of Building Sciences (NIBS). It is a standardized, nationally applicable earthquake loss estimation methodology. The PC-based software is designed to produce detailed maps and analytical reports that describe a community's potential earthquake-related loss. At the simplest level, one can use default data to for rapid output of expected damage based on an earthquake "scenario" – a likely event researchers forecast for any seismically active region.

Default data for the program were created from existing state and national databases. The data include regional building inventories and economic conditions of earthquake-prone communities. Those who desire more accurate output must input data based on a city or county's actual records. Trained users can provide detailed information about local geology, liquefaction and landslide susceptibility, building inventory, and utility and transportation systems. With more accurate input the program can produce increasingly better loss estimates and also aid in mitigation planning and emergency planning, response and recovery.

Numerous research groups, government agencies and public and private corporations in northern California have recognized the value of this tool, and have formed the Bay Area HAZUS User Group (BAHUG), funded largely by FEMA. The user group is made up of organizations from 11 counties in the area: more than 300 individual users are from city and county governments, private industry, utilities, nonprofit organizations, universities and national research laboratories.

SOUTHERN CALIFORNIA NEEDS A TEACHING LAB, TRAINING FACILITY AND USER GROUP

Fifty percent of the expected average dollar loss caused by earthquakes in the U.S. is due to extreme earthquake-related risk (potential loss due to casualties, building and infrastructure damage, business disruption, etc.) in southern California. Twenty-five percent of the risk is in Los Angeles County alone. Despite these facts, no southern California GIS laboratory, training facility and HAZUS user group exists.

We believe we are uniquely qualified to establish a GIS laboratory, training facility and HAZUS user group for the region. For the last decade, SCEC has fostered strong working relationships among its community of end-users: engineers, building officials, technical professionals, local government agencies, emergency planners – all who are concerned with the earthquake threat.

We have established a strong reputation and enjoy the trust of the community-at-large – essential ingredients to creating a southern California GIS laboratory, training facility and HAZUS Users group.

SCEC's working group leaders and Board of directors, who have become familiar with the capabilities offered by new GIS tools and specifically HAZUS, agree that we are well positioned to play an important role in improving the earth science data and resulting calculations and models. SCEC staff and scientists have received initial HAZUS introduction and training. Topics addressed would include similar ones to that of BAHUG: user applications and emergency management protocols for creation and distribution of damage assessment maps and reports.

SCEC conducted a survey June-August 2000, of possible participants in a southern California HAZUS Users Group. A carefully selected group of 30 professionals in occupations related to earthquake preparedness, response, and recovery were queried as to what they know and think about GIS-based loss estimation tools such as HAZUS, and whether a southern California user group would benefit their organization.

SURVEY RESULTS

- When asked what their exposure was to earthquake risk, about half the people their risk is high; the remainder either didn't understand the question or didn't know the answer when they did. This lack of understanding by a community of people responsible for mitigation and safety shows that GIS based tools such as HAZUS are greatly needed.
- Most commented that loss estimation or hazard analysis tools are important to their work – especially those concerned with building damage and emergency response.
- When asked about GIS based tools, particularly HAZUS, most had heard of it but few have used the application. All were interested in learning more. Some knew of GIS capabilities but very few had hands-on experience. No one had worked directly with ArcView or MapInfo and only a few had heard of either software. All but two people were interested in learning more about GIS to accurately depict earthquakes or damage scenarios.
- When presented with a list of HAZUS capabilities such as damage and functionality estimates of certain types of buildings, facilities and lifelines, most recognized a versatile tool that could be programmed to give them specific information would be useful
- All but two people said that they were interested in learning more about the program and were reasonably enthusiastic. One of the two people that didn't seem interested stated that his company was using "Early Post Earthquake Damage Assessment Tool" (EPEDAT) – and didn't realize that the program, formerly supported by California's Office of Emergency Services, has been replaced by HAZUS.
- After hearing about the accomplishments of BAHUG, most agreed that forming a southern California users group is a very good idea. Many went on to say that combining the users groups would be desirable.
- Most said their organization would send a representative to participate in a GIS training program and user group if one was created.

2000 SCEC Abstracts

Shallow Site Response at Precariously-Balanced Rock Sites Near the San Andreas Fault

Robert E. Abbott, John N. Louie, James N. Brune, and Rasool Anooshepoor
University of Nevada, Reno

We present results from the analysis of 3-component digital recordings of approximately 20 LARSE-II explosions and approximately 300 Hector Mine aftershocks (M2 to M5.1) at precarious- and semi-precarious rock sites near the San Andreas fault. We recorded seismograms near precarious rocks at two buttes (Lovejoy and Piute), both within 20 kilometers of the Mojave section of the San Andreas Fault. This section of the fault has ruptured numerous times in the last thousand years, most recently in 1857. We also made simultaneous recordings at Mill Creek Summit, location of the USC strong motion station MCS, and a rock site (not precarious) 7 kilometers southeast of Pearblossom and a few kilometers northwest of the fault. In addition, we recorded simultaneous seismograms at Alpine Butte and at a rock outcrop less than 3 kilometers north of Black Butte. Reconnaissance of the Alpine Butte and the near-Black Butte sites revealed no precarious rocks, but a more detailed search is needed.

Amplitude spectra of the horizontal components of seismograms recorded at Lovejoy Buttes and Piute Butte exhibit significant de-amplification relative to Mill Creek Summit in the 1 to 6 Hz frequency range. Preliminary velocity analysis suggests that the rock at MCS, previously categorized as an engineering class A site (>760 m/s shear wave velocity to 30-m depth), has significantly slower seismic velocities than the rock at the buttes, partially explaining the de-amplification at the precarious rock sites relative to MCS. MCS has an average 30-m shear wave velocity of 461 m/s. Lovejoy and Piute Buttes have average 30-m shear wave velocities of 1046 m/s and 1465 m/s, respectively.

Inconclusive Evidence for Fault Zone Trapped Waves on the Bullion Fault

Marie C. Ammerman and Ralph J. Archuleta
University of California, Santa Barbara

Aftershocks recorded by stations in the Bullion Wash Array lacked the arrival of seismic waves that characterize the fault zone trapped waves observed by Li et al., 1994. The arrivals following the S wave were more prominent on fault parallel and vertical components of the seismometers than on the fault perpendicular components-inconsistent with a Love wave type mode trapped in a fault zone. The waves following the S wave did not show consistent amplitudes on stations within the fault zone with a decrease in amplitude for stations farther away from the fault trace. The apparent lack of fault zone trapped waves may be due to the juvenile nature of the Bullion fault zone, i.e., it is not well enough developed to generate trapped waves. The observed post-S waves may be basin edge generated waves caused by a wedge of sediments that underlies the array (Dibblee, 1967). The presence of edge generated surface waves would explain why the waves are more prominent on fault parallel and vertical components.

Fault Roughness and High Frequency Seismic Wave Generation

John G. Anderson, James N. Brune, and Steven G. Wesnousky
University of Nevada, Reno

In three large earthquakes that are well-recorded on strong motion accelerographs, the peak accelerations were surprisingly low. The first was the Michoacan, Mexico earthquake of Sept. 19, 1985 ($M_w=8.0$), where peak accelerations at four stations on rock directly above the fault had peak accelerations of 13%-17% of gravity. The second is the Kocaeli, Turkey, earthquake of August 17, 1999 ($M_w=7.6$), where peak accelerations on rock within ~10 km of the fault recorded peak accelerations of 23%-40% of gravity, a factor of two below predictions. The third is the ChiChi, Taiwan, earthquake of September 21, 1999, where peak accelerations at numerous sites with uncertain conditions were generally a factor of two smaller than regression models. These may represent the three best cases of near-fault strong ground motions from earthquakes with magnitudes over 7.5 on major, highly active faults. The peak accelerations are taken to represent the amplitudes of the high-frequency end of the seismic spectrum, and therefore suggest that in these three cases the high frequencies have been systematically depleted, compared to extrapolations from smaller-magnitude earthquakes. Of the various possible physical explanations, one strong contender must be that the amount of high-frequency radiation is related to the total amount of slip on the fault. Wesnousky (1988) recognized that strike-slip faults with large total offset have smoother fault traces than those with little cumulative offset, and suggested that the degree of heterogeneity decreases as the cumulative offset increases. This is a reasonable consequence of large cumulative slip wearing off the rough places on the fault phenomenon that would happen at all depths and not just at the surface. It is therefore reasonable that faults with large total offset would tend to systematically radiate high-frequency ground motion than faults with less total offset.

The Communication, Education and Outreach (CEO) Program

Jill Andrews

In collaboration with **Mark Benthien, John Marquis, and Bob de Groot**
Southern California Earthquake Center

From the beginning, SCEC scientific activities were strongly influenced by a series of timely, moderate earthquakes, in most cases damaging, that occurred from 1987 - 1999. Center leaders recognized the urgent need to communicate the results of their research with the multiple millions of citizens who live and work in this seismically active region (and other populous regions affected by earthquakes), and established in 1992 what is now the SCEC Communication, Education and Outreach (CEO) program. We represent over 150 leading earthquake scientists from more than 30 academic institutions (a total of 423 people make up today's SCEC community of researchers, including principal investigators, post-doctorals, graduate and undergraduate students). We enjoy working partnerships with more than 50 other earthquake science, engineering, education, and government organizations worldwide.

With ongoing expert advice from constituents and partners, SCEC leaders formed a CEO program mission that has evolved as Center activities matured: to increase earthquake awareness and knowledge so that people take actions that improve safety and reduce loss.

To fulfill this mission, SCEC leaders and CEO professionals emphasize the importance of programmatic flexibility as new communications tools, technologies and methods arise. We recognize that we must be responsive to change as research results emerge and understanding of earthquakes increases. Although we strive to maintain a cutting-edge approach, the basic program components remain constant: public awareness programs and products for media reporters and writers, civic groups and the general public; education programs and products for

students, educators, and working professionals; and knowledge transfer programs and products for technical professionals, scientists and engineers. We manage an array of activities based on the Center's scientific research results and processes. Products such as fact sheets, maps, posters, videos, working group reports, news briefs, public awareness brochures, educational modules and curricula, proceedings, consensus documents and databases are disseminated through mechanisms such as workshops, seminars, short courses, field trips, a web service, email list-services, print and electronic newsletters, museum exhibits, and media briefings and interviews.

We recognized early on that partnerships could greatly enhance our efforts. Our partners are individuals and organizations who co-sponsor, support, or otherwise aid in development and implementation of CEO activities and products. They have helped us bring together disparate groups (scientists, engineers, government officials, educators, the general public) to attempt to solve the very complex problems posed by our active faults. (A distinction should be made here, through our partnerships for knowledge transfer with agencies charged with producing official products that feature our scientific results, we conduct workshops that promote understanding and support of these items, such as official maps, databases, technical reports and documents.)

Our partners in academia, government, industry and education aid us in assessment, evaluation and follow through by participating in our advisory groups and providing cost-sharing and matching funds. They also provide us with the ability to reach larger audiences far beyond the borders of our study region. Since 1995, SCEC CEO professionals have been invited to conduct workshops and make presentations at earthquake science and engineering meetings throughout the United States as well as other countries such as Canada, Italy, New Zealand, China, Greece, and Japan. Earthquake researchers and CEO experts in many of these countries have based their public awareness, education and knowledge transfer programs on the SCEC CEO model. We recently learned that Istanbul, Turkey, with an at-risk population of more than 11 million, is creating an earthquake public awareness and education program that will be modeled on the SCEC CEO program.

Shake Table and Numerical Tests of Precarious Rock Models: Implications for Constraints on Response Spectra and Seismic Hazard

Rasool Anooshehpour and James N. Brune
University of Nevada, Reno

Strong motion data from Izmit, Turkey, and Chi-Chi, Taiwan earthquakes have pointed out the uncertainties in current strong motion attenuation curves for large earthquakes. Near-source strong motion data from these two earthquakes was considerably below the median for current attenuation curves. However, the data from these two earthquakes is consistent with constraints estimated from precarious rocks. Thus the recent evidence suggests that the attenuation curves assumed in the recent USGS-CDMG hazard maps give values which are too high at short distances, and thus may lead to serious overestimation of seismic hazard in some cases. In this study we use shake table experiment, as well as two-dimensional numerical modeling, to further quantify the precarious rock methodology for constraining ground motion attenuation curves and seismic hazard maps. We investigate the rocking response of 13 wooden rectangular blocks of various sizes and aspect ratios to realistic synthetic seismograms. The input motions consist of forty horizontal components of M7.9 synthetic accelerograms that were generated using the composite source model of Zeng et al. (1994). The recording station is located 15 km from the center of a 310-kilometer fault, analogous to Lovejoy Buttes (a precarious rock site near Palmdale, California) which is about the same distance from the Mojave section of the San Andreas fault. For each block the peak toppling ground acceleration (PGA) and the dynamic toppling accelerations at 0.2 sec, 0.3 sec, and 1.0 sec are calculated. At the time of meeting we will present results showing comparison of the precarious rock estimates of ground motion with those predicted by the USGS-CDMG hazard maps for 2%, and 10% probability of exceedence in 50 years.

A Reassessment of GPS Derived Coseismic Displacement Fields of the 1999 Hector Mine Earthquake

Kenneth E. Austin, M. Meghan Miller, and Daniel J. Johnson
Central Washington University

The fortuitous occurrence Hector Mine earthquake within a regional GPS network established during 1991 in Mojave Desert allows assessment of earthquake-related deformation and evaluation of the reference frame. Annual and earthquake-response campaign-mode GPS observations record active deformation in the Mojave Desert over the past decade. Data were analyzed using GIPSY point positioning in ITRF 97 combined with regional stabilization. The difference between ITRF96 and ITRF97 was significant in this region, particularly in the north component. We present a new displacement field for the Hector Mine earthquake. Well-established 1993-1999 velocities provide a robust constraint on pre-earthquake station positions. Rapid response to the Hector Mine event, including continuous observations at two GPS stations yields a robust co-seismic velocity field, and assessment of short term transient deformation. The co-seismic displacement field is compared to predictions from a geologically and seismologically constrained elastic dislocation model.

LARSE II: What Caused the Focusing Related Damage in Santa Monica During the Northridge Earthquake?

Shirley Baher and Paul Davis, University of California, Los Angeles
Gary Fuis, U.S. Geological Survey, Menlo Park
Rob Clayton, California Institute of Technology

The city of Santa Monica sustained concentrated damage from the anomalous amplification of seismic energy during the 1994 Northridge earthquake. Several hypotheses have been developed to explain the high amplitudes of ground motion. These include 1) focusing by a deep geological structure which acted like an acoustic lens, 2) a combination of focusing and shallow basin effects, 3) shallow (less than 1 km) basin edge effects involving constructive interference of surface and bodywaves. As part of LARSE (Los Angeles Region Seismic Survey) we conducted a high resolution seismic survey of Santa Monica to test the various hypotheses. The experiment took place in two parts: 1) a refraction survey in October 1999 which involved recording arrivals from shots and earthquakes (including Hector Mine) on ~200 sensor array, and 2) a 10 km Vibroseis reflection survey in June 2000 through Santa Monica and Pacific Palisades with vibes every 60 m and geophones every 30m. In addition to local shots to study the structure, two distant (4000lb) shots were detonated designed to reproduce the focusing of seismic energy that occurred during the Northridge Earthquake. The wave amplitudes of these shots along with Northridge aftershocks were examined to confirm the existence of focusing. Travel times of first p arrivals for shots and vibes have been used to obtain a 2D velocity structure. The velocity structure confirms existence of sub-basin in Santa Monica beneath the damage zone bounded to the north by the Santa Monica fault. The vibroseis experiment shows coherent reflections south of the Santa Monica fault related to sedimentary layers in the basin. We located the Santa Monica fault at depth about 1km north of the location of a surface trace that was previously mapped. We also located the unmapped Potrero Canyon fault using shots detonated in the Santa Monica Mountains.

Afterslip Models of Postseismic Deformation from the 1999 M7.1 Hector Mine Earthquake

Teresa Baker, Massachusetts Institute of Technology,
Susan Owen, University of Southern California

Following the October 16, 1999 M=7.1 Hector Mine earthquake there has been a focused effort by SCEC researchers to collect postseismic surface deformation data in the region surrounding the fault rupture. Using campaign and continuous GPS data collected by SCIGN, the USGS, USC, UCLA, UCSD and MIT, we calculated postseismic velocities at more than 50 sites. By measuring the postseismic deformation we can quantify the crustal response to the earthquake and model the distribution of afterslip on the fault at depth. This is important for understanding the mechanics of the lower crust and the postseismic period of the earthquake cycle.

The postseismic deformation field follows the expected pattern of continued right-lateral displacement. The highest velocities occur 20-40 km from the surface rupture and the velocities subsided significantly over a nine month period. The velocities decay rapidly in the first month following the earthquake and more slowly afterwards. Taking this into account, we have modeled the distribution of slip over three time periods. In the model, the fault extends from the surface rupture to 40 km depth and also extends 20 km beyond the ends of surface trace. This fault surface was then discretized into 2 km by 2 km squares, and we estimated the slip on each square, applying a smoothing constraint to regularize the slip distribution. While variations in data quality over these different time periods affect our model resolution, it appears that the region of maximum slip moves northeast along the fault over time.

High Resolution Imaging of the Geometry and Seismic Properties of the Karadere-Duzce Branch of the North Anatolian Fault at Depth

Yehuda Ben-Zion, **David Okaya**, and **Zhigang Peng**, University of Southern California
Andrew J. Michael, United States Geological Survey
Leonardo Seeber and **John G. Armbruster**, Lamont-Doherty Earth Observatory
Naside Ozer, The University of Istanbul, Istanbul
Serif Baris and **Mustafa Aktar**, Bogazici University, Istanbul

A week after the August 17, 1999, Mw7.4 earthquake on the North Anatolian Fault, we deployed a 10-station PASSCAL seismic network along and around the Karadere-Duzce branch of the fault, in a region where the surface rupture is in bedrock. The network straddles the eastern end of the August 17 rupture and the western end of the Mw7.1 event that occurred about 3 months later on November 12. In January-February 2000 we deployed 16 additional sensors in a "T" array along and normal to the fault for 14-19 days, before removing both arrays. Preliminary aftershock locations exhibit diffused patterns in a broad region between the north and south strands of the North Anatolian Fault, rather than in the immediate vicinity of the 1999 ruptures, pointing to a broad complex deformation on many secondary faults. Two weeks before the November 12 mainshock, seismicity increased in the region around our local fault network.

A major goal of the deployments was to provide a high resolution imaging of the fault zone structure at depth using waveform modeling of seismic fault zone guided waves. We identified in the data sets recorded by the initial and "T" arrays waveforms that may contain seismic phases that are trapped in a damaged low velocity rock around the surface rupture of the August event. The observations, however, are not very clear, probably due to structural complexity at the Karadere-Duzce branch of the fault. The candidate FZ waveforms are modeled with a genetic inversion algorithm (GIA) that maximizes the correlation between observed and synthetic waveforms [Michael and Ben-Zion, ms. in preparation]. The synthetic seismograms are

generated with a two-dimensional analytical solution for a scalar wavefield in a layered vertical fault zone between two quarter-spaces [Ben-Zion and Aki, BSSA, '90; Ben-Zion, JGR, '98].

Preliminary results suggest the presence of a damaged near-vertical fault zone layer close to, but not necessarily coincident with, the surface trace of the August Karadere-Duzce rupture. The model fault zone layer is characterized by a thickness of 75-100 m, a velocity decrease of about 30% relative to the surrounding rock, and an S-wave quality factor of about 30. The current results, however, have large uncertainties because of other mechanisms (e.g., shallow structure) that can produce similar waveforms, and trade-offs in model parameters. To overcome these difficulties we are developing now a multi-faceted analysis that combines seismic travel time tomography to provide regional information, array analysis techniques to determine the direction the wavefield comes from, simultaneous GIA modeling of multiple FZ waveforms, and analysis of additional signals (e.g., anisotropy, non-linearity) that may be indicative of damaged FZ rock at depth. Results from the combined analysis will be presented in the AGU meeting.

Validation of Airborne Laser Swath Mapping (ALSM) of the 1999 Hector Mine Earthquake Fault Zone

Adrian Borsa and Jean-Bernard Minster, University of California, San Diego
Ken Hudnut, United States Geological Survey, Pasadena
Craig Glennie, Aerotech, LLC

The fault zone encompassing the 1999 Hector Mine earthquake was mapped in April 2000 by a commercially-operated airborne scanning laser altimeter at extremely high resolution. Although the instrument was calibrated prior to flight, validating the data set postflight is the only way to confirm altimeter system performance throughout the experiment. Determining altimetry error sources and the repeatability of the altimeter measurements is important for generating accurate absolute topography, and even more crucial for determining change in topography from overflights separated by months or years.

We use three complementary approaches to validate the Hector Mine data set. First, the altimetry-derived topography is compared to "ground truth" measurements -- in this case topography derived from a combination of static GPS and photogrammetry over the open pit "Hector" mine (which was overflown for validation purposes) as well as mobile GPS surveys of several areas within the mine. The two topographic surfaces are matched in 3-D space using optimization techniques and any uncalibrated systematic errors are identified from the fit.

Next, repeatability statistics of the altimetry are determined by comparing multiple passes over the same ground. The perimeter of the Hector mine was flown several times in both directions to build up enough repeated measurements for a detailed comparison. In addition, the entire fault zone was overflown once in each direction, which yields many duplicated points along the flight path that can be examined for errors related to the location of the aircraft or temporal drift in the output of the altimeter system components.

Finally, data generated from a series of roll and pitch maneuvers over the dry Lavic Lake bed is analyzed for departure from the hypothetical plane to which the lake topography is expected to fit. This serves as a second independent method to validate the laser pointing accuracy.

Validation is essential to determining the error budget for the laser mapping process (with the benefit of providing calibration information that can be used to reprocess the raw altimeter data), and sets limits on the detection of temporal change in topography using laser altimetry -- an important consideration for mapping coseismic deformation or surface changes due to volcanism, erosion, and human activity.

The Relationship of Fault-Slip Rate to Fault Lengths

Richard Briggs and Steve Wesnousky
University of Nevada, Reno

The relationship between fault length and fault slip rate is explored by examining a global data set of continental faults for which geologically determined Holocene and Late Pleistocene slip rate have been published. Preliminary results indicate a tendency for slip rate to increase with fault length for strike-slip faults. This tendency is most apparent for fault lengths beyond 90-100km. No correlation between fault length and slip rate is observed for dip-slip (normal and reverse) faults.

A gross positive correlation of slip rate with fault length in strike-slip systems may reflect alignment of the slip vector with fault growth direction and the tendency for lateral strain to organize along discrete zones in the course of continual regional deformation. In contrast, the lack of correlation between slip rate and fault length in dip-slip systems may be attributed to a number of factors: (1) Slip vectors are perpendicular to fault growth direction; (2) Continued dip-slip on individual faults may be impeded by isostatic and gravitational forces, particularly in extensional environments, resulting in a more distributed fault system; and (3) Our analysis does not differentiate between dip-slip faults in extensional regions and those in strike-slip and thrust regions.

Ground Motions for Large Thrust, Strike-Slip and Normal Faults: Evidence from Physical and Numerical Models, Precariously Rocks and Shattered Rocks

James N. Brune
University of Nevada, Reno

Recent physical and numerical models of large thrust, strike-slip, and normal faults have indicated strong differences in ground motion between the hanging wall and footwall sides of the fault, and strong differences between fault types. However, the input parameters for modeling are too poorly known to allow confidence in the results, in large part because the strong motion database for near-fault ground motions for large earthquakes is too limited to constrain modeling parameters. The same limitations exist for non-modeling attempts to extrapolate the limited ground motion database to near-source large-earthquake ground motions. However, recent field evidence of various types has opened the possibility of independently constraining modeling and extrapolation parameters. The types of field evidence include objects thrown in the air, shattered rock, and precariously balanced rocks.

For thrust faults, on the near-fault (<several km) hanging wall, objects thrown in the air and the common existence of shattered rocks indicate the most intense ground motions. The field evidence, along with physical and numerical modeling, suggests inertial decoupling of the shallow hanging wall from the footwall, leading to failure of traditional dislocation theory and erroneous estimates of fault slip using teleseismic waves. Failure of the traditional equation relating fault slip to seismic moment may be a partial explanation for "tsunami earthquakes". On the other hand on the foot wall of some thrust faults the existence of precariously balanced rocks indicates relatively low ground motions.

For strike-slip faults the intensity of shaking appears to depend on whether or not there is a local component of tectonic normal stress. Where the shallow part of a strike-slip fault is locked by high tectonic normal stress the near-fault ground motions can be high, but for extensional strike-slip faults, where the shallow part of the fault is not locked by tectonic normal stresses, physical and numerical modeling, along with precarious rock evidence, indicates that the ground motions are relatively low.

For normal faults the tectonic stress is extensional and cannot lock the fault at shallow depths. This fact, and the geometry of the stress release, lead to very low near-fault ground

accelerations, especially on the foot wall. This result is supported by the existence of numerous precarious rocks on the foot wall of large normal fault earthquakes in Nevada and California.

The pattern of ground motion suggested by the field studies is generally similar to that indicated by the physical and numerical studies, depending on the parameters chosen for the models. The precarious rock evidence is in agreement with ground motion data from two recent earthquakes, the Izmit, Turkey, earthquake and the Chi-Chi, Taiwan, earthquake. However the combined field evidence does not support some recent published predictions of ground motions, which, for example, may be too low for the hanging wall of thrust faults, too high for the foot wall of normal faults, and too high for low probability motions. Further quantitative studies of precarious rocks can lead to critical control on parameters used in numerical models, and consequently a greatly improved understanding of the near-source seismic hazard from large earthquakes of all types.

Rupture Complexity of the 1999 Hector Mine, California, Earthquake

Ji Chen and Donald V. Helmberger, California Institute of Technology
David J. Wald, U.S. Geological Survey, Pasadena

We present a rupture model of the Hector Mine earthquake (M_s 7.1) determined from the joint inversion of strong motion records, P and SH teleseismic body waves, Global Positioning System (GPS) displacement vectors, and geological surface breaks. Our fault parameterization involves multiple fault segments, variable local slip, rake angle, rise time and rupture velocity. The inversion methodology combines a wavelet transform approach with a nonlinear (simulated annealing) algorithm. The final model is checked by forward simulating the Interferometric Satellite Aperture Radar data. Our estimation of the seismic moment is 6.28×10^{26} dyne-cm, which is comprised of three segments with 37% associated with the west branch of Lavic Lake fault, 41% with the east branch of Lavic Lake fault, and 22% with Bullion fault. Although the average slip is 1.5 m, the peak amplitude is as high as 7 m. The fault rupture has a long average rise time of 3.6 s and slow average rupture velocity of 1.9 km/s as averaged in the 14 s rupture propagation history. Our approach permits a large variation in rupture velocity and rise time, and indicates shorter rise times are associated primarily with the rupture of asperities. We also find evidence for nearly simultaneous rupture of two northern branches.

Comparing Mechanical and Geodetic Models of Los Angeles Basin Faults

Michele Cooke and Susan Murphy, University of Massachusetts, Amherst
Susan Owen, University of Southern California

Our knowledge of slip rates along Los Angeles faults is constrained to limited paleoseismic observations [e.g. Clark et al, 1984, McNeilan et al, 1996, Grant et al, 1997], and indirect fault modeling efforts [e.g. Davis et al, 1989; Shaw and Suppe, 1996, Cooke and Kameda, in prep]. Dip slip rates along buried faults in the Los Angeles Basin have been inferred from two dimensional kinematic reconstructions using geometric rules [Davis et al, 1989; Shaw & Suppe, 1996] and from two-dimensional forward models based on continuum mechanics [Cooke and Kameda, in prep]. Although the forward mechanical models show promising correlation with paleoseismic data in parts of the basin, other regions do not match observations indicating errors in the interpreted fault configuration. Additionally, these studies have not considered the important strike-slip component of deformation within this complex transpressional system. Additional data is needed in order to constrain three-dimensional fault configuration and slip rates; we are fortunate to have GPS data available for this purpose.

Our main goal is to better assess the hazards associated with buried faults within the Los Angeles basin. We present our work to date on estimating fault geometry and slip rates by

combining kinematic models of geodetic data from SCIGN with continuum mechanics models that evaluate mechanical efficiency. SCIGN data delineates deformation within the Los Angeles basin with unprecedented spatial resolution. However, even with this excellent data set, a fairly wide range of kinematic models will be consistent with the observed surface velocities [Johnson, 1995]. We will further constrain the set of plausible fault models by analyzing the distribution of work within particular fault system models, with the assumption that the most efficient model is potentially the most physically realistic. The continuum mechanics model will also be used to evaluate fault interactions and identify regions that are close to failure and may contain additional faults.

Seismic Sleuths 2001: Revision of a Tool of Scientific Literacy and a Renewal of Outreach Partnerships at the Southern California Earthquake Center

R. M. de Groot and K. E. van Rosendaal
Southern California Earthquake Center

Seismic Sleuths, an earthquake education curriculum for grades 7-12, was developed jointly by AGU and FEMA in 1995. In 1999, NSF funded a revision of the curriculum under the direction of the Southern California Earthquake Center (SCEC). Revisions will reflect advances in science and technology especially the use of geodesy in earth science. This effort will provide an innovative opportunity to improve earth science education in several domains. Instruction in the classroom generally centers on teaching the conclusions of scientific investigation. Seismic Sleuths 2001 will be a resource for a basic integrated approach to the study of seismic phenomena while being a doorway into current research and controversies in earth science. The curriculum will harness the power of the World Wide Web forming partnerships across academe, government, and industry in order to tap the multi-disciplinary nature of earth science. The primacy of relevance, so well demonstrated in the original curriculum, will be enhanced and expanded to include issues related to all hazards that face citizens in the United States. Seismic Sleuths 2001 will allow individuals to make sense of the world around them, take action to reduce risk, and use technology that is an integral part of their lives without eclipsing the science that comprises the backbone of the curriculum.

Paleoseismology of the San Andreas Fault at Plunge Creek, near San Bernardino, California

Safaa A. Dergham, California State University, Long Beach
Sally F. McGill, California State University, San Bernardino

Preliminary interpretation of relationships exposed in several trenches across the San Bernardino segment of the San Andreas fault near Plunge Creek suggests that the most recent earthquake on this portion of the fault may have occurred between 350 and 560 years ago (Dergham and McGill, 2000). Calibrated radiocarbon dates on detrital charcoal from Trench 8 appear to constrain a surficial faulting event to between A.D. 1411 and-1652 (2-sigma). The younger bound on the age of this earthquake is not firm because the detrital charcoal samples could overestimate the ages of the layers from which they were collected. This issue is discussed further below.

An earthquake of similar age (A.D. 1442-1643) was documented in trench 7 at this site (McGill and others, 1998). In trench 7, no younger events were visible, but neither could they be ruled out. In trench 8, the stratigraphy may preclude the occurrence of younger events. In trench 8 there are five dated samples that are older than AD 1652 (at the 2-sigma level) from layers that cap some of the faults, and there are no younger dates from within or below this stratigraphic

interval. The lack of clear stratigraphy immediately above the remaining fault strands prevents us from determining whether or not these strands rupture higher in the stratigraphic section. Nonetheless, the stratigraphically highest two of the five charcoal samples mentioned above are from layers that appear to cap all of the faults within the trench, and this is our basis for inferring that the most recent event occurred prior to about AD 1650, if the charcoal ages are taken at face value (see further discussion below). We are in the process of reviewing the stratigraphy of the trench to reinforce or disprove our initial interpretations of the stratigraphic bounds on the event horizon(s).

It is possible that younger earthquake(s) may have occurred if the rupture(s) were entirely limited to fault strands beyond the limits of trench 8. The north end of trench 8 stopped 2-3 meters south of the topographic break- in-slope at the base of the mountain front, in order to avoid damaging a major water pipeline. Our work in trench 6 and logs of four consultants trenches, all of which extended up to the mountain front, did not reveal a fault at the mountain front. The fact that no secondary fault strands or other deformation is apparent near the north end of trench 8 also leads us to suspect that any fault that may exist at the mountain front has not been active recently. We plan to test this hypothesis by excavating across the mountain front at a location where the pipeline lies several meters outboard of the mountain front, if permission is granted by the East Valley Water District.

We are also in the process of trying to evaluate how old the detrital charcoal samples may have been at the time they were deposited. The vegetation within the drainage basin of trench 8 consists of chaparral and coastal sage scrub. The chaparral in both southern California (where fire control is practiced) and in Baja California (where fire control is not practiced) burns 2-3 times per century (Minnich, 1983). Although some wood may survive on charred stumps for more than one fire cycle, it seems likely that the vast majority of the wood in the drainage basin that feeds trench 8 is probably no more than about 30-50 years old when it burns, and we expect that the majority of the charcoal deposited in trench 8 was not much older than this at the time it was deposited. We plan to test this hypothesis by dating charcoal from layers of known age, where possible, and by dating the oldest wood on existing shrubs within the drainage basins that feed the trench site.

In the meantime, it seems unlikely to us that any of the faults exposed in trench 8 ruptured in the 1812 earthquake. This interpretation would require both of the two samples from layers that cap all of the faults in Trench 8 to have been 180-190 years old at the time they were deposited. Even though the dates are not strictly consistent with interpreting the event in trenches 7 and 8 as the AD ~1680-1700 earthquake, which has been documented at Wrightwood and Pitman Canyon, this interpretation would not be unreasonable, given the possibility that the charcoal samples may be up to 30-50 years older than the layers in which they were deposited.

These interpretations are preliminary and may change as more samples from the trenches and from the drainage basin are dated. Four additional samples from trench 8 are pending.

Paleoseismologic Trench Results from the Eastern Sierra Madre Fault, Shuler Canyon Site, San Dimas, California: Implications for Age of Most Recent Event

James F. Dolan and Allan Z. Tucker
University of Southern California

The Sierra Madre fault is a major reverse fault that extends east-west for 75 km across the northern edge of the Los Angeles metropolitan region. The size and frequency of earthquakes on this fault system has been the subject of much recent debate within the SCEC community. Specifically, does the Sierra Madre fault typically rupture during infrequent, large-magnitude events (Mw 7-7.5?), as suggested by paleoseismologic evidence from the central (Rubin et al., 1998) and eastern (Tucker and Dolan, in review) reaches of the fault? Or does it commonly rupture in much smaller, more frequent events similar to the 1971 Mw 6.7 San Fernando event?

As part of SCEC's ongoing efforts to address these questions, during May 2000 we excavated a 30-m-long, 5-m-deep trench across the main active strand of the eastern Sierra Madre fault at the mouth of Shuler Canyon, in San Dimas, California. This site is located ~1 km west of our 1998 trench site, which yielded evidence for a >8,000-year-long quiescent period since the most recent surface rupture on the eastern part of the fault. Our 2000 trench exposed three gently north-dipping ($\leq 15^\circ$ N) fault strands that have thrust colluvium and highly fractured Miocene-aged Puente Formation mudstone over a buried A horizon and underlying alluvial strata. Total brittle fault slip on the lowest of the three main fault strands exposed in the trench measures ~90 cm, whereas the 3-4 m of slip on the upper two fault strands is expressed at the paleo-ground surface as folding of a colluvial gravel bed. Thus, ~75% of the total 4-5 m of displacement that reached the surface at this site during the most recent event(s) is expressed as folding, rather than brittle fault slip. This is similar to many observations from the surface rupture of the 1999 Chi-Chi, Taiwan, earthquake. It is not clear whether thrust displacement observed at the Shuler Canyon site occurred during more than one event. If all of this displacement occurred during a single event, it would suggest that the most recent surface rupture on the eastern Sierra Madre fault was of large magnitude ($M_w \geq 7$). Accelerator Mass Spectrometer (AMS) ^{14}C dates on 10 samples of detrital charcoal (pending) will help constrain the age(s) of the most recent surface rupture(s).

The Source Process of the Hector Mine, 1999 Earthquake ($M_w 7.2$) and Use of Finite Source Models in Automated Near-Fault Strong Ground Motion Prediction

D. Dreger, A. Kaverina, and E. Price
University of California, Berkeley

We investigate the finite source process of the October 16, 1999 Hector Mine earthquake in the context of a 3-segment, multiple time window fault model by simultaneous inversion of seismic and geodetic data. The earthquake is located only 20 km east-northeast of the Landers - Emerson - Camp Rock fault system which ruptured in the Landers, 1992 event. Similarly to the Landers event, the Hector Mine earthquake had a slow rupture initiation and ruptured a complex system of faults. The constrained, non-negative least-square inversion of the data from 6 broadband stations at regional and local distances revealed that the time history of the earthquake is complicated and indicates a slow rupture process with a variable dislocation rise time, which can be on the order of 7 seconds. The results indicate that the event is bilateral and that the majority of slip is located close to the hypocenter. The overall dimensions of the rupture extend from 15 km NW of the epicenter to approximately 20 km to the SE giving a total length of 35 km. The peak slip was found to be about 8.5 m; the total seismic moment of 8.2×10^{19} Nm yields a M_w of 7.2. We tested a possible northeast coseismic bifurcation of rupture suggested by aftershock locations, however we found that the data do not require any appreciable slip on the fault located east of the Lavi Lake fault. Our seismically derived slip model correlates well with the post-Landers Coulomb stress change (Parsons and Dreger, 2000), and agrees with static slip distributions inferred from radar interferometry. These results, a new slip model derived by simultaneous inversion of seismic and InSar data, and the use of automated finite-fault information for near-fault ground motion prediction will be presented.

Applications of Ground Penetrating Radar to Imaging Faults

D. Eason and R. Clayton
California Institute of Technology

We have applied a Ground Penetrating Radar (GPR) system to the problem of imaging subsurface faults. The goal is to image not only the faults themselves but also candidate piercing point features that could indicate the amount of strike-slip offset. The technique has the potential to extend direct fault measurement determined by trenching.

We applied the method to the Simi Fault that was trenched by Hitchcock, Weaver, Helmswall and Lindvall in June, 2000. Our cross-fault lines show the thrust fault that was mapped in the trench. Our parallel lines show a possible buried channel that has 4m of left-lateral displacement. We have also applied GPR to thrust faults on the north side of the San Bernardino Mtns and to normal faults near Mono Lake.

RELM - A Working Group for the Development of Regional Earthquake Likelihood Models

Edward H Field
U.S. Geological Survey, Pasadena
(<http://www.scec.org/research/RELM>)

SCEC's Phase II report (WGCEP, 1995) represented the first large-scale effort to integrate seismic, geodetic, and geologic constraints into a complete probabilistic seismic hazard analysis (PSHA) source model. However, the model predicted that magnitude 6 to 7 earthquakes will occur about twice as often as they have historically, which led to a widely publicized debate on whether the apparent deficit was real, an artifact of the limiting magnitude implied by fault size, or simply a reflection of uncertainties (Jackson, 1996; Hough, 1996; Schwartz, 1996; Stirling and Wesnousky, 1997; Stein and Hanks, 1998; Field et al., 1999). A similar discrepancy exists for the USGS/CDMG statewide hazard maps (Petersen et al., 1996).

An alternative, mutually consistent source model has since been put forth by Field et al. (1999), which appears to solve the problem in that neither $M > 8$ earthquakes, nor an accelerated earthquake rate, are required to satisfy available data. However, neither phenomenon can be ruled out either. For example, time-dependent recurrence models generally predict a rate acceleration because most faults are deemed overdue. In addition, some models allow a finite probability of $M \sim 8.5$ earthquakes (Kagan, 1999). Because these models cannot be excluded, it behooves us to evaluate their implications for seismic hazard.

To this end, a joint SCEC-USGS sponsored working group for the development of Regional Earthquake Likelihood Models (RELM) has been established. The goals are as follows: 1). To develop and test a range of viable earthquake-potential models for southern California (not just one "consensus" model; 2). To examine and compare the implications of each model with respect to probabilistic seismic hazard analysis. This will not only define existing uncertainties in seismic hazard, but will also identify what research topics should be targeted in order to reduce these uncertainties; 3). To test these models for consistency with existing geophysical data (e.g., historical seismicity), and to design and document conclusive tests with respect to future observations. An important part of the effort will involve updating and documenting the geological fault database, the earthquake catalog, and the geodetic strain-rate map. We are also contemplating the development of object-oriented PSHA code that will lend itself to web-based applications and tutorials.

Accounting for Site Effects in Probabilistic Seismic Hazard Analyses of Southern California: Overview of the SCEC Phase III Report

Edward H Field and the Phase-III Working Group
U.S. Geological Survey, Pasadena

This poster presents an overview of the Southern California Earthquake Center (SCEC) Phase III effort to determine the extent to which probabilistic seismic hazard analysis (PSHA) can be improved by accounting for site effects. The contributions made in this effort are represented in the various papers that compose a special issue of BSSA.

Given the somewhat arbitrary nature of the site effect distinction, it must be carefully defined in any given context. With respect to PSHA, we define the site effect as the response, relative to an attenuation relationship, averaged over all damaging earthquakes in the region. A diligent effort has been made to identify any attributes that predispose a site to greater or lower levels of shaking. The most detailed maps of Quaternary geology are not found to be helpful - either they are overly detailed in terms of distinguishing different amplification factors, or present southern California strong-motion observations are inadequate to reveal their superiority. A map based on the average shear-wave velocity in the upper 30 meters, however, is found to delineate significantly different amplification factors. A correlation of amplification with basin depth is also found to be significant, implying up to a factor of two difference between the shallowest and deepest parts of the Los Angeles basin. In fact, for peak acceleration the basin-depth correction is more influential than accounting for the 30-meter shear-wave velocity. Questions remain, however, as to whether basin depth is a proxy for some other site attribute.

In spite of these significant and important site effects, the standard deviation of an attenuation relationship (the prediction error) is not significantly reduced by making such corrections. That is, given the influence of basin edge induced waves, subsurface focusing, and scattering in general, any model that attempts to predict ground motion with only a few parameters will have a significant intrinsic variability. Our best hope for reducing such uncertainties is via waveform modeling based on first principals of physics.

Finally, questions remain with respect to the overall reliability of attenuation relationships at large magnitudes and short distances. Current discrepancies between viable models produce up to a factor of 3 difference among predicted ten-percent in 50-year exceedance levels, part of which results from the uncertain influence of sediment nonlinearity.

The Gutenberg-Richter Distribution: From the Inside Out

S. A. Fontaine and Steve Wesnousky
University of Nevada, Reno

We combine paleoseismic data with the NCSN and CIT-USGS earthquake catalogs to examine the physical processes that result in broad regions of seismicity satisfying the Gutenberg-Richter magnitude-frequency relationship. Magnitude-frequency plots are constructed for both the northern and southern portions of the San Andreas fault, starting with 20x20 km polygons at the center of each fault section and incrementally increasing the length of the polygons along strike to encompass the entire fault. The same initial 20x20 km polygons are then increased both along and perpendicular to fault strike. Along the southern San Andreas fault, the magnitude-frequency distribution for a volume of crust 20 km wide and 500 km long along strike has a characteristic earthquake shape, while increasing the width to just 100 km (a 100x100 km polygon) yields a distribution with a Gutenberg-Richter shape. The 100x100 km polygon includes seismicity from the 1952 Kern County, 1971 San Fernando, and 1994 Northridge earthquakes. Along the northern San Andreas, the magnitude-frequency distributions for volumes of crust with 20 km width and increasing lengths show a characteristic earthquake shape

until the aftershocks from the 1989 Loma Prieta earthquake are included, after which, the distribution has a Gutenberg-Richter form. Incrementally increasing the width as well as the length of the original polygon to 140x140 km yields a magnitude-frequency distribution with a Gutenberg-Richter shape. The 140x140 km polygon includes seismicity along the Rodgers Creek, Concord, Green Valley, Hayward, Calaveras, and Grenville faults. In both cases, plotting the seismicity associated with only the San Andreas fault results in a magnitude-frequency distribution with a characteristic earthquake shape. The transition from characteristic earthquake to Gutenberg-Richter is thus directly attributed to seismicity from specific off-fault sources. Our observations imply that either, 1) the Gutenberg-Richter relationship between earthquake size and frequency is satisfied only when seismicity from multiple sources is considered or 2) if the magnitude-frequency distribution for an individual fault is Gutenberg-Richter in shape, then the seismicity associated with the fault is not evenly distributed in time throughout the seismic cycle of the fault.

Upper Crustal Structure and Tectonics along the LARSE Transects, Southern California

G. S. Fuis, J. M. Murphy, and V. E. Langenheim, U.S. Geological Survey, Menlo Park
T. Ryberg, GeoForschungsZentrum, Potsdam, Germany
N. J. Godfrey and D. A. Okaya, University of Southern California
W. J. Lutter, University of Wisconsin, Madison

The Los Angeles Region Seismic Experiment (LARSE) consists of two transects (Lines 1 and 2) which are approximately centered on the San Andreas fault in southern California. The goal of these two transects is establish sedimentary basin depths and structure and interconnection of faults, in order to better assess earthquake hazards in southern California. Airgun, explosion, and earthquake data were collected onshore on these transects, and are discussed here; airgun data only were collected offshore. Line 1 (1994, 160 km long) crosses the Los Angeles basin, central Transverse Ranges (San Gabriel Mountains), and Mojave Desert; Line 2 (1999, 150 km long) crosses the Santa Monica Mts, San Fernando Valley, Santa Susana Mts, central Transverse Ranges (Sierra Pelona and Liebre Mountain blocks), and western Mojave Desert. Along both transects, the San Andreas fault is located at or near the geographic boundary between the central Transverse Ranges and the Mojave Desert. Chief crustal-structure results from Line 1 are as follows: (1) In the upper 20 km of crust, the current San Andreas fault separates low-velocity rocks (5.8-6.0 km/s--chiefly Pelona Schist) on the south from low- to intermediate-velocity rocks (5.5 -6.3 km/s--chiefly batholithic and metamorphic rocks) on the north. (2) Beneath the San Gabriel Mountains, at 20-km depth, a sequence of subhorizontal bright reflectors terminates 3 km north of the surface trace of the San Andreas fault, leading us to infer an average northward dip for the San Andreas fault of over 80 degrees. A sequence of reflectors is also seen at approximately the same depth (20 km) in the southern Mojave Desert, but these reflectors are unconnected to the reflectors in the San Gabriel Mountains. (3) A thin (500-m) layer of anomalously low velocity rock (4 to 4.5 km/s) is seen between two of the reflectors in the San Gabriel Mountains, leading us to infer the presence of fluid-filled cracks in the mid-crust. (4) In the lower crust, below 20-km depth, the San Andreas fault is poorly defined in our data but appears to separate higher velocity rocks on the south (~6.5 km/s) from lower-velocity rocks on the north (~6.3 km/s). (5) The Moho is depressed by about 7 km (to 35-km depth) in a 40-km-wide region centered on the San Andreas fault.

Chief tectonic interpretations from Line 1 are as follows: (1) The geometry of the bright reflections beneath the San Gabriel Mountains suggests they are linked to a master decollement that extends from the San Andreas fault southward to the hypocenter of the 1987 M 5.9 Whittier Narrows earthquake, and perhaps even farther south. A symmetrical decollement is interpreted in the southern Mojave Desert. (2) The Sierra Madre fault and the Puente Hills blind thrust fault of Shaw and Shearer (1999) appear to sole into the decollement beneath the San Gabriel

Mountains. (3) From our above inference of fluid-filled cracks in the mid-crust of the San Gabriel Mountains, we further interpret that the decollement here is lubricated by fluids. (4) We have constructed a tectonic model in which the brittle upper crust and ductile lower crust are approximately separated by the decollements in the San Gabriel Mountains and Mojave Desert. In response to a large component of compression across the San Andreas fault, the brittle upper crust imbricates along reverse and thrust faults, and the ductile lower crust flows toward the San Andreas fault, from both north and south directions, creating a crustal root centered beneath the trace of the San Andreas fault.

Preliminary velocity-modeling results from Line 2 indicate the following: (1) The San Andreas fault is a steeply dipping structure that separates upper-crustal blocks having low velocities on the south and intermediate velocities on the north, similar to results from Line 1. (2) The thickness of sedimentary rocks in the vicinity of the Santa Susana Mts (eastern Ventura basin) may reach 7- to 8-km depth. (3) A moderately north-dipping low-velocity zone is observed in the upper crust beneath the Santa Susana Mts, and a similar but fainter such zone may be present in the Santa Monica Mts. Preliminary reflectivity results for the middle and lower crust indicate the following: (1) A moderately north-dipping zone of reflectivity is seen from the beneath the north edge of the eastern Ventura (near the San Gabriel fault) to the base of the crust at the San Andreas fault. This zone projects upward toward the low-velocity zone described above beneath the Santa Susana Mountains and may represent a major crustal fault zone. (2) A reflector is seen dipping gently to moderately southward beneath the Santa Monica Mts from the vicinity of the Northridge hypocenter.

Lower-Crustal Structure, Tectonics and Gravity Modeling Along the LARSE Transects, Southern California

Nicola Godfrey and David Okaya, University of Southern California
Gary Fuis and Janice Murphy, United States Geological Survey, Menlo Park
Rob Clayton, California Institute of Technology
Trond Ryberg, GeoForschungsZentrum, Potsdam
Bill Lutter, University of Wisconsin, Madison
Gerry Simila, California State University, Northridge

Combination of all data from the 1994 and 1999 LARSE active-source experiments produce two transects which image crustal structure under the Los Angeles region. We present P-wave velocity models derived from land explosion, onshore-offshore refraction/wide-angle reflection, ocean bottom seismometer (OBS) refraction/reflection, and vertical-incidence airgun reflection profiles.

Transect I is 270- km long and extends from San Clemente Island to the Mojave Desert, crossing the Continental Borderlands, the Los Angeles and San Gabriel basins, the San Gabriel Mts and San Andreas fault. This transect was collected in 1994.

Transect II, west of Line 1, is 300-km long and traverses the Continental Borderlands, the Santa Monica Mts, the San Fernando Valley basin (1994 M 6.7 Northridge epicenter), the San Andreas fault and the Mojave Desert, terminating at the Garlock fault/Tehachapi Mts. This transect was begun in 1994 but completed in October 1999 with the USGS-SCEC Northridge-to-Mojave land explosion profile. Data merging of the 1999 data was completed in Summer 2000; preliminary analyses have only recently commenced.

High resolution seismic tomography methods have been applied to the onshore upper crust using the 1994 and 1999 land explosion data - see adjacent poster for results. These shallow results along with shallow crust results for the continental Borderlands from OBS tomography (ten Brink et al., 2000) can be used to constrain the tomographic inversion of the deeper crustal structure.

Along Transect I, the Mojave Desert crust north of the San Andreas fault has a low-velocity (6.3 km/s) mid- and lower crust and 28-km-deep Moho. South of the San Andreas fault,

beneath the Los Angeles and San Gabriel Valley basins, there is a fast (6.6 – 6.8 km/s), thick (10-12 km) lower crust with a 27-km-deep Moho. Further south still, the lower crust of the Continental Borderland is fast (6.6 – 6.8 km/s) and thin (5 km) with a shallow (22-km-deep) Moho.

Tomographic reconstruction of the deep structure along Transect II combining the 1994 and 1999 data has recently begun. Crustal thickness in the continental Borderlands west of San Clemente and Santa Catalina is similar to that seen along Transect I (~22 km). Gentle deepening of the crust begins north of Santa Catalina and extends to under the northern San Gabriel Mts at a depth of 35+ km. Mojave crustal thickness is approximately 28-30 km based on nearby industry seismic reflection profiles.

There is an 8-km-thick crustal root centered beneath the surface trace of the San Andreas fault, north of the highest topography in the southern San Gabriel Mtns. A simple mass-balance calculation suggests ~36 km of north-south shortening across the San Andreas fault in the central Transverse Ranges could have formed this root. If north-south compression began at 2 - 5 Ma (either when the 'Big Bend' in the San Andreas ft formed or when the Transverse Ranges formed), 36 km of shortening implies a north-south contraction rate of 7 - 18 mm/year across the central Transverse Ranges.

Is the Salton Sink Still Sinking? First Order Leveling, GPS and Other Observations

J. Javier Gonzalez-García and J. Alejandro Gonzalez-Ortega,
CICESE, Ensenada

The Salton Trough is a physiographic province in the contact between the Pacific and North American plates at the international border between USA and México. It is the NW continuation of the en echelon transforms and spreading centers in the Gulf of California and includes (at least) two small segments of crustal extension (Brawley and Cerro Prieto).

In order to look for current deformation, we compare leveling data obtained by Dirección de Estudios del Territorio Nacional and Comisión Federal de Electricidad (DETENAL/CFE) in Mexicali Valley during 1977-1979, with recent GPS observations obtained near the Cerro Prieto Geothermal Field (CPGF) made during 1993-1997. We also use observations obtained by the USGS in the Imperial Valley.

The USGS reports 3.5 cm/yr subsidence, measured by three first order leveling surveys over 1972-1977, for the SE part of the current Salton Sea, i.e. the SE end of the San Andreas Fault. For this region, campaign mode GPS observations (STRC), indicate horizontal strain with NW slip accounting for 70-80% of the strain predicted by the NUVEL-1A model for the motion between the Pacific and North American plates.

Besides detecting the ground subsidence around CPGF, the three Mexicali Valley leveling surveys record coseismic vertical motion caused by the Imperial, October 15, 1979, earthquake. A maximum vertical slip of 11.5 cm occurred in the central part of the Imperial fault, at the Mexico/USA border. There is evidence of ~1 cm uplift of the region between the Cerro Prieto Volcano and the SE end of the Cucapah Ranges, where we have identified a left lateral fault, here named the Puente-Cruz Fault.

Moreover, the differential motions caused by the Imperial earthquake, allow speculation about the existence of a branch of the Cerro Prieto Fault, which joins with the Imperial Fault. We designate this probable feature as the Yarzalonso Fault with a N 28°E strike and 16 km length. This fault would be the counterpart of the San Adrian Fault (González-García, 1998) which joins the Imperial and the Cerro Prieto Faults with a S 27°W strike.

The GPS results for 1993-1997 show a clear subsidence zone between the Imperial and Cerro Prieto Faults. Vertical deformation rates near the Imperial and Cerro Prieto faults are 11 cm/yr and 4 cm/yr respectively. 60% of this deformation is induced by aquifer depletion and about 40% is tectonic.

Because of its similar tectonic setting, the SE end of the SAF (Salton Sink) may experience likeness deformation. The tectonic horizontal (GPS) and vertical (leveling) motions are of the same order of magnitude in these zones of critical deformation within the Salton Trough Basin. Preliminary results from 3 SCIGN sites in this region confirm this hypothesis.

Gonzalez-García, J. J., Mapa Sismo y Neo-tectonic del Valle de Mexicali. Abstract in Primera Reunión Nacional de Ciencias de la Tierra, September 21-25, 1998, p. 105, Fac. de Ciencias, UNAM, México, D. F.

Characterization of the Most Recent Earthquake And Uplift Of The San Joaquin Hills, Southern Los Angeles Basin

Lisa B. Grant and Leslie J. Ballenger
University of California, Irvine

The historic record of earthquakes in California begins in 1769 with an account by Spanish explorers of a strong temblor in the southern Los Angeles basin. Since then, the largest known earthquakes in the Los Angeles (LA) basin were the destructive but moderate-size Long Beach (M 6.3), San Fernando (M 6.7) and Northridge (M 6.7) earthquakes in 1933, 1971 and 1994. A significantly larger earthquake may have occurred in the San Joaquin hills, southern LA basin, just prior to or during the early historic period. We have mapped, measured and dated late Holocene shorelines and marsh deposits that are above the active shoreline or marsh at 20 sites around the coastal margin of the San Joaquin Hills and upper Newport Bay. The paleo-shorelines are 1.6 m (average of 60 measurements) above the active shoreline. Several measurements exceed 3 m along the rocky coastline between Laguna Beach and Dana Point, with a maximum of 3.6 m. The average elevation is greater along the open coast between Corona Del Mar and Dana Point (1.8 m from 39 measurements at 13 sites) than in Newport Bay. The elevated shorelines and emergent marsh deposits are best explained by tectonic uplift of the San Joaquin Hills. Radiocarbon dating of plant material and a shell from an elevated "marsh bench" in Newport Bay indicate that emergence occurred sometime after 1635 A.D. Assuming the uplift occurred in a single earthquake, the magnitude can be estimated from empirical relationships of Wells and Coppersmith (1994) with correction factors for application to paleoseismic data (Hemphill-Haley and Weldon, 1999). The estimated magnitude (M) is 7.0-7.3 from average uplift of 1.6 m. Average slip on the fault would be greater than uplift at the surface. Therefore, the magnitude may be underestimated.

Observed Basin Response and 3D Ground Motion Simulations for the 1999 Hector Mine Earthquake

Robert W. Graves and Arben Pitarka, URS Corporation, Pasadena
David J. Wald, United States Geological Survey, Pasadena

The 1999 Hector Mine earthquake is the largest event to be recorded on the recently installed TriNet strong motion system. The availability of high dynamic range digital recordings throughout the Los Angeles metropolitan region allows for an unprecedented analysis of source, wave propagation, and basin response effects during a major earthquake. The earthquake rupture occurred over three main fault segments about 150 km east of Los Angeles. As the waves propagated westward into the San Bernardino and Los Angeles basins, significant amplification of the motions occurred. Relative to sites adjacent to the basins, peak ground velocities and displacements were 2 to 4 times higher for sites within the basins. The basin amplification was strongest at longer periods (5 - 10 sec), due partially to the strong source radiation at these periods, but also suggesting a preferential mechanism for the trapping of basin generated surface

wave energy at these periods. To better understand the effects of basin geology on ground motion response in the San Bernardino basin during this event, we have performed finite difference simulations utilizing complex 3D structural models. The calculations are limited to periods longer than 2 seconds and incorporate the variable slip finite-fault rupture model of Ji et al. (www-socal.wr.usgs.gov/slipmodels.html). Using this source model not only allows us to accurately model the near source ground motions, but also ensures that the energy propagating into the basins is modeled accurately as well. We use the Version 1 SCEC 3D Seismic Velocity Model as the starting point for the simulations. This model predicts significant amplification for the basin sites and qualitatively matches the observed pattern of amplification. However, the model overpredicts the amplification for sites in the northern San Bernardino basin by about a factor of two. Based on well data and preliminary USGS seismic reflection profiling, we have modified the SCEC V1 model to have a shallower basin depth along the northeastern basin margin and to also have a gentle basement dip toward the southwest. This modified structural model produces a significantly better match to the observed ground motion response. These results demonstrate the utility of using recorded ground motion data to refine and validate 3D structural models.

New Methods of Accessing Waveform Data from the Data Center

Katrin Hafner and Robert W. Clayton
California Institute of Technology

In the past year, the Data Center has been working closely with the TriNet Seismic System to develop new types of waveform data archives, particularly for the newly installed digital broadband stations. In addition to the traditional event triggered waveforms, the Data Center has been archiving continuous waveforms (20 sps and less) since October of 1999. In response to these new data types, we have developed a number of new interfaces to waveform data. These include implementation of the BREQ_FAST e-mail and WWW waveform request system used by the IRIS DMC and the NCEDC. This interface allows users to retrieve SEED volumes of broadband data based on net, station, channel and time requests.

In addition the Data Center has focused on developing web interfaces to the triggered waveform archives of the TriNet system. These include "EQUEST", which allows users to retrieve precompiled waveform data sets for large earthquakes in Southern California, e.g. for the Hector Mine earthquake. These data sets include triggered waveforms in SAC binary, I*4 binary, and SEED volume formats. Users can download these data directly via an Internet browser, or download a Java tool to run the application remotely.

The Data Center has also developed a "seismogram transfer program" called "stp", that can copy seismograms from the continuous or triggered archive directly to the user disk in a manner similar to 'ftp'. The user portion of this interface is available as a download from the Data Center. It is written in C and can currently be compiled and run on SunOS and Linux platforms. Waveforms that are returned are in SAC format with instrument gains removed and necessary byte-swapping done. An example of its usage is

```
stp scedc      (connect to the Data Center waveform server)
STP> help     (get a listing of help topics)
STP> sac      (output will be converted to SAC format)
STP> WIN CI PAS BHZ 2000/05/16,13:15:16 2000/05/16,14:25:14.3
              (get a window of data from CI.PAS.BHZ)
STP> TRIG 9501793
              (get the seismograms for event 9501793)
STP> quit
```

This example transfers to the user's disk one seismogram for the PAS station from the continuous archive, and six seismograms from the triggered archive. A web version of this interface is under construction.

All of these waveform interfaces will be demonstrated at the meeting.

The Crustal Stress Field in Southern California

Jeanne Hardebeck, University of California, San Diego
Egill Hauksson, California Institute of Technology

We determine stress orientations in the crust in southern California, and make an order of magnitude estimate of the deviatoric stress magnitude at seismogenic depths. A high resolution image of the orientations of the principal stress axes at seismogenic depths is found from the inversion of earthquake focal mechanisms. Approximately 50,000 events recorded by the SCSN from 1981 to 1999 were relocated using the 3D velocity model of Hauksson [2000], and focal mechanisms were found using FPFIT [Reasenber and Oppenheimer,1985]. Earthquakes were grouped spatially in bins with 5 km to 20 km radius, and inverted for stress orientation using the method of Michael [1984, 1987]. The stress field appears to be highly spatially heterogeneous, with variations related to differences between geologic provinces, fault complexity, and major earthquakes. The 1992 Landers earthquake appears to have rotated the local stress axes by approximately 20 degrees. This rotation can be used to estimate the magnitude of the deviatoric stress because it is controlled by the ratio of the magnitude of the stress change caused by the earthquake to the magnitude of the deviatoric stress. The results of a 2D analytic solution imply that the deviatoric stress magnitude in the vicinity of Landers is on the order of 100 bar.

The 1999 Izmit, Turkey Earthquake - A Test of the Dynamic Stress Transfer Model for Intra-Earthquake Triggering

Ruth A. Harris, U.S. Geological Survey, Menlo Park
James F. Dolan and **Ross Hartleb**, University of Southern California
Steven M. Day, San Diego State University

Before the 1999 Izmit earthquake theoretical studies of earthquake ruptures and geological observations had estimated how far an earthquake might jump laterally to get to a neighboring fault. Both numerical simulations and geological observations suggested that 5 km might be the upper limit of such a jump if there were not any transfer faults. The 1999 Izmit earthquake appears to have followed these expectations. It did not jump across any stepover wider than 5 km and was stopped by a wide stepover at its eastern end. Records of surface slip show a small amount of slip just beyond the eastern stepover. This observation is consistent with one class of numerical models whereby a rupture has enough energy to just make it across a stepover, but not enough energy to continue propagating on the other side of the step. An interesting feature of the Izmit earthquake is that a 5-km along strike surface gap followed by a 25 degree restraining bend in the fault zone did not stop the earthquake.

Seismotectonics of the 1999 Mw7.1 Hector Mine Earthquake Sequence, Southern California

Egill Hauksson and Kate Hutton, California Institute of Technology,
Lucile M. Jones, U.S. Geological Survey, Pasadena

We synthesize and interpret the seismological observations from the 1999 Mw7.1 Hector Mine earthquake sequence, including occurrence of the foreshock sequence, spatial and temporal distribution of aftershocks, state of stress inferred from focal mechanisms. We relocate the sequence and determine 5 km horizontal and 4 km vertical grid Vp and Vp/Vs models. We use these models to determine refined first motion focal mechanisms and use coulomb stress modeling of the mainshock to explain the spatial distribution of the aftershocks.

The Hector Mine mainshock that was preceded within 24 hours by small foreshocks of $M \leq 3.8$ at the focal depths of the mainshock, showed right-lateral strike-slip faulting, with an initial strike of N6°W on an almost vertical fault. The Hector Mine earthquake ruptured mostly to the south for a distance of 15 km and rotating its strike to the south-southeast for an additional 10 km distance. The Hector Mine mainshock also had an unusual additional rupture segment, extending from about 5 km south of the hypocenter, to the north-northwest for a distance of 20 km, thus forming a trilateral rupture zone. The aftershocks delineate the entire rupture zone. The Hector Mine aftershocks form an asymmetric spatial distribution, where the aftershocks do not center on the main surface break with most of the aftershock occurring to the east and north of the surface rupture. Several pockets of high aftershock activity have persisted, near bends in the fault rupture, near the northernmost end of the rupture, and one approximately 10 km further to the north. The 1992 Mw7.3 Landers and Mw7.1 Hector Mine mainshocks occurred near the southernmost extent of the Eastern California Shear Zone, an 80 km-wide, more than 400 km-long zone of deformation. This zone extends into the Death Valley region and accommodates about 10 to 20% of the plate motion between the Pacific and North American Plates. These earthquake sequences illuminate the slip transfer zone between the ECSZ to the southern San Andreas fault.

Collaborative Paleoseismic Investigations After the Hector Mine Earthquake

Hector Mine Geologic Working group

(Funded by SCEC through Tom Rockwell, Scott Lindvall, Charlie Rubin)

The 1999 Hector Mine earthquake presented an excellent and important opportunity to showcase cooperative efforts between SCEC, USGS and CDMG scientists. Following the earthquake, the Hector Mine Geological Working Group, composed of near 50 geologists and over half of which are from SCEC institutions, mapped the surface rupture and surveyed offset geomorphic and cultural features. During this phase, a number of promising paleoseismic sites were identified that should yield recurrence information on the Lavic Lake fault, a previously unnamed minor fault of the Eastern California Shear Zone which was the source for October's earthquake.

As a continuation of this collaborative effort, SCEC and USGS geologists initiated a paleoseismic program this past year to establish the timing of past events on a number of faults on the 29 Palms Marine base. Four sites were included in this study this past year: two along the Lavic Lake fault, one along the Bullion fault, and one along the Mesquite Lake fault. The occurrence of the earthquake on the Marine base resulted in unprecedented access to some of the most important and least studied faults of the Eastern California shear zone, and outstanding cooperation between the Marines and the scientific community. For each site, a SCEC or USGS scientist generally took the lead during the trenching phase, and Tom Rockwell (SCEC) and Dave Schwartz (USGS) provided overall review of trenches.

The Drainage Divide site was chosen because of geomorphic evidence for a prior event along a ~1 km-long section of the fault. This is also the region where maximum slip was reported after the earthquake. We excavated six trenches, and clear stratigraphic and structural evidence was found in several of these trenches for the prior event. Scott Lindvall took the lead on this site and was joined by up to nine SCEC and USGS scientists. No charcoal was found in any of the trenches so we relied on surface exposure dating techniques and correlation of surface and subsurface deposits. Dates are pending but current thought is that the penultimate surface rupture may be as many as several tens of thousands of years ago based on the degree of soil development in the affected alluvial deposits.

Two trenches were excavated at the Bullion Fan site, where only minor cracking and perhaps a couple of cms of strike-slip was observed after the earthquake. One of the major questions to be addressed is whether the Bullion fault had recently failed, as suggested by the geomorphology. TL dates on faulted alluvium place this event at less than about 1 ka in age, similar to most other faults in the Eastern California Shear Zone, and indicate that this fault has also been involved in the cluster of recent earthquakes in the Mojave. Tim Dawson, Heidi Stenner and Tom Rockwell shared the lead at this site.

Four trenches were excavated at Lavic Lake, with Mike Rymer as the lead scientist. This site was ideal because stratigraphy was generally found to be excellent and abundant detrital charcoal allows for radiocarbon age control. In addition to trenching the 1999 rupture, a parallel vegetation lineament was trenched: a paleoevent was identified along this other fault but was not recognized on the 1999 trace. Radiocarbon dates are pending.

Finally, Charlie Rubin and Chris Madden opened two trenches across the Mesquite Lake fault on the southern part of the Marine base to test for recency of movement. A relatively massive clayey section, interpreted as the Holocene alluvial component, overlies well-bedded and lithified fluvial sediments interpreted as Pleistocene. At least one Holocene event is evident in the section; radiocarbon dates are pending.

All of these trench studies will shed further light on the observations of earthquake clustering in the Eastern California shear zone. Two important conclusions arising out of prior work are that: large surface ruptures have apparently clustered over relatively short time intervals, with longer intervening periods of seismic quiescence, and that the 1992 Landers earthquake is apparently unique over the past several recurrence cycles in rupturing multiple faults and fault segments (Rockwell et al., 2000 in press). The 1999 Hector Mine earthquake is also unusual in that it ruptured a minor, unnamed fault with a low slip rate and apparently long return period. A larger set of observations on other faults of the eastern California shear zone are required to test whether clustering affects the entire shear zone, or whether seismic activity has simply migrated from one part of the shear zone to another. It is still uncertain if the clustering that has been observed is an artifact of a sampling bias, since we currently only have data from those faults in the southwestern part of the shear zone. Inclusion of paleoseismic data from the Lavic Lake, Bullion, and Mesquite Lake faults will greatly expand our observations and allow for a more rigorous analysis of apparent temporal clustering. Preliminary results from the Bullion fan site support the idea that clustering is a regional phenomenon.

Paleoseismic Studies of the Simi Fault at Arroyo Simi, Simi Valley, California

Christopher Hitchcock, John Helms, Kristin Weaver, and Scott Lindvall
William Lettis & Associates
Jerry Treiman, California Division of Mines and Geology

The Simi fault zone is a 28-km-long, north-dipping, left-lateral-oblique-reverse fault that forms the linear, southern boundary of the Santa Susana Mountains in Southern California (Figure 1). The Simi fault is the eastern portion of the Simi-Santa Rosa fault system that extends to the Oxnard Plain and includes the Springville and Camarillo faults. This fault zone, which is 40 km in length, exhibits strong geomorphic evidence of Quaternary deformation. Despite this

geomorphic evidence, however, the recency of activity, slip rate and sense of fault movement are not well constrained. Our investigation of the Simi fault was designed to address the timing and style of Holocene surface deformation along the fault.

This on-going paleoseismic study of the Simi fault at Arroyo Simi within northwestern Simi Valley was initially funded by the Southern California Earthquake Center (SCEC) in 1997 and the U.S. Geologic Survey's National Earthquake Hazards Reduction Program (NEHRP) in 1999-2000. Currently we are planning additional focused investigations, including further exploratory drilling and trenching, to refine the timing of the most recent event and assess slip rate on the fault. We have also collaborated with Rob Clayton and his students who have run ground-penetrating radar (GPR) at this site. We hope that their subsurface imaging may find a linear feature, such as a stream channel or terrace riser, that could be used to quantify the slip vector and rate (see poster by Deborah Eason et al. also at this poster session).

In our initial phase of work we investigated the Simi fault at the western end of Simi Valley, where the fault crosses Arroyo Simi and appears to tectonically impound the drainage (Figure 2). At this location a fault zone is exposed in the western bank of Arroyo Simi. Tectonic geomorphology of the Simi fault in the vicinity of the Arroyo Simi site was analyzed through interpretation of aerial photography and detailed geologic and geomorphic mapping. This confirmed that the fault within the stream exposure is a major fault strand of the Simi fault. We cleaned and logged the stream bank exposure in October 1997 and documented the presence of deformed and faulted Holocene deposits. Bucket auger holes were drilled into the stream terrace southwest of the arroyo to better understand the lateral extent of the stratigraphy observed in the arroyo wall (Figure 3). Using the stream-cut exposures, we were able to constrain the age of the most recent surface rupture on the Simi fault to between 7666 ± 50 years BP, the age of faulted ponded clay deposits, and 1205 ± 80 years BP, the age of overlying unfaulted colluvium (Fig. 4).

In April 2000 we logged stratigraphically higher portions of the arroyo wall following a slump failure that revealed previous unexposed material (Figure 5). The newer arroyo exposure revealed faulting higher in section characterized by ductile shearing of clays and brittle offset of sands. These units are capped by unfaulted buried soils and sands. The clays lie stratigraphically above the deposits exposed in the lower 1997 exposure (Figure 4) and exhibit a north-side-up dip-separation of about 60 cm. Charcoal collected from these units have been submitted for AMS dating.

In order to further document Holocene activity, and constrain the timing and sense of slip of the Simi fault, this past summer we excavated a trench on a mid- to late-Holocene stream terrace across the fault at this site (Figures 2 and 6). Our trench revealed gently- to moderately-south-dipping silts and silty sands (units C through E in Figure 6) overlying massive sandy clay deposits (units A and B). The fault is expressed as a steeply north-dipping half flower structure with multiple strands exhibiting north-side-up (reverse) sense of slip. The sandy clay deposits, as well as much of the overlying stratigraphy, are warped and faulted in a north-side-up manner along six vertical to steeply-north-dipping faults. The brittle vertical separation across all strands totals ~ 1 meter, with no more than ~ 30 cm on any given strand. The thin, sharp nature of these offsets, and the poorly expressed shear fabric suggests that this slip was produced in a single event. If we restore the brittle slip, the basal subunits of unit C, which have a relatively uniform thickness, still appear to be warped significantly across the top of units A and B. This implies that a significant component of non-brittle deformation accompanied the brittle faulting event and/or an earlier event that produced only plastic deformation.

The main strand exposed in our trench juxtaposes units A and B, two noticeably different sandy clay deposits, suggesting that this strand has experienced a significant amount of strike-slip. Units A through D appear to have been faulted and/or warped by the Simi fault, while unit E has not. A detrital charcoal sample collected from above the red clays north of the fault yielded an uncorrected age of 4310 ± 40 years B.P. and a corrected age of Cal B.P. 4960 to 4830. This indicates that the most recent surface rupture at this site occurred sometime since ~4800 years ago. We collected and submitted for age analysis several additional detrital charcoal pieces from unit C and unit E that should further constrain the age of the most recent surface rupture on these strands of the Simi fault zone.

Inferring Fault Rupture Length from Early Aftershock Distributions: Bridging the gap Between Big and Small Earthquakes

Susan E. Hough

United States Geological Survey, Pasadena

A considerable database of fault rupture parameters has been assembled for both small ($M < 4$) and large ($M > 6$) earthquakes. Typically, high-resolution empirical Green's function methods are now commonly used to determine the fault dimensions for small events, while finite fault inversions are used to determine the rupture dimensions of large events. In a few cases, sufficient data exist to obtain finite fault models for events smaller than $M 6$. However, rupture parameters of intermediate ($M 4-6$) events are relatively scarce. To help bridge this gap, I analyze aftershock distributions of 50 $M_w > 5$ earthquakes in southern California between 1975 and 1998. Early (within the first 24 hours) aftershocks are commonly assumed to delineate the mainshock rupture. Using the relocated catalog of Richards-Dinger and Shearer (1999), I find that 41 of the 50 events--many large aftershocks with their own subsequences--have clustered aftershock distributions from which a rupture length can be inferred. Most of the remaining nine are large aftershocks for which a subsequence cannot be distinguished. Two lines of evidence suggest that the inferred rupture dimensions are reasonable: 1) finite fault models have been obtained by previous studies for eight of the events, and the rupture lengths determined from the two methods compare quite well, and 2) the inferred radii for $M < 6$ events are shown to be consistent with expectations for self-similar (i.e., constant stress drop) scaling given previously inferred results for small earthquakes. These results support the use of early aftershock distributions to infer mainshock rupture parameters.

Evidence for spatially complex Late Cenozoic uplift and exhumation of the Eastern San Gabriel Mountains from (U-Th)/He thermochronometry

Martha A. House, California Institute of Technology

Ann E. Blythe, University of Southern California

New helium ages were collected in order to document the Late Cenozoic exhumation history of the easternmost San Gabriel mountains, as well as to assess the role of NE-SW trending strike slip faults in accommodating uplift of the range. Preliminary helium ages from a vertical transect at Cucamonga Peak are 5.2-5.5 Ma over ~100 m, while a vertical transect extending between Stockton Flat Campground and Thunder Mountain (spanning 524 m) yields helium ages of 1.8-10.9 Ma. The slopes of these age-elevation profiles suggest that the Cucamonga samples were exhumed more rapidly (0.3 km/my) than the Thunder Mountain transect (0.05 km/my). However, assuming a closure temperature of ~65 C for helium ages and a geothermal gradient of ~25 C/km implies that exhumation accelerated in both regions since ~5 Ma (0.5 km/my at Cucamonga Peak and 1.4 km/my at Thunder Mountain). In addition to different rates of exhumation, there also appears to be a vertical offset of ~300 m between the two profiles since ~5 Ma. Furthermore, comparison of these data with those previously reported from Mt. San Antonio (5.1 Ma, Blythe et al., 2000) suggests that there has been approx. 500 m of vertical offset between Mt. San Antonio and Cucamonga Peak since ~5 Ma.

The apparent offsets between Cucamonga Peak and Mt. San Antonio, coupled with the difference in cooling histories and vertical offset documented between the Cucamonga Peak and Thunder Mountain transects suggests that the eastern San Gabriel Mountains are comprised of a number of individual fault blocks with different exhumation histories. Additional sampling is required, however, in order to fully resolve the spatial pattern of exhumation in the eastern San Gabriel Mountains.

Dynamic Rupture on an Interface Between a Compliant Fault Zone Layer and a Stiffer Surrounding Solid

Y. Huang and Y. Ben-Zion
University of Southern California

Natural fault zones are often more compliant than the surrounding medium and ruptures tend to propagate on their interfaces. Dynamic rupture along a material interface occurs as narrow self-healing pulse with low generation of frictional heat, in agreement with inferred properties of earthquake ruptures [e.g., Brune, '70; Heaton, '90]. Weertman ['80] obtained a 2D steady-state analytical solution for dynamic in-plane rupture pulse along a material interface governed by Coulomb friction, in which spatial variations of slip induce local changes of normal stress that can reduce dynamically the frictional strength of slipping regions. Spontaneous rupture occurs only in one direction, that of slip in the more compliant medium. Adams ['95] showed that this problem is unstable to perturbations with an instability growth rate proportional to the wavenumber. Physically this implies that rupture along a material interface with Coulomb friction would be associated with pulse sharpening during propagation. Mathematically the Adams instability makes the response to perturbation ill posed, and introduces grid-size dependency into numerical calculations. Schallamach ['71], Anooshehpour and Brune ['99], and Samudrala and Rosakis ['00] observed in sliding and fracture experiments uni-directional narrow slip pulse along material interface with tendencies to become narrower and break up with propagation distance. Andrews and Ben-Zion ['97] and Ben-Zion and Andrews ['98] simulated numerically slip pulses with similar features in calculation of dynamic rupture along a material interface governed by Coulomb friction. Ranjith and Rice ['00] clarified the conditions associated with the Adams instability and showed that the problem can be regularized by a friction law, motivated by lab data of Prakash and Clifton ['93] and Prakash ['98], where the instantaneous response of Coulomb friction to variations of normal stress is replaced by a gradual evolution. Cochar and Rice ['00] calculated numerically a self-sustaining slip pulse along a material interface governed by the regularized friction that appeared stable (no self-sharpening) in the range of their calculations.

Here we use 2D plane-stain finite-difference calculations to study dynamic rupture in a model with several different media, employing in most calculations the regularized friction. Harris and Day ['97] used a similar model with a slip-weakening friction which (like the Coulomb and standard rate-state frictions) does not regularize the Adams instability. We first extend the calculations for the self-sustaining case of Cochar and Rice ['00] and find that in this case too the self-sharpening phenomenon exists for large enough propagation distance (although in subdued form and without grid-size dependency). The pulse is in general unstable and the parameters of the regularized friction have to be fine-tuned to produce apparent stability for a given propagation distance. However, eventually the pulse will always either diverge or die. We then introduce a low velocity layer between two identical elastic materials and systematically change the width and velocity of the layer. For very narrow layer, the amplitude of the pulse decreases to zero, approaching the limiting case of two identical solids. For very wide layer, there is self-sustaining propagation and the results approach those of the case with two different elastic materials. For intermediate layer width, we observe that the strength of the pulse increases first with the width up to a maximum and then decreases. The envelope of the pulse strength is modulated by oscillations related to waves reflecting from the layer walls. Ben-Zion and Andrews ['98] explored the influence of velocity contrast on the strength of self-sustaining slip pulse for the case of only two materials with Coulomb friction and found that the pulse strength increases with velocity contrast up to a maximum at about 35% contrast. We find similar results for a configuration with a low velocity layer of moderate width (about one quarter of the size of the imposed source) between two identical materials and regularized friction. However, the envelope of the pulse strength is again modulated by oscillations. The results suggest that rupture along an interface between a low velocity layer and a half space, growing initially in a crack-like mode from a nucleation size, can become a self-sustaining pulse when it reaches a certain size

related to the layer width and velocity. If the rupture grew to a much larger size, transition to a pulse-mode is not favorable.

High Resolution Topography along the October 16, 1999 Hector Mine Earthquake (Mw7.1) Surface Ruptures using Airborne Laser Swath Mapping (ALSM)

Kenneth W. Hudnut, U. S. Geological Survey, Pasadena
A. Borsa and J.-B. Minster, University of California, San Diego
C. Glennie, Aerotec, LLC

The Hector Mine earthquake produced extensive surface ruptures along more than 70 km of breaks that offset geomorphic features by up to 5.25 meters. Across the surface of the Lavic Lake playa, slip in the range of 2.0 - 3.0 meters displaced the formerly quasi-planar lake bed surface along the fault zone into remarkable geomorphic expressions of compressional and dilatational jogs and steps. In order to document the surface rupture, in particular the maximum slip area and the deformed surface of Lavic Lake, we acquired a high resolution topographic data set. A raster laser scan of the main surface breaks along the entire rupture zone, as well as along an unruptured portion of the Bullion fault, was performed. Airborne Laser Swath Mapping (ALSM), also known as Light Detection and Ranging (LIDAR) and by other names such as simply laser scanning, is becoming an increasingly precise and commercially available topographic mapping method.

On April 19, 2000, the field team acquired the data set using a helicopter based instrument platform. Ground control was supplied by remotely and sequentially setting several of the Southern California Integrated GPS Network (SCIGN) continuously operating GPS stations to record at high (up to 2 Hz) sampling rate during the flight segments. On-board GPS and an integrated inertial navigation system allowed very precise positioning of the platform and its scanning system optics; the laser scanned at a rate of 7,000 pps. Precise ground waypoint navigation was provided by the surface rupture mapping by Kendrick et al. (USGS Open-File Report, in press). A swath width of 150 meters on average, along over 70 km of fault lines, was obtained in a single day. Along the maximum slip area and Lavic Lake, a swath width of 300 meters was obtained in overlapping, multiple data passes. Calibration maneuvers were performed to assess instrumentation and software unknowns and error sources. As well, a fault-perpendicular swath was run across Lavic Lake to attempt to detect longer wavelength deformation of the dry lake bed. We also collected redundant data over an open pit mine that had previously been mapped in great detail using conventional photogrammetric methods. This will allow both a comparison with other methods, and an assessment of the geodetic capabilities attainable by repeat passes that are separated temporally. We also expect to be able to use these data to estimate slip distribution along the fault, and compare this result with measurements made by other methods (e.g., field mapping, seismological, and geodetic), despite the lack of pre-earthquake high resolution topographic data in this case.

Laser scanning practice is becoming sufficiently precise that repeat-pass use should allow differential positioning at the centimeter level in both horizontal and vertical components (with some spatial averaging) to be obtained after future earthquakes, as long as pre-earthquake data are obtained with which to form a difference image. Within discussions on the scope of the Plate Boundary Observatory, it has been proposed that systematic topographic mapping of all active faults within the region of interest should be made in order to improve over the digital elevation models available currently from the USGS, or soon to be from the Shuttle Radar Topographic Mission. One possible method for obtaining such data is laser scanning, although radar and other methods will be considered as well. Our results show that laser scanning can be done cost-effectively, in combination with other imaging, to very high level of detail if desired.

For post-earthquake damage assessment, we suggest that at the same time as such strip mapping along active faults is performed, major lifelines that cross these faults should also be scanned. This would facilitate post-earthquake damage assessment and disaster recovery efforts, through the implementation of the same rapid pre- and post-earthquake differencing methods.

The use of a Regional Reference Frame in Realizing the Inherent Precision of Regional GPS

Ken Hurst, Mike Heflin, David Jefferson, and Frank Webb
Jet Propulsion Laboratory

A new analysis of the January 1998 to April 2000 SCIGN data demonstrates daily station coordinate repeatabilities of 1.3 mm for the East, 1.2 mm for the North, and 4.4 for the Vertical in ITRF97.

This analysis used fixed precise GPS orbits and clocks in a precise point positioning mode, followed by double difference ambiguity resolution, followed by transformation into a regional definition of the ITRF97.

This last step, transformation into a regional definition of ITRF97 allows recovery of the inherent internal precision of the network into the station coordinates.

Geodetic GPS has strong information about the relative positions of the stations - the shape of the network - but relatively weak information about the location and orientation of the network as a whole. Resolution of the doubly differenced carrier phase ambiguities provides even stronger constraints on the baselines between stations, but still does little to improve the position and orientation of the whole network.

This leads to a situation familiar to many GPS geodesists in which the precision attainable on a baseline is better than the precision of the position of either one of the stations in the baseline.

By defining a regional realization of the ITRF, and then using a helmert transformation on each day into the regional reference frame, we are able to reduce the noise in the station coordinates to a level commensurate with the baseline precision. In this solution, the baseline precision is $\sqrt{2}$ times the precision of the individual stations.

Another way to think about this problem is to realize that it is possible to ask 2 questions of the data: 1) Where is the "centroid" of the network. and 2) What is the vector from the "centroid" to each individual station. The GPS solution can give very precise answers to question 2, and the daily transformation can answer question 1.

The definition of the regional ITRF must be done with great care in order to avoid biasing the positions and velocities of the stations in the network. When done properly, the velocity of the stations defining the regional reference frame should be identical to the velocities for those stations from the global solution.

Hector Mine: Postseismic Deformation from ERS InSAR

Allison Jacobs, David Sandwell and Lydie Sichoix
University of California, San Diego

The Hector Mine earthquake occurred on October 16, 1999, in the Mojave Desert of California. Four days later, the European Space Agency satellite, ERS-2, flew over the region, bouncing radar waves off the desert surface to produce the first co-seismic synthetic aperture radar (SAR) image of the area. The collection of this data was also highly important for studying postseismic deformation since the most significant earthquake deformation usually occurs within the first 40 days after the main shock. We were fortunate to match this key image with data received on June 21, 2000, at the Scripps Institution of Oceanography satellite ground station,

and create a postseismic interferogram covering this critical time period. Using the interferogram we contoured the line-of-sight (LOS) displacement in the fault region. The three main deformation features seen in the line of sight displacement map are a region of subsidence (40 mm line of sight increase) on the northwestern side of the fault, a region of uplift (65 mm line of sight decrease) located to the northeast of the primary fault bend, and a linear trough running along the main rupture of the fault. These features coincide well with a characteristic left-bending, right-lateral strike-slip fault that ideally exhibits contraction on the restraining side of the fault bend and extension along the opposite side. In this initial postseismic interferogram, the areas of subsidence and uplift combine to display a maximum amount of displacement of nearly 105 mm. A second interferogram made from images taken 39 days and 139 days after the earthquake shows a significant decrease in the amount of displacement (maximum displacement of 50 mm). This smaller deformation indicates that most of the relaxation occurs within about 40 days of the main shock. The co-seismic and postseismic interferograms created for this study are on display at <http://topex.ucsd.edu>.

Long-Term and Short-Term Earthquake Forecasting

David D Jackson and Yan Y Kagan
University of California, Los Angeles

We present long-term and short-term forecasts for magnitude 5.8 and larger earthquakes for scientific testing only. We optimizing both forecasts and test their skill using the likelihood function. For our long-term forecast we assume that the rate density (probability per unit area, magnitude, and time) is proportional to a smoothed version of past seismicity. This differs considerably from the seismic gap model (e.g., McCann et al., 1979; Nishenko, 1991), which assumes that recent earthquakes deter future ones. The estimated rate density depends linearly on the magnitude of past earthquakes and approximately inversely on a power of the epicentral distance out to a few hundred km. We assume no explicit time dependence, although the estimated rate density depends on the catalog, which evolves with time. The forecast applies to the ensemble of earthquakes during the test period, rather than any single earthquake. We assume that one percent of all earthquakes are surprises, assumed uniformly likely in those areas with no cataloged earthquakes. For plate boundaries with high seismicity we use the Harvard CMT catalog. Using focal mechanisms we construct an anisotropic smoothing kernel that concentrates the estimated rate density along the presumed strike direction of an earthquake fault. We have made specific forecasts for calendar years 1999-2000 for the North-west Pacific and South-west Pacific regions. For continental areas we use the PDE catalog because the Harvard catalog has too few events. However, the PDE catalog does not report focal mechanisms, so we use an isotropic smoothing kernel. Here we present forecasts for South-east Asia and the continental USA. We plan eventually to expand the forecast to the whole Earth. We tested the 1999 forecasts for the western Pacific against the earthquake catalog using a likelihood test. The results confirm the effectiveness of the forecast for the North-west Pacific. For the Southwest Pacific the model forecast a broader distribution of earthquake locations than actually occurred. We'll present results for 2000 at the meeting. Our short term forecast, updated daily, makes explicit use of statistical models describing earthquake clustering. Like the long-term forecast, the short-term version is expressed as a rate density. However, the short-term model will change significantly from day to day in response to recent earthquakes. The model is designed to forecast all dependent events, including aftershocks, aftershocks of aftershocks, and mainshocks preceded by foreshocks. However, there is no need to label each event, and the method is completely automatic. According to the model, nearly ten percent of moderate sized earthquakes will be followed by larger ones within a few weeks.

Three-Dimensional Modeling of Wave Propagation in Fault Zone Structures

**Gunnar Jahnke and Heiner Igel, Ludwig-Maximilians-Universität, München
Yehuda Ben-Zion, University of Southern California**

Fault zone (FZ) structures play dominant roles in fault mechanics and strong ground motion in seismically active regions. Although a huge amount of seismograms recorded in FZ areas exists, the structure of FZ at depth is not well understood. One reason is the low FZ thickness which makes the structure invisible for seismic tomography because the properties of body waves crossing the fault are hardly altered. A better approach to reveal the structure of a FZ is the use of FZ guided head and trapped waves (FZ-waves) which sometimes arise in the fault region and which are caused by low seismic velocities in the FZ. These waves can travel many kilometers inside the fault before reaching the surface and therefore are strongly altered by the FZ properties. Currently modeling of FZ-waves is mostly done in 2D and is not able to handle realistic sources like double-couple point sources or strong deviations from a 2D geometry of a FZ. In this study we present simulations of 3D elastic wave propagation through various FZ models. Our algorithm is based on a high-order staggered-grid finite-difference scheme. We discuss the influence of some fault geometries and the seismic properties on seismograms observed at the earth surface, with a focus on the envelope and the frequency content of the seismic traces.

Our simulations show that a fault which is continuous at depth and splits into two fault segments towards the surface is capable of guiding FZ-waves. Even for a source which is located beneath one of the segments clear FZ-waves can be measured also on the other fault segment. Therefore the detection of FZ-waves on different fault segments can be used to find out whether the segments are continuous at depth or not. Fault models with an increasing lateral disruption at depth lead to a decrease of FZ-wave amplitude and to a spatial smearing at the surface. If the lateral shift of the FZ exceeds its own width, no more distinct FZ-waves arrive at the surface. The spectra for models with increasing amounts of lateral disruption look similar, whereas the FZ-wave amplitude decreases and the wave train becomes longer and merges with the coda. Thus the appearance of FZ-waves and their properties contain information on how continuous the fault is at depth. The effect of varying fault width, e.g., a flower-type structure, on the amplitudes is moderate. Therefore moderate changes of the fault's properties with depth hardly alter FZ-waves; such features would be difficult to resolve from seismograms. Cases with vertical gradients of seismic properties show that the FZ-wave amplitude, the spectrum and the length of the wave train are hardly affected by realistic levels of the gradient. Thus it would be very difficult to derive information about seismic gradient from waveform modeling of observed FZ waves.

Earthquake Potential Estimated from Tectonic Motion

Yan Kagan, David D. Jackson, Peter Bird, and Heidi Houston
University of California, Los Angeles

We analyzed the tectonic moment rate and the earthquake magnitude distribution for several types of tectonic environment, including subduction zones, plate bounding transform faults, deforming continental regions, oceanic transform faults, and spreading ridges. In each region we estimate the strain rate or relative plate motion from a plate tectonic model, active fault data, or geodetic data, and we compile a sub-catalog of earthquakes from the Harvard CMT catalog. We then estimate the range of b-values and corner magnitude values consistent with the sub-catalog, assuming a modified Gutenberg-Richter distribution as defined in Jackson and Kagan [SRL, 1999]. The ratio of earthquake rate to tectonic moment rate (the normalized seismicity) depends on the b-value, corner magnitude, and effective seismogenic thickness. We studied subduction zones and continental transforms defined by McCann et al.

[PAGEOPH,1979] and Nishenko [PAGEOPH, 1991]. The normalized seismicity does not vary systematically with the time since the last major earthquake, the relative plate velocity, the ratio of parallel to perpendicular plate motion, Nishenko's estimate of characteristic earthquake size, or his probability of a future characteristic earthquake. Because the normalized seismicity depends strongly on corner magnitude and effective thickness, apparently neither one varies strongly with tectonic environment. The normalized seismicity correlates with age of the subducted lithosphere, but large residuals inspire doubt. The b-value and corner magnitude are about 0.95-1.0 and 8.0-8.5 throughout the Pacific rim, regardless of tectonic style. For the Western United States [Shen-Tu et al., JGR, 1999] and South-east Asia (including China) [Holt et al., JGR, 2000], the b-value and the corner magnitude are similar to those for the circum-Pacific Rim. There is no systematic dependence of these parameters on geographic region or strain rate. The distribution of oceanic spreading earthquakes is consistent with "normal" $b = 1$ (although b is not well constrained) and with uniform corner magnitude of 5.8. Oceanic transform faults also have "normal" b , but their corner magnitudes decrease from about 7.1 to about 6.3 with increasing relative plate velocity. Spreading ridges and oceanic transform faults both appear to have low seismic efficiency, because if efficiency were unity it would require unreasonable stress drops or aspect ratios to explain the largest earthquakes. These results show that past seismicity is proportional to tectonic moment rate, estimated from plate tectonics, fault slip rates, or geodesy. The proportionality factor depends on the magnitude distribution and effective lithospheric thickness, which can be estimated using the models we have developed. We are using these relationships to develop a testable model of earthquake likelihood as a function of location and magnitude.

Geometry and Quaternary Slip of the Pitas Point, North Channel and Red Mountain Faults, California

Marc J. Kamerling, Christopher C. Sorlien, and Ralph Archuleta
University of California, Santa Barbara

We created structure-contour maps of the Pitas Point, North Channel, Red Mountain, and offshore Padre Juan faults beneath northern Santa Barbara Channel. Fault plane reflections from these faults were observed on the 3D and 2-D seismic lines used for mapping, and faults were also mapped from the sea floor geology and detected by repeated sections and abrupt dip changes in wells. We revised and extended the mapping of the North Channel fault by Hornafius et al. (1996), mapped the additional faults, performed a preliminary depth conversion, and created digital structure contour maps in geographic coordinates of all the faults. The N-dipping Pitas Point fault and the North Channel fault are distinct from each other in cross section but are stacked to map along the same E-W trend. Both faults intersect in the upper 1 km, with the Pitas Point fault dipping more steeply to diverge downdip. Shallow thrusts, folds, and south dipping reverse faults occur in the hanging wall and the footwall of the Pitas Point and North Channel faults. The south branch of the offshore Red Mountain fault is a separate parallel structure 6 km to the north. The Red Mountain fault splays into two main branches near the Carpinteria coast. The northern branch decreases in displacement to the west and continues west of the UCSB campus where it may die into folding. The south branch also decreases in displacement to the west and dies out in a syncline south of Santa Barbara. The North Channel and Red Mountain faults probably intersect with depth, detaching the intervening upper crustal block. Displacement is transferred from one fault to another via NE-SW cross faults and probably by vertical axis local block rotations. Major cross faults are mapped or inferred near Santa Paula, along the Ventura River, at Rincon Point, and at Fernald Point. Abrupt changes in shortening and fault-fold style along the strike of the Pitas Point and North Channel faults occur across these NE-SW faults. We created 34 digital structure-contour maps on fault-bounded blocks of the top Lower Pico horizon through onshore and offshore Ventura basin and adjoining areas to the north and south. Unfolding and restoration of these maps on the 1.8 Ma horizon indicates shortening

varying from 1-3 km along strike, with a local higher amount interpreted south of Santa Barbara. The total shortening across these fault systems decreases to the west. This 1-2 mm/yr rate is much less than the GPS rate of ~6 mm/yr across this area. The difference is probably due to shortening in the hanging-wall north of the Red Mountain fault, acceleration of the shortening rate since 1.8 Ma, and because sediment compaction within offshore Ventura basin causes an apparent shortening in the GPS data.

Hornafius, J. S., Kamerling, M. J., and Luyendyk, B. P., and, 1996, Seismic mapping of the North Channel fault near Santa Barbara, California, 1995 Annual Report, Southern California Earthquake Center, v. II, University of Southern California, p. D13-D17.

Results from the SCIGN Analysis Committee

Nancy King, Jeff Behr and Keith Stark, United States Geological Survey, Pasadena
Ken Hurst and Mike Heflin, Jet Propulsion Laboratory
John Langbein, United States Geological Survey, Menlo Park
Matt van Domselaar and Hadley Johnson, University of California, San Diego

GPS data from the Southern California Integrated GPS Network (SCIGN) is routinely processed by SCIGN's precise processing centers (JPL, SIO), as well as by USGS-Pasadena. The SCIGN Analysis Committee is investigating the differences between the results. This is crucial to understanding the effects of different processing methods (software, orbits, and strategies), detecting problems, estimating accuracy and precision, and forming a combined SCIGN solution. The Analysis Committee has undertaken several investigations, including comparison of positions, velocities, and coseismic displacements associated with the October 16, 1999 Hector Mine earthquake. The committee's December 1999 combined coseismic displacements were an official SCIGN product. There are still puzzling discrepancies at the level of a few mm or mm/yr. The committee is also investigating the effect of offsets (both man-made and geophysical) on the precision of our estimates of velocity.

Earthquake Nucleation and Early Propagation as Affected by Prior Events in Elastodynamic Simulations of Earthquake Sequences

Nadia Lapusta and James R. Rice
Harvard University

We study earthquake nucleation and early propagation during sequences of model earthquakes in a 2-D model of a vertical strike-slip fault with standard depth-variable rate and state friction. The methodology (Lapusta et al., JGR, 2000, to appear) incorporates both truly slow, tectonic loading and all dynamic features. It allows us to treat accurately, within a single computational procedure, loading intervals of thousands of years and to calculate, for each earthquake episode, initially aseismic accelerating slip (nucleation process), the resulting dynamic rupture break-out and propagation, post seismic deformation, and ongoing slippage throughout the loading period in creeping fault regions.

Rate and state friction incorporates a characteristic slip distance L for evolution of frictional strength. For fixed other parameters, the nucleation size (size of the quasi-statically slipping patch that precedes the dynamic rupture break-out) is proportional to L . We study how earthquake sequences change as we decrease L , approaching the laboratory range of tens of microns (too small to be computationally feasible). As L decreases, small events appear near the brittle-ductile transition at the bottom of the seismogenic (velocity-weakening) zone. For the particular depth-variable fault model studied by Lapusta et al. (ibid), a simulation with $L = 8$ mm produces a periodic sequence of large events (sequence I), while a simulation with $L = 2$ mm results in the sequence of a large and a small event (sequence II), as do the simulations with $L =$

1 mm and 0.5 mm. In the case with $L = 0.14$ mm (done so far only quasi-dynamically; we intend to redo it with full dynamics), the sequence is more elaborate, with large events interspersed by three smaller events.

The nucleation of the large and small events is very similar, as manifested by plots of slip, slip velocity, moment rate, and moment acceleration. This means that observing the nucleation and beginning of a model earthquake, it is impossible to tell whether the final size of the event will be large or small. The final size of the event is determined by the conditions on the fault region that the event is propagating into, rather than by the nucleation process.

We observe that moment acceleration during initial stages of dynamic rupture propagation can have "bumps" and subsequent "speed-ups". This is consistent with observations, e.g. as reported by Ellsworth and Beroza (Science, 1995), who attribute these features to either processes in the preslip region or a special cascade structure of the fault. Our simulations show that such irregular moment acceleration (to which velocity seismograms are proportional) can be caused by heterogeneous stress distribution left by previous events. For the large event of the sequence II, moment acceleration grows initially, then decreases almost to zero during rupture propagation over the region that slipped in the previous small event, and then again abruptly grows, even faster than initially, when the rupture reaches the region of stress concentration left by the arrest of the previous event. Such a "bump" and "speed-up" is not observed for an event of the sequence I which does not have small events.

Modeling of Nonlinear Strong Ground Motion during the 1994 Northridge, Earthquake at the Van Norman Dam Complex

D. Lavallee, L. F. Bonilla, and R. J. Archuleta
University of California, Santa Barbara

SCEC sponsored studies and strong motion data recorded at the Van Norman Dam Complex (VNDC) during the 17 January 1994 Northridge earthquake (Mw 6.7) have been used to determine the presence of nonlinear effects in strong ground motion. The data available included borehole velocity profiles, weak to strong motion records, and dynamic soil laboratory tests. Measurements of ground motion observed at the Jensen Generator Building (JGB) site located on bedrock, have been coupled with the nonlinear model to generate scenarios of ground shaking at the Jensen Main Building (JMB) site. The nonlinear model formulation includes effects such as anelasticity, hysteretic behavior (also known as the memory effect) and cyclic degradation due to pore water pressure. In this study, two situations have been investigated; one that includes the effect of pore pressure and the second without it.

The results of the numerical experiments conducted with this site support the assumption that pore pressure cyclic mobility did contribute significantly to the ground shaking observed at the surface. A characteristic features of simulations including pore pressure effects for this site is the depletion of the high frequency in the signal in good agreement with the recorded acceleration. None of the scenarios generated without pore pressure were able to reproduce this feature. Also spiky waveforms in the tail can be detected in both synthetic and observed accelerograms. Similar conclusions applied to both horizontal components of the JMB site. We have to stress that in this study, conclusive finding of nonlinearity is based on direct simulations of nonlinear soil dynamics and the quantification of the nonlinearity in terms of the model parameters.

Fault Story: Two Big Ones That Got Away

Mark R. Legg, Legg Geophysical
Chris Goldfinger, Oregon State University,

Two of the largest active faults in the southern California region lie submerged offshore, inaccessible to conventional land-based paleoseismology. The San Clemente and the San Diego Trough fault zones are major strike-slip faults that appear to have sustained a substantial part of the late Cenozoic right-slip along the Pacific-North America plate boundary. Together, they comprise the transform fault system most active during the middle to late Miocene phases of the PAC-NOAM plate boundary evolution. During this time, when the northern San Andreas fault system grew northward following the Mendocino triple junction, the San Clemente-San Diego Trough transform fault system grew southward following the East Pacific Rise at the Rivera triple junction. Although at a slower rate than during Neogene time, movement on these fault zones continues at present as shown by historical seismicity in the region. Sea Beam swath bathymetry combined with high-resolution seismic reflection profiles show well-defined fault traces with prominent seafloor displacement over fault lengths exceeding 400 km (600 km for San Clemente). The major sections of the San Clemente fault system include, from north to south: 1) Santa Cruz-Santa Catalina Ridge fault zone; 2) Santa Barbara Island fault zone; 3) Kimki Ridge fault zone; 3) San Clemente Ridge fault zone; 4) San Clemente Island fault zone; 5) East San Clemente Basin fault zone; 6) Bend Region fault zone; 7) San Isidro fault zone; and other unnamed sections west of northern Baja California. The major sections of the San Diego Trough fault system include: 1) Santa Catalina Escarpment fault zone; 2) San Pedro Basin fault zone; 3) San Diego Trough fault zone; 4) Bahia Soledad fault zone; and possibly other unnamed sections west of Baja California. The great length of these fault zones combined with recent observations of large (1-3 m high) vertical seafloor fault scarps show that large earthquakes ($M > 7$) have occurred during pre-historic time on these prominent offshore faults. Substantial seafloor uplift during large earthquakes at major restraining bends, Bend Region offshore San Diego and Ensenada, and Santa Catalina Island offshore Los Angeles, will generate local tsunamis that may be destructive to these heavily populated coastal cities. Submarine geologic data combined with geodetic measurements suggest that 20% of the PAC-NOAM relative plate motion is presently occurring offshore of southern California. The San Clemente and San Diego Trough fault systems likely accommodate the major portion of this right-slip. Both fault systems were ignored in recently published probabilistic seismic hazard assessments. Consequently, the seismic hazard along the heavily populated southern California coastline may be seriously understated.

Characterization of Rupture Zones of the Hector Mine and Landers, California, Earthquakes using Fault-Zone Trapped Waves

Yong-Gang Li, University of Southern California
John E. Vidale, University of California, Los Angeles

The 1999 M7.1 Hector Mine earthquake and the 1992 M7.5 Landers earthquake in southern California, both of them with sterling surface exposure, provide us excellent sites for recording fault-zone trapped waves. The two earthquakes occurred only ~25 km apart from each other in the eastern Mojave shear zone and showed right-lateral strike-slip faulting and high stress drops. The Landers event produced surface breaks of total 80 km in the length with the maximum slip of 7 m. The Hector Mine event produced 40-km-long surface breaks with the maximum slip of 5 m. Observations and modeling of fault-zone trapped waves from aftershocks allowed us to characterize the internal structure of the rupture zone and physical nature of fault segmentation with a high resolution at the seismogenic depth. We have delineated a low-velocity zone (waveguide) along the surface ruptures at Landers and Hector Mine, respectively. Within

the waveguide, the shear velocity is reduced by 40-50 percent from the wall-rock velocity and Q is 20-40 either for the Landers rupture zone or the Hector Mine rupture zone, suggesting that the degree of rock damage in dynamic rupture of these two earthquakes is similar. The waveguide width inferred by trapped waves on the Hector Mine rupture zone is 75-100 m, only a half of the width on the Landers rupture zone. However, the ratio of the waveguide width to the rupture length for both earthquakes is consistent with the scale of the process zone width to the fault length predicted by the cohesion-zone fault growth model [Cowie and Scholz, 1992]. Trapped wave data also revealed that multiple faults were associated with each of these two earthquakes. At Landers, the rupture is segmented at stepovers between pre-existing faults. At Hector Mine, the rupture branches into sub-parallel strands in the northern and southern portions of the rupture zone as oppose to the single slip plan in the middle rupture segment.

A Stochastic Model for Earthquake Fault Geometry Revisited

Eric Libicki and Yehuda Ben-Zion
University of Southern California

Kagan develops in the paper "Stochastic Model of Earthquake Fault Geometry" [Geophys. J.R. Astr. Soc., 1982] a method to synthesize fractal fault geometry. The work was motivated by observations of fault traces and epicenter/hypocenter distributions that are indicative of fractal geometry. Since fractals are characterized by power laws, the model is based on various power-law probability distributions. Using power laws for determining fault geometry complements other observed power-law statistics associated with earthquakes, such as the Gutenberg-Richter relationship and Omori's law. Kagan's model provides an opposite end member to the standard Euclidean-continuum framework and as such it is important to understand the properties and consequences of the model. The stochastic branching model of Kagan [1982] consists of numerous circular dislocations joined by a lineage tree generated with a critical Poisson distribution. The disks do not reside on a plane, but are rather rotated individually according to a given power law distribution, $P(x)$. Using power law probability distributions requires including a minimum cutoff parameter to avoid the problem of $P(x)$ approaching infinity for small values of x .

In the past decade, there has been a significant increase in computer processing speeds in addition to the large increase in papers that claim to observe fractal features. Therefore, it is important to revisit both the observational basis of the model and its theoretical foundations. Here we focus on the latter, following most aspects of Kagan's original model. However, there are also slight differences between our simulations and those of Kagan [1982], involving the rotation of the dislocations and the values used for the parameters. This poster shows preliminary results from an early stage of our analysis. We have tested various power-law rotations and began looking at 2-D and 3-D representations of the synthetic faults. We have also started using fractal dimensional analysis, and exploring the merit of using critical Poisson branching versus other distributions. Work for the near future includes looking at the synthetic fault traces over a broader range of scales and examining how the synthetic faults propagate through time.

The Effect of a Low-Velocity Surface Layer on Simulated Ground Motion

Peng-cheng Liu and Ralph J. Archuleta
University of California, Santa Barbara

With the advance of computational efficiency, the finite difference method (FD) has frequently been used to calculate seismic wave-field simulations for more realistic three-dimensional velocity models. A common feature of the FD simulations is that low-velocity

surface layers are rarely incorporated into the 3D velocity models because of the severe computational and memory requirements imposed by the low velocity material. However, the wave velocity near the free surface is generally small relative to most of the volume and can strongly affect the ground motion. To include a low-velocity layer into FD simulation one optimal approach is to generate a grid with variable spacing. Here we extend the method of Aoi and Fujiwara (1999) from a second-order staggered grid to a fourth-order staggered grid. The grid system is divided into two regions: Region I is the volume that includes the free surface, and Region II is all the volume below the Region I. The grid spacing is three times more coarse in Region II compared to Region I. We have used this FD approach and the SCEC southern California velocity model (version 2) to study the effect of low-velocity surface layer on simulated ground motion. Because the Q structure is not yet available in the 3D model, we assume that QS and QP are one tenth of the S or P velocity (given in m/s), respectively. For comparison, we also fix the minimum S-wave velocity at 500 m/s, a value that is currently used by many researchers.

Analysis of Acoustic Emission and Stress-Strain Lab Data with a Damage Rheology Model

Yunfeng Liu and Yehuda Ben-Zion, University of Southern California
Vladimir Lyakhovsky, The Hebrew University, Jerusalem
Dave Lockner, United States Geological Survey, Menlo Park

Lyakhovsky et al. [JGR, 1997] developed a damage rheology model to describe evolving non-linear properties of rocks under conditions of irreversible deformation. The model adds to the parameters of linear Hookean elasticity λ , μ a third parameter γ to account for the asymmetry of the response of rocks under loading or unloading conditions, and makes all three parameters a function of an evolving damage state variable α . Conceptually, damage evolution in rock deformation leading to brittle failure can be divided into the following three stages: frozen initial damage, distributed material degradation, and localization of damage culminating with macroscopic failure. In the first stage, the elastic moduli λ , μ and γ are all constant and γ is equal to zero for damage-free rocks. During the second stage with distributed damage, effective moduli of stress-strain can be used to describe evolution of average elastic properties in the deforming solid. In the third localized stage, the heterogeneity of the material must be taken into account. Along with damage evolution, we also consider damage-dependent viscous deformation. On the time scale of laboratory experiments, viscous strain based on values of viscosity η typically used for crustal deformation (e.g. $\eta \geq 10^{19}$ Pa s) is too small to contribute appreciably to deformation. However, the viscous deformation may be accelerated by increasing damage and we thus assume that the viscosity η is a function of the rate of α .

Here we analyze acoustic emission and stress-strain data obtained in a recent experiment with Westerly granite (BZ05) at the USGS Menlo Park laboratory of D. Lockner in terms of the above damage rheology model. The analysis of the experimental data is done with the following three procedures: (1) damage rheology without viscosity, (2) damage rheology with constant viscosity, and (3) damage rheology with damage-dependent viscosity. We find that model predictions with procedure (1) can fit the observations well beyond the range of Hookean elasticity, but the predicted curves diverge from observed ones about 2/3 of the way between the initial deviation from linearity and the final brittle failure. The fitted range with procedure (2) is much larger than that with (1); however, the required value of constant viscosity η is about 10^{15} Pa s, which is unrealistically low for the early stages of deformation. The calculated results with procedure (3) can fit the observations very well in a range almost up to the final brittle failure of the rock.

Shallow Shear-Velocity Structure Below Strong-Motion and Precarious-Rock Sites Near the San Andreas Fault

John N. Louie and Robert E. Abbott
University of Nevada, Reno

Microtremor noise recordings made on 200-m-long lines of seismic refraction equipment can estimate shear velocity with 20% accuracy, often to 100 m depths. With no source, densely urbanized locations give better results than quiet rural settings. We have performed hammer refraction and passive microtremor surveys at eight sites near the Mojave segment of the San Andreas. Thirty-meter average velocities estimated from P-wave hammer refraction agreed with surface-wave results to better than 10%, under the assumption that soils have Poisson's ratios of 0.25-0.30. Surface-wave dispersion modeling cannot duplicate the detail in the velocity profile yielded by a suspension logger. However, we were able to match the average velocity of 10-20 m depth ranges and suggest structure below the 100 m depth of the Rosrine hole at the Newhall Fire Station. The so-called "rock" sites of strong-motion recording we have surveyed at Newhall, Mill Creek Summit, and Palmdale have 30-meter average shear velocities well below the 760 m/s standard used in creating the predictive ground-motion maps. The precarious-rock sites all have 30-meter velocities significantly above the 760 m/s standard.

Preliminary Paleoseismic Results from the Mesquite Lake fault, Twentynine Palms Marine Base, California

Christopher Madden, Charles Rubin, and Ashley Streig
Central Washington University

We report preliminary results from two excavations across the Mesquite Lake fault located on the Mesquite Lake playa at the Marine Corps Air Ground Combat Center, Twentynine Palms, California. The Mesquite Lake fault is the southern extension of the Calico Blackwater fault [Jennings, 1994] and shows evidence of prehistoric surface rupture. The surface rupture of the October 1999, magnitude 7.1 Hector Mine earthquake is located only 30km northwest the playa site. Degraded northeast and southwest facing scarps, vegetation linaments, a pronounced groundwater barrier and fault parallel longitudinal dunes mark the trace of the Mesquite Lake fault. The excavation site is located between two sand dunes at the edge of the playa where the fault splays into two parallel strands. This is an ideal site for preserving event stratigraphy as dune sands appear to regularly wash across the fault onto the playa surface. In addition, lacustrine sediments favor preservation of detrital charcoal and offer an excellent depositional record.

Two fault-perpendicular trenches, 15 and 25 meters long, expose a 4 meter section of well-bedded, reworked sand dune deposits overlain by weakly-bedded, bioturbated, lacustrine deposits. These strata are overlain by a thin, massive to cross-bedded sand dune unit. The Mesquite Lake fault appears in the trench walls as a 2.5m wide fault zone. Trench wall exposures suggest evidence for three prehistoric events and tenuous evidence for perhaps an additional event. The thin uppermost sand dune unit exposed in the trenches is not cut by the fault and provides a minimum age estimate for the most recent event. The penultimate event occurs near the base of the lacustrine deposits and is marked by an abrupt upward termination of in-filled fissures exposed in both trench wall exposures. The pre-penultimate event is marked by a distinct deformation horizon in the well-bedded sands below the lacustrine deposits. We have collected detrital charcoal samples at each event horizon. Although radiocarbon dates are pending, our current interpretation, based on work done on nearby faults, suggests that the lacustrine deposits are Holocene age. Therefore, we propose that at least two prehistoric earthquakes occurred in the last 11,000 years. This suggests that the Mesquite Lake Fault experiences long recurrence intervals, similar to other faults of the eastern California shear zone.

The SCEC Southern California Reference 3D Seismic Velocity Model: Version 2

**Harold Magistrale and Steve Day, San Diego State University
Rob Clayton, California Institute of Technology
Rob Graves, URS Corporation, Pasadena**

We present Version 2 of the SCEC southern California 3D seismic velocity model. Version 2 includes the following enhancements over Version 1: shallow (<200 m depth) Vp and Vs constraints from geotechnical borehole data and a soil classification map, a model of the Imperial Valley basin, tomographic velocities for regions outside the basins, and a laterally varying Moho depth based on receiver-function estimates.

Well-constrained shallow properties are desirable because near-surface seismic velocities can have a strong influence on earthquake ground motions. We use seismic velocities measured in boreholes in the greater Los Angeles area by various organizations and compiled by W. Silva. We determined generic velocity-depth profiles for each of the soil types defined on a soil classification map developed by the CDMG; generic profiles for softer soil types vary by basin. The velocity at a particular point is a weighted combination of the appropriate generic profile and nearby boreholes. The Imperial Valley contains many potential earthquake sources and it influences regional wave propagation. We incorporate a crude Imperial Valley model based on existing seismic refraction results.

Areas outside of the Imperial Valley and Los Angeles area basins are assigned velocities interpolated from the tomographic Vp and Vs results of E. Hauksson based on local earthquake travel times. Moho depths are from receiver function analysis of teleseismic events recorded on broad band stations by L. Zhu with the depths and uncertainty estimates incorporating 3D tomographic crustal Vp and Vs.

The model is conveniently parameterized as a set of objects and rules that are used to generate any 3D mesh of seismic velocity and density values at length scales appropriate for different uses. The model will be available on the SCEC Data Center at <http://www.scecdc.scec.org>.

A Latest Pleistocene-Holocene Slip Rate on the Raymond Fault Based on 3-D Trenching, East Pasadena, California

M. Marin, J. F. Dolan, R. D. Hartleb, S. Christofferson, A. Tucker
University of Southern California
L. Owen, University of California, Riverside

The Raymond fault is a 20-km-long, left-lateral strike-slip fault that extends east-north eastward through the San Gabriel Valley, northeast of downtown Los Angeles. The Raymond is one of several strike-slip faults that lie at the heart of a controversy concerning the mechanism of plate boundary deformation in the greater Los Angeles metropolitan area. Walls et al., (1998) have proposed that a significant percentage of north-south shortening across the region is accommodated by east-west extrusion of major crustal blocks along east-northeast left-lateral faults (e.g. Raymond, San Jose) and west-northwest trending right-lateral and oblique-reverse faults. In contrast, Argus et al., (1999) suggest that almost all north-south shortening is accommodated on east-trending contractional faults (e.g. Sierra Madre-Cucamonga). The extrusion model would therefore predict faster rates of strike-slip, whereas the contractional model would predict much slower rates of strike-slip. In order to test these competing hypotheses, we excavated a 3-D network of more than 25 trenches and incrementally excavated trench faces across the Raymond fault at a site in eastern Pasadena. Our excavations exposed a 10-m-wide zone of closely spaced sub-parallel faults, with a single 10-cm-wide main strand near the southern end of the zone. We traced in 3-D the buried western margin of a distinctive

southward-flowing, > 8-m-wide, pebble- and cobble-filled gravel channel that is offset by the fault. Forty-two meters of the total channel offset of 44 +/- ~ 1m is accommodated on the main strand of the fault. A single AMS 14C date of a charcoal fragment obtained from a silty sand into which the offset channel was incised yielded a radiocarbon age of 25,400 +/- 160 yBP (~ 29,000 calendric years ago; Voelker et al., 1999). These observations yield a minimum left-lateral slip rate for the Raymond fault of 1.5 mm/yr. The faulting is almost pure left-lateral strike-slip at this location, with < 50 cm of north-side-down vertical separation of deposits below the offset channel. Additional (pending) age determinations of charcoal and OSL samples will allow us to refine our maximum and minimum slip rate estimates for the Raymond fault. Our data indicate that significant left-lateral motion is occurring along the Raymond fault consistent with either: (1) active westward extrusion of the Santa Monica Mountains block; and/or (2) transfer of slip westward from the Sierra Madre fault to the Verdugo-Eagle-Rock fault. This slip rate provides a critical constraint for any future kinematic models of deformation in Southern California.

Weaver and Dolan (2000) suggest an average recurrence interval for Raymond fault surface ruptures of < = to ~ 3 ky. If correct, this RI, combined with our minimum slip rate, suggests that Raymond fault surface ruptures are characterized by large offsets (~ 4-5 m). This, in turn, implies that these would be large-magnitude events ($M_w > 7$). If such large events do characterize the Raymond fault, then we speculate that they may involve simultaneous rupture of the Raymond fault together with the Hollywood-Santa Monica fault system to the west. Alternatively, many (most ?) paleo-surface ruptures on the Raymond fault must be missing from the paleoseismological record.

PBIC Activities Summary for 2000

Aaron J. Martin, Elizabeth Cochran, Carrie Glavich, Jon Schuller and Ralph Archuleta
University of California, Santa Barbara

The PBIC provided equipment to nine different research experiments over this past year. Substantial field assistance was provided on several of the larger projects including the active phase of LARSE II and the Hector Mines deployment. The PBIC has completed the basic timing corrections and preliminary event associations of the Hector Mines data. Further processing steps are already underway and new data sets will be available in the next few months. This preliminary data set is available via the web at <http://www.crustal.ucsb.edu/scec/hectormines>. The Santa Barbara Array, delayed by the Hector Mines deployment and subsequent experiments, now has nine stations operational. The equipment was used heavily over the past year with the exception of a several month period following the completion of the Hector Mines deployment. This time was used to perform further maintenance on DASs and to upgrade all the GPS units to correct a bug introduced by the WNRO and Y2K upgrades performed in mid 1999. ARGOS satellite telemetry systems from PBIC and PASSCAL were used to monitor equipment status of the hector mines deployment and allowed researchers to better gauge battery replacement intervals and the rate of data collection.

The PBIC web page registered over 21000 hits from over 2000 different users and is being redesigned to provide easier and expanded access to user documentation and legacy information. Summaries and repair histories for all major pieces of PBIC equipment are now available online. Response information as well as the equipment information is being migrated to a web accessible database form. Links to this online format will be provided in the SCEC legacy document.

Pressure Solution Slip-faulting Associated with the Quatal Thrust Fault

Kevin Mass and Jan Vermilye
Whittier College

This study is based on the analysis of pressure solution strain structures to infer stress orientations. Sandstone and conglomerate outcrops located in Quatal Canyon (northern Ventura County, CA) have many types of pressure solution deformation structures. Small pressure solution slip-faults (cm to m in length) are a type of deformation structure that can be analyzed to infer the local and regional principal stresses. Field measurements of these faults are recorded at six locations in Quatal Canyon. These six data locations are then combined in order to determine the regional inferred stress axes.

The geometric and kinematic data are analyzed using the methodology of Michael (1984) and a program written by Allmendinger et al. (1992). The Michael (1984) analysis produces the orientation of the principal stress axes in the form of eigenvalues and eigenvectors. Allmendinger's program produces contour stereoplots of the P-axis (contraction) and T-axis (extension), as well as a fault plane solution plot representing the maximum strain directions for the combined data set.

The results of these analyses show the inferred stress and strain orientations at six locations throughout Quatal Canyon. The stress and strain orientations are displayed as stereoplots. The contraction and extension strain axes appear remarkably similar to the tension and compression stress axes, respectively. Therefore, it is valid to assume that the principal stress axes can be found using strain deformation structures. While a composite strain analysis indicates a typical thrusting regime, with sub-horizontal compression and near-vertical tension, individual outcrops show variability. A spatial explanation for this involves inhomogeneous stress around the fault due to the irregular shape of the Quatal fault. A temporal explanation involves translation of the Quatal fault along the San Andreas fault from the Garlock fault intersection to its present location.

Paleoseismologic Work in Progress on the San Andreas fault at the Plunge Creek Site, near San Bernardino, California

Sally McGill
California State University, San Bernardino

Excavations have continued at the Plunge Creek site within the past year. The original goal of the new excavations was to search for evidence for earthquakes older than the one exposed in trench 8, which is thought to be the most recent event (see Dergham & McGill, this volume). Within the past year, trench 4 was deepened from about 2.5 meters deep to 5 meters deep. Trench 4 reveals well stratified, granite- and gneiss-bearing fluvial gravel and sand from Oak Creek that interfingers with poorly stratified, gneiss-bearing colluvium from the mountain front. Several fault strands are visible in the lowest of the four tiers within this benched trench, and some of these faults probably extend up into the third tier beneath the ground surface. A laminated silt layer near the top of the 3rd tier is interpreted as filling and then overtopping a depression behind an uphill-facing scarp. A detrital charcoal sample from this silt layer has a calibrated age of AD 1420-1500 (2-sigma). Additional radiocarbon dates are pending, including others from this silt layer. Until these additional dates are available, it is not possible to judge how representative this single date is. No faults are visible above this silt layer, but the poorly stratified colluvium in the north end of the trench makes it difficult to preclude the possibility of younger events. Another silt layer in the lowest tier of trench 4 may have ponded behind a scarp from an earlier earthquake. Individual fault strands also appear to terminate at two other stratigraphic horizons with the trench. At this time, I do not consider these terminations of individual fault strands to be convincing evidence for additional earthquakes, but they do suggest

that possibility and serve as reminders that additional faulting events within this stratigraphic range can not yet be ruled out.

In April 2000 excavations began at trench 9, which was sited closer to the mouth of Oak Creek in an effort to find a place where the fault zone would intersect the well-stratified fluvial deposits from this drainage. Trench 9 does indeed lie entirely within the well-stratified deposits of Oak Creek. Faults are only visible in the lowest of the four tiers of this trench, and are most clearly visible on the east wall. The top of a poorly sorted fine sand layer (debris flow?) near the base of the third tier beneath the surface is clearly unfaulted for the entire length of trench 9. A detrital charcoal sample from above this layer has a calibrated age of AD 1425-1520 or AD 1575 to 1625. Additional radiocarbon dates are pending. Until they are available it is not possible to judge how representative this single date may be.

Dislocation Modeling of the East Coyote Anticline in the Eastern Los Angeles Basin

Daniel J. Myers, John L. Nabelek, and Robert S. Yeats
Oregon State University

The 1994 Northridge and 1987 Whittier Narrows earthquakes warned Los Angeles residents of the threat of earthquakes due to unmapped, blind reverse faults and emphasized the importance of identifying and characterizing blind reverse faults in assessing the seismic hazard to the region. The Coyote Hills in the eastern Los Angeles basin are the surface expression of blind reverse faulting. Folded Quaternary strata indicate that the hills are growing, and that the faults underlying them are active. Detailed subsurface mapping in the Hualde dome of the East Coyote oil field shows that the previously mapped Stern fault is predominantly an inactive strike slip fault with approximately 1.2 km of left-lateral displacement measured from offset pinchouts of Delmontian and Repetto strata. A major south flank fault is absent in the Anaheim dome of the East Coyote oil field. Structural similarities between the Stern fault and the South Flank fault of West Coyote support the hypothesis that they are the same fault. These results suggest that the fault responsible for growth of the East and West Coyote oil fields does not cut wells in either oil field. Elastic dislocation modeling of the folded upper Repetto-Pico and Pico-San Pedro contacts suggests that the best fitting thrust fault would have 3000 m of reverse displacement since the beginning of deposition of the Pico member of the Fernando Formation, and 1400 m of reverse displacement since the beginning of deposition of the San Pedro Formation. Using ages determined by interpolating between a dated ash bed (Nomlaki tuff) in the upper Repetto member and the Brunhes-Matuyama chron boundary yields slip rates of 1.0 mm/yr based on the folded Pico-upper Repetto contact and 1.2 mm/yr based on the folded San Pedro-Fernando contact.

Constraints on the SCEC 3D velocity Model from Gravity Data: Two Dimensional Gravity Modeling of the Central and Eastern Transverse Ranges in the Los Angeles Region

Nancy Natek and Mousumi Roy
University of New Mexico

The goals of this project are to test the consistency of crustal seismic velocity structure and gravity data in the Transverse Ranges. Following earlier work by Roy and Clayton, we use 2D gravity models based on density structures inferred from crustal tomography. We use version 2 of the Southern California Earthquake Center (SCEC) velocity model and an empirically derived scaling relation between seismic velocities and density. The density structures thus inferred are used to forward model gravity along 2D profiles.

We plan to compare predicted gravity along four 2D topographic profiles across the central and eastern Transverse Ranges to the observed gravity. This poster shows our preliminary results for ONE of the profiles, with work in progress on the other three profiles. We find that, in general, gravity data and crustal tomographic structures are consistent with each other. However, we find that there are significant misfits in the eastern LA Basin and in the Mojave Desert. In order to obtain a good fit in the LA Basin, we were required to increase average densities in the basin, reducing the size of the negative Bouguer signal from basin sediments. The gravity anomaly in the Mojave Desert section of the profile is more negative than predicted, suggesting the presence of a subsurface crustal mass deficit. This region can be well-matched by increasing the depth to the Moho under the Mojave Desert, or, as shown by Roy and Clayton, by reducing average crustal densities in the Mojave.

Re-Evaluation of Fault Slip, Geodetic Strain, and Seismic Hazard Studies in the Light of Active Subsidence, Compaction, and Footwall Deformation

Craig Nicholson, Christopher C. Sorlien and Marc J. Kamerling

University of California, Santa Barbara

Jean-Pierre Gratier, Universite Joseph Fourier, Grenoble

Leonardo Seeber, Lamont-Doherty Earth Observatory, Columbia University

Across Ventura and Los Angeles basins, high rates of oblique crustal strain have been measured by space geodesy. This deformation represents a significant seismic hazard and is presumed to be largely accommodated by active faulting, folding, and hanging-wall uplift. Most models used to infer subsurface geometry, or used to resolve geodetic strain into fault slip typically presume rigid footwall blocks, non-deforming planar fault surfaces, and deformation that is largely restricted to the hanging-wall. Preliminary results from the 1999 M7.6 Chi-Chi earthquake suggest that such models are not unreasonable. In California, however, deep, subsiding basins are often bounded by oblique reverse faults that thrust early-Cenozoic and older rocks over young, unconsolidated sediments, suggesting that footwall deformation, subsidence and compaction may play an important role in accommodating regional tectonic strain. Even in the absence of active crustal shortening, 3D sediment compaction alone will produce surficial motions that mimic deep fault slip. This implies that inferred slip rates and the derived seismic hazard can be under- or over-estimated depending on what model assumptions are made. For example, in the presence of regional subsidence, reference to sealevel or paleo-sealevel can underestimate the rate of tectonic uplift (and fault slip) if subsidence is ignored. On the other hand, differential subsidence, pressure solution, and 3D compaction of footwall sediments relative to hanging-wall basement rocks can lead to increased vertical separation and fault rotation about horizontal axes, even in the absence of active fault slip. Such effects would contribute to net horizontal and vertical motions in both geologic and geodetic data, resulting in overestimates of the inferred seismic hazard. Preliminary results suggest that these horizontal and vertical motions may be as large as 1 to 2 mm/yr.

Variation of Dynamic Rupture Velocity in a Heterogeneous Stress Field

Kim B. Olsen, University of California, Santa Barbara

Eiichi Fukuyama, National Institute for Earth Science and Disaster Prevention, Tsukuba, Japan

We have investigated the transition from sub-Rayleigh to super-shear rupture velocity in a heterogeneous stress field by numerical experiments using the boundary integral equation method. In order to measure the rupture velocity independent of the rupture initiation process, we assume a long rectangular fault. Slip is assumed to occur along the long dimension of the fault, thus the in-plane rupture dominates. We set up a background stress field which makes the rupture

propagate with sub-Rayleigh speed by assuming appropriate slip-weakening frictional coefficients. Under this condition, we place an asperity at the middle of the fault where the initial stress is raised by a certain amount. When the rupture encounters the asperity it either accelerates to a super-shear velocity or it maintains the sub-Rayleigh speed. We have systematically examined the criterion to excite the super-shear velocity by changing the size and amplitude of the asperity.

We observe a critical boundary between sub-Rayleigh and super-shear rupture propagation. This boundary includes two corners between which the critical boundary is located where the product of the width and height of the asperity becomes constant. This result is expected since the rupture velocity is determined by the balance between the fracture energy consumed at the crack tip and the supplied elastic strain energy released by the stress drop on the fault. The corner corresponding to the smaller amplitude / larger width of the asperity is produced by the critical stress level for a homogeneous initial stress distribution. This could be interpreted that as the asperity width becomes large enough, the rupture behaves as the asperity dominates the stress field. The corner of the critical boundary corresponding to the larger amplitude / smaller width might be produced by insufficient spatial resolution in the stress field compared to the critical slip weakening distance (D_c).

Our results implicitly show that if the spatial wavelength of the stress distribution is short, locally high initial stress does not excite super-shear rupture. However, if the wavelength becomes long, asperities of high stress can produce super-shear rupture propagation. The short-wavelength stress heterogeneity is insensitive to the rupture acceleration and thus rupture remains stable with sub-Rayleigh wave velocity.

Hybrid Modeling of Curved Fault Radiation in a 3D Heterogeneous Medium

Kim B. Olsen, University of California, Santa Barbara

Eiichi Fukuyama, National Institute for Earth Science and Disaster Prevention, Tsukuba, Japan

Raul Madariaga, Ecole Normale Supérieure, Paris

We are in the process of the development of a hybrid method for flexible and efficient modeling of dynamic rupture propagation and its radiation in a heterogeneous three-dimensional medium. The dynamic rupture propagation is computed using the boundary integral equation (BIE) method. The computation of radiated waves outside the fault is carried out by an efficient fourth-order staggered-grid finite-difference (FD) method. The hybrid method enables dynamic modeling of rupture propagation on curved or multi-segmented faults in laterally and vertically heterogeneous earth models with an accurate free-surface. In addition modeling dynamic rupture on a single fault, the hybrid method can be used to model the statistics of recurrent ruptures on multiple, arbitrarily-shaped fault systems. Finally, the method may be used to improve the accuracy of kinematic source implementation on extended faults. Here, we show preliminary results for the rupture propagation and radiation from a spontaneous rupture on a curved fault.

Accuracy of the Explicit Planar Free-Surface Boundary Condition Implemented in a Fourth-Order Staggered-Grid Velocity-Stress Finite-Difference Scheme

Kim B. Olsen, University of California, Santa Barbara

E. Gottschammer, Karlsruhe Universitaet, Karlsruhe

We compare the accuracy of two implementations of the explicit planar free-surface boundary condition for 3-D fourth-order velocity-stress staggered-grid finite-differences, $1/2$ grid apart vertically, in a uniform halfspace. Due to the staggered grid, the closest distance between the free surface and some wavefield components for both implementations is $1/2$ grid spacing.

Overall, the differences in accuracy of the two implementations are small. When compared to a reflectivity solution computed at the staggered positions closest to the surface, the total misfit for all three components of the wavefield is generally found to be larger for the free surface co-located with the normal stresses (FS1), compared to that for the free-surface co-located with the xz and yz stresses (FS2). At an epicentral distance/hypocentral depth (EDHD) of 10, we find the total misfit for FS2 to be about 25% smaller compared to that for FS1. However, this trend is reversed when compared to the reflectivity solution exactly at the free surface (the misfit encountered in staggered-grid modeling). When the wavefield is averaged across the free surface, thereby centering the staggered wavefield exactly on the free surface, the free surface condition FS2 generates the smallest total misfit for increasing epicentral distance. At an EDHD of 10 the total misfit of FS2 is about 15% smaller than that for FS1, mainly controlled by the misfit on the Rayleigh wave. Our recommendation is to use the averaged free surface condition FS2 which generally produces the most accurate results.

Three Dimensional Paleoseismic Investigation on the South Break of the Coyote Creek Fault, Southern California

A. Orgil and Tom K. Rockwell
San Diego State University

High-resolution paleoseismic studies have been utilized to better understand segment controls on the rupture history of the southern San Jacinto fault (Rockwell et al., 2000). Trenches have been excavated at seven sites along the southern San Jacinto fault zone to better understand the relationship between the Coyote Creek (CCF) and Superstition Mountain (SMF) faults. Our study, located on the south break of the Coyote Creek fault, has the unusual status that it is possibly the transitional element between the two above noted faults to the northwest and southeast, respectively. Detailed three-dimensional paleoseismic study on this break, exposing paleo-surfaces by removing sets of sediment layers from above key contacts, has been a great tool for recognizing each individual earthquake and determining the slip per event in order to better understand fault segmentation in conjunction with other studies in the area.

In the main two dimensional trench excavated across to the 1968 rupture trace, we exposed about 10 lacustrine discrete deposits representing highstand phases of ancient Lake Cahuilla. Unfortunately, between the third lake and the previous one believed to be the fourth lake, we found a depositional hiatus of about 2500-3000 years. Nevertheless, five events can be demonstrated above that hiatus. Evidences for those events were established and quantified by excavating trenches both parallel and across to the 1968 fault trace. Three-dimensional trenching analysis by removing sediments layer by layer confirmed that the 1968 slip is the only event recognized as post-dating the 300 year-old lake stand. The penultimate event is represented by liquefaction and is recognizable at the Middle Break site to the north as well as at Carrizo Wash and Shoreline sites to the south (Rockwell et al., 2000). The third event back appear to shatter a 15 meters wide zone, with clear evidences of several faults truncating up to the same stratigraphic level. Likewise, the fourth and fifth events also represented by wide zones of faulting and are correlated to the same events described for Superstition Mountain fault at Carrizo and Northern Shoreline sites.

From these observations it appears that only some of the moderate 1968-type earthquakes with short recurrence intervals rupture the southern segment of the Coyote Creek fault, and almost all of the less frequent larger Superstition Mountain events blast through this segment. With the application of concepts of the relationship between seismicity at the surface and at depth, the above noted assumption is important in understanding of fault segmentation and the forecasting of future earthquakes.

Refinement of Near-Surface P and S Wave Velocities in the SCEC 3-D Velocity Model Using 3-D Waveform Modeling

Tracy Pattelena, University of California, Santa Cruz
Kim Olsen, University of California, Santa Barbara

An important part of ground motion studies is to predict full theoretical seismograms for an earthquake at a given site. Our study focuses on the ground motion in a portion of the San Fernando Valley (SFV) where control on the near-surface S wave velocity, a critical parameter for accurate prediction of strong ground motion, is mostly indirect and in many areas not well constrained. We use 1-Hz 3D finite-difference simulations to propagate waves for a M=5.1 Northridge aftershock through two 10 km by 10 km by 5 km models of the SFV subsurface: (1) a subset of the SCEC southern California reference 3D seismic velocity model (version 2.0), and (2) model 1 modified with slower velocities in the near-surface material taken from a tomographic model. Model 2 contains near-surface P and S velocities up to 70% and 50% less than those of model 1, respectively, in the upper 500 m. Compared to the response of model 1, the tomographically refined model (2) generates peak ground velocities (PGV) and cumulative kinetic energies (CKE) up to a factor of two in localized areas of the model. While the synthetics for model 2 improve the fit to data at the five stations only slightly, our simulations suggest that version 2.0 of the SCEC velocity model is not complex enough to reproduce the 1-Hz duration and peaks in the SFV basin.

Inversion of Seismic Fault Zone Waves in the Rupture Zone of the 1992 Landers Earthquake for High Resolution Velocity Structure at Depth

Zhigang Peng and **Yehuda Ben-Zion**, University of Southern California
Andrew J. Michael, United States Geological Survey, Menlo Park

Waveform modeling of seismic fault zone (FZ) trapped waves provides a potentially high-resolution means of investigating seismic velocities, seismic attenuation, width of FZ, and structural continuity at depth. The 1992 Landers aftershock sequences generated a wealth of seismic data. From a digital waveform data of 238 Landers aftershocks [William Lee, per. Com., '99], we identified about 60 events with good candidate trapped waves. Each event was recorded by 33 three-component, short-period (2 Hz), L-22 seismometers. In general, clear trapped wave candidates are generated when both event and receiver are close to or in the FZ, and the S-P time is smaller than about 2 seconds. Most of the Landers trapped wave energy is in the 3 to 6 Hz frequency range.

The candidate FZ waveforms are modeled with a genetic inversion algorithm (GIA) that maximizes the correlation between observed and synthetic waveforms [Michael and Ben-Zion, ms. in preparation]. The synthetic seismograms are generated with a two-dimensional analytical solution for a scalar wavefield in a layered vertical FZ between two quarter-spaces [Ben-Zion and Aki, BSSA, '90; Ben-Zion, JGR, '98]. When enough models (more than 5000) are tested, the GIA provides very good fits for FZ waveforms with a model consisting of a single uniform FZ layer in a half space. However, it is possible to get equally good fits for a wide range of parameters. This is due to significant trade-offs between FZ width, propagation distance along the fault, source offset from the fault, velocity contrast, and attenuation. Additional uncertainties stem from the possibility that the candidate trapped waves are produced by shallow structure. To overcome these difficulties we are developing now a multi-faceted analysis that combines seismic travel time tomography to provide regional information, array analysis techniques to determine the direction the wavefield comes from, and simultaneous GIA modeling of multiple FZ waveforms. Results from the combined analysis will be presented in the AGU meeting.

Interaction between the Landers and Hector Mine earthquakes from space geodetic techniques and boundary element modeling

Evelyn Price and Roland Burgmann
University of California, Berkeley

The October 16, 1999 M7.1 Hector Mine earthquake ruptured only 30 km to the east of the 1992 M7.2 Landers earthquake in a region whose individual faults break during an earthquake of this size every 1500-5000 years. The proximity of these two earthquakes in space and time suggests that they are mechanically related. However, using a simple Coulomb failure criterion to test the hypothesis that the Hector Mine earthquake was triggered by the Landers earthquake has failed to show that static stress interaction is the dominant process linking the two events. In fact, the Hector Mine rupture was nearly everywhere moved away from right-lateral shear failure by stress changes resulting from the Landers earthquake and experienced unclamping only on its northern half.

We hypothesize that, at the time of the Landers earthquake, the faults involved in both the Landers rupture and the Hector Mine rupture were near failure and that the occurrence of the Landers earthquake delayed the Hector Mine earthquake. We test this hypothesis by combining detailed distributions of earthquake slip in elastic half-space boundary element models. Detailed distributed slip models are first obtained from joint inversions of InSAR and GPS data. We then compute how the background stress was changed by the occurrence of each earthquake and compare this change to independent estimates of equivalent regional strain rate and direction in the Mojave before Landers. From this analysis, we can determine a range of delay times between the two earthquakes and examine the possibility of this simple explanation for earthquake interaction.

Southern California 2D Wavefield Reconstruction

Kenton Prindle and Toshiro Tanimoto
University of California, Santa Barbara

Southern California high-density network data provides an opportunity to view the seismic wavefields as time-varying two-dimensional fields at the surface of the Earth. The primary goals of this project is to bring forth media friendly methods to display wave propagation in Southern California as well as provide a new way in which to visualize wave propagation in areas of high complexity and see the spatial extent of seismic disturbances directly. The data set consists of contributions from AMOES, USGS, and TERRASCOPE and the number of stations reach more than 100 for events in year 2000.

There are some characteristics that one can immediately notice in the reconstructed wavefields; The first such feature is the basin resonance. After the passage of P-wave wavepackets, the Los Angeles basin shows many more cycles of oscillations that are clear indication of basin oscillations. These features are also recognizable in a stack of one-dimensional time series for such stations as SWS (Santa Monica), USC and COO (Compton), but movies depict such features more dramatically. Similar features can be seen in the Indian Well Geothermal region.

The second feature is the wavefront split, particularly from earthquakes from South Pacific. P-wave wavefront that arrives from due west shows clear split, on the order of 0.5 seconds, between north and south of the transverse range. This split also shows up in the detailed timing measurement at each station, which we also perform in our algorithm. There are some indications that basins are the cause of wavefront break-up, probably because seismic velocities are slow in basins.

We will discuss other features and limitations of our approach.

Elastodynamic Crack-Tip Fields for Shear Ruptures and Off-Axis Secondary Faulting

Alexei Poliakov, University of Montpellier II, France
James R. Rice, Harvard University

We consider singular crack or slip-weakening rupture models for which the residual dynamic shear strength τ_r on the fault can be considered as effectively constant at distances from the rupture tip larger than the slip-weakening (process) zone size. An important feature of the dynamic near-tip stress field is the growth of the maximum off-fault shear stress τ_{off} with an increase of velocity of rupture propagation v_r . At least according to the leading term in the singular crack solution, the ratio of τ_{off} to the stress τ_{main} on the main fault plane, at a fixed distance from the rupture tip, approaches infinity as v_r approaches the limiting crack speed c_{lim} (which is the Raleigh speed c_R for mode II and the shear speed c_s for mode III). For example, for mode III, this ratio is

$$\tau_{\text{off}} / \tau_{\text{main}} = [1 - (s^2)/2]^{1/2} / [1 - s^2]^{3/4}.$$

where $s = v_r / c_s$. High off-fault stress may contribute to the explanation of the following: (i) secondary faulting (activation of damaged border zone, like observed along the exhumed San Gabriel and Punchbowl faults), (ii) bifurcation of fracture path and self-arrest of a crack as $v_r \rightarrow c_{\text{lim}}$, and (iii) jump of a rupture to a sub-parallel segment (e.g., Landers and Izmit events).

To study the location and directions of highest stressing on secondary faults we plot, for the singular crack model, (i) isolines of the maximum ratio of shear stress to Coloumb shear strength for the local normal stress, and (ii) directions of potential fractures (planes on which that ratio is maximum) around a crack tip. This augments a study by Rubin and Parker (USGS O-F Rpt. 94-228). Coordinates are scaled with what would be the length of the slip-weakening zone (w_0) at $v_r = 0+$, which is estimated to be 5 to 100 meters (based on 0.5 - 5 MJ/m² fracture energy and 50 - 100 MPa peak to residual strength drop). For given pre-stress states, we varied v_r and τ_r .

For both rupture modes we found that the zone of potential secondary faulting (i) contracts in front of the rupture while (ii) it stretches in the direction perpendicular to the main fault as $v_r \rightarrow c_{\text{lim}}$ and (iii) decreases (in all directions) with an increase of τ_r . At low τ_r (relative to the slip-weakening strength drop), directions of the secondary faults tend to be perpendicular to the main fault, and for high τ_r they tend to be parallel. The main difference between modes is an asymmetry of secondary faulting for mode II compared to symmetrical faulting for mode III.

To conclude, our calculations predict activation of faults in the damage zone of the size in the range of (0.1 - 1) w_0 (i.e. 0.5 - 100 meters) in vicinity of the main fault. The directions of secondary fractures depending on the mode of rupture, τ_r and pre-stress state.

The study is in preparation for finite-element modeling of spontaneous activation of secondary faults during dynamic rupture.

Seismic Hazard Assessment of the San Joaquin Hills Using GIS

Daniel E. Raymond and Lisa Grant
University of California, Irvine

The San Joaquin Hills region of Orange County is undergoing rapid commercial and residential development. The anticlinal structure of the area is likely due to a combination of tectonic uplift and seismic activity on local fault systems. The goal of this project was to determine the hazards of the fault zones in the area while there may still be time to translate these findings into sound planning practices for the area.

Geotechnical and fault investigation reports were collected for as many sites as possible in the San Joaquin Hill region. The findings from these reports were then collected and transferred to a GIS-based map. This map was designed in such a way to allow a convenient regional view of report coverage and findings, and was linked to a more complete bibliography created to display report titles, conclusions and relevant trench logs. Because little conclusive or comprehensive information was found during this study, a strong case can be made for the need for further fault investigations in the San Joaquin Hills region.

Seismic Gaps and Earthquakes

Yufang Rong, David D. Jackson and Yan Y. Kagan
University of California, Los Angeles

The "seismic gap" model of McCann et al. [1979] ascribes earthquake potential to 125 Pacific Rim zones. Nishenko [1991] updated and revised the model, adding probability estimates and characteristic earthquake magnitudes. After twenty and ten years, respectively, sufficient data exist to test the models rather conclusively. For the McCann et al. forecast, we counted qualifying earthquakes in the several categories (colors) of zones. We assumed a probability consistent with the model (e.g., red zones have twice the probability of green zones) and tested against the null hypothesis that all zones have equal probability. The gap hypothesis can be rejected with a high confidence: the data suggest that the real seismic potential is lower in the red zones than in the green ones. For the Nishenko hypothesis, we tested the number of filled zones and the likelihood ratio relative to a Poissonian null hypothesis with a modified Gutenberg-Richter magnitude distribution. The new seismic gap model predicted 17.5 zones filled by characteristic earthquakes during 1989-1999. Only 5 zones were actually filled, an outcome of miniscule probability according to the gap model. If we admit earthquakes 0.5 units below the tabulated characteristic magnitudes, then 12 or 13 zones were filled, consistent with the gap hypothesis. However, for either threshold, the new seismic gap hypothesis can be rejected with 95% confidence in favor of the null hypothesis. We also test the modified Gutenberg-Richter magnitude distribution against the Harvard CMT catalog by a likelihood test. For both McCann et al.'s zones and Nishenko's zones, the modified G-R distribution passes the test. The seismic gap models assume that most slip occurs in characteristic-size earthquakes. However, the magnitude distributions in McCann et al's red, orange, and green zones all had the same shape as the global distribution. This fact suggests that the characteristic earthquake hypothesis is not valid, or that the estimated characteristic earthquake size was severely underestimated in Nishenko [1991]. The rate of earthquakes over magnitude 5.8 in the several types of zones is closely proportional to the plate-tectonic moment rate, implying that the long-term rate of large earthquakes is proportional to the observed rate of moderate ones. The long-term moment rate depends on the overall earthquake rate as well as the slope of the magnitude distribution, the upper magnitude limit, the degree of seismic coupling, and the stationarity of earthquake occurrence. The observed proportionality between plate-tectonic moment rate and decade-scale earthquake rate suggests that the effective coupling and the shape of the magnitude distribution are nearly constant; only the overall seismicity varies much from place to place.

Late Holocene Timing of the Penultimate Earthquake on the Lavic Lake Fault, Mojave Desert, Southern California: Preliminary Results

Michael J. Rymer, U.S. Geological Survey, Menlo Park
Gordon Seitz, Lawrence Livermore National Laboratory

Trench exposures were dug and analyzed at four sites across the Lavic Lake fault on Lavic Lake playa, near the northern end of the 1999 Hector Mine rupture; exposures in one of

these trenches revealed evidence of the penultimate earthquake. Three of the four trenches were dug across the 1999 rupture; the fourth trench, trench D, the one with evidence of the penultimate event, was across a vegetation lineament that did not rupture during the 1999 event. Aerial photographs of the area show that the vegetation lineament that did not rupture in 1999, along with other vegetation lineaments that did rupture, has persisted for several decades, at least back to 1951. The four trenches ranged in depth from about 2.2 to 4.0 m; trench D was the shallowest. Strata exposed in trench D revealed horizontal bedding along with local warping and offset by faults. Faults revealed in the trench exposures line up with the vegetation lineament at the ground surface and indicate a zone of shears with a width of about 1 m. A depositional contact about 80 cm below the ground surface acts as the upward termination of fault breaks in trench D. Thus, this contact may be the event horizon for a surface-rupturing event prior to 1999. Carbon 14 dating of detrital charcoal samples from one sample above and two below the event horizon (1940 +/- 40, and 1730 +/- 40 and 3040 +/- 40 radiocarbon years B.P., respectively) indicates that the earthquake associated with the faulting occurred a maximum of 1700 to 2000 years ago. The 1300-year age variation between the two samples below the event horizon suggests the potential for long residence time of detrital charcoal in the area. This, considered with a lack of bioturbation, suggests that the age estimates are maximum bounding ages and the recognized penultimate event may be considerably younger. A late Holocene age of the probable penultimate event at trench D is significantly younger than for the penultimate event as indicated at more southerly trench sites across the 1999 rupture.

Repeating Earthquakes as Low-Stress-Drop Events at a Border between Locked and Creeping Fault Patches

Charles G. Sammis, University of Southern California
James R. Rice, Harvard University

The source of repeating earthquakes on creeping faults is modeled as a weak asperity at a border between much larger locked and creeping patches on the fault plane. The decrease in stress concentration with distance x from the boundary is shown to lead directly to the observed scaling between the average repeat time and average scalar moment for a repeating sequence. The stress drop in such small events at the border depends on the size of the large locked patch. For a circular patch of radius R and representative fault parameters, we calculate stress drops between 0.1 and 1.0 MPa (1-10bars) for R between 5 km and 100 m. These low stress drops are consistent with estimates of stress drop for small earthquakes based on their seismic spectra. However, they are orders of magnitude smaller than stress drops calculated under the assumption that repeating sources are isolated stuck asperities on an otherwise creeping fault plane, whose seismic slips keep pace with the surrounding creep rate. Linear streaks of microearthquakes observed on creeping fault planes are trivially explained by the present model as alignments on the boundaries between locked and creeping patches.

Comparison of Seismicity on Locked and Creeping Segments of the San Andreas Fault near Parkfield, CA

Charles G. Sammis, University of Southern California
M. Wyss, University of Alaska
Stefan Wiemer, ETH Hoenggerberg; Zurich
R. M. Nadeau, Lawrence Berkeley Laboratory and University of California, Berkeley

The b -value, fractal dimension, and stress tensor orientation were measured on both locked and creeping segments of the San Andreas Fault near Parkfield, CA. The locked segment near Middle Mountain is characterized by a low b -value ($b \sim 0.5$), a low fractal dimension ($D \sim 1.0$)

and a principal stress σ_1 oriented at a high angle (60° - 90°) to the fault plane. The creeping segment to the north is characterized by a higher b-value ($b \sim 1.3$ - 1.5), a higher fractal dimension ($D \sim 1.7$) and a principal stress σ_1 oriented approximately 45° to the fault plane. These observations are consistent with higher stress and lower fluid pressures at the asperity relative to the creeping segment. Stress orientations suggest fluid pressure near lithostatic in the creeping segment. At the asperity we observe $D=2b$ expected for self-similar events and constant stress drop. The low D and b values at the asperity can be interpreted either as reflecting high stress or as a consequence of a linear distribution of hypocenters at the edge of the asperity.

Hector Mine Earthquake: Vector Coseismic Displacement from ERS InSAR

David T. Sandwell, Lydie Sichoix, and Bridget Smith
University of California, San Diego

Two components of fault slip can be uniquely determined from two ERS line-of-sight (LOS) measurements by assuming that the fault-normal component of displacement is zero. We use this approach with ascending and descending co-seismic interferograms to estimate surface slip along the Hector Mine earthquake rupture. The LOS displacement is determined by visually counting fringes to within 1 km of the outboard ruptures. These LOS estimates and uncertainties are then transformed into strike- and dip-slip estimates and uncertainties; the transformation is singular for a N-S oriented fault and optimal for an E-W oriented fault. In contrast to our previous strike-slip estimates, which were based only on a descending interferogram, we now find good agreement with the field geology measurements of slip. The ascending interferogram reveals significant dip-slip (~ 0.5 m) that reduces the strike-slip estimates by 1-2 m especially along the northern half of the rupture. A spike in the strike-slip displacement of more than 6 m occurs in central part of the rupture. This large offset is confirmed by sub-pixel cross-correlation of features in the before and after amplitude images. Our main conclusion is that at least two look directions are required for accurate estimates of surface slip even along a "pure" strike-slip fault; models and results based only on a single look direction could have major errors.

We use these estimates of strike-slip and dip-slip along the rupture as a starting point for dislocation modeling. Initial models assume the surface slip varies with depth in a variety of simple vertical positive modes and we then solve for the best fitting vertical structure. Results will be compared with the full interferograms as well with GPS vector displacements. So far the major anomalous feature is a zone of uplift in the epicentral area where post-seismic interferograms show 65 mm of continued rebound. (see <http://topex.ucsd.edu/hector>)

The Southern California Integrated GPS Network (SCIGN) and The Scripps Orbit and Permanent Array Center (SOPAC), Supporting Involvement

**Michael Scharber, Yehuda Bock, Peng Fang, Brent Gilmore
Paul Jamason, Rosanne Nikolaidis, and Matthijs van Domselaar**
University of California, San Diego

The Scripps Orbit and Permanent Array Center (SOPAC) was established to collect, archive, analyze, and disseminate data and data products from various continuous GPS arrays around the world. Specifically, supporting the SCIGN continuous GPS network is the top priority at SOPAC. With over 200 stations already in place and producing data on a daily basis, building and maintaining an efficient and effective data storage and information management system for SCIGN has been, and will continue to be one of SOPAC's top priorities. Already one of the largest homogeneous GPS networks in the world, and still growing, SCIGN continues to provide the GPS community with high-quality continuous GPS data, accurate and timely site information

and metadata, and insightful scientific products and research opportunities. The focus of this poster is to point out the magnitude and importance of SCIGN in the global GPS community, from an archive and information management perspective, as well as highlight some of the various means employed at SOPAC in order to stay in front of SCIGN's development. By providing useful and intuitive on-line services to SCIGN analysts and information managers alike, SOPAC, in direct partnership with the Jet Propulsion Laboratory and the United States Geological Service - Pasadena, hopes to make SCIGN a model for the continuous GPS community.

Seismogenic Faulting at the Juncture of the two Mw7+ 1999 Ruptures of the North Anatolian Transform in Northwestern Turkey

Leonardo Seeber and John G. Armbruster, Lamont-Doherty Earth Observatory,
Naside Ozer, The University of Istanbul
Serif Barif and Mustafa Aktar, Kandilli Observatory of Bugazici University, Istanbul
Yehuda Ben-Zion, David Okaya, and Zhigang Peng, University of Southern California

We operated a temporary 10-station seismic network along and around the Karadere segment of the 1999 rupture on the North Anatolian transform for about 1/2 year, from a week after the Iznik mainshock on 17 August, to 3 months after the second mainshock on 12 November. The Karadere rupture is confined in time and space between the two main ruptures: It occurred several seconds after the Iznik rupture and 86 days prior to the Duzce rupture. We base our preliminary observations on about 3000 quality-selected hypocenters and 500 focal mechanisms. We are improving these data by the cross-correlation technique and by including data from additional seismic stations. The Karadere segment strikes N70E, about 20° from the local E-W trend of the right-lateral transform. This transpressive geometry is not reflected by the purely transcurrent subvertical rupture, but is manifested by relative high topography and by thrust earthquakes. The relatively small 1.5 m right-lateral surface displacement and a remarkable scarcity of aftershocks with corresponding kinematics may manifest slip-induced locking of this segment by increased fault-normal compression. Both ends of the segment are marked by changes in strike, gaps in surface rupture, and intense clusters of aftershocks involving many faults. These clusters are sharply bounded by surfaces extrapolated eastward and westward, respectively, from the Iznik and Duzce ruptures. Some of the secondary seismogenic faults may accommodate transform motion by clockwise rotation. Most of the aftershocks along the Karadere segment are concentrated on a subhorizontal 2-3km-wide strip marking the 13-to-15-km-deep floor of the seismicity. Focal mechanisms suggest a subhorizontal plane with slip parallel to the rupture. This kinematics is consistent with a vertical right-lateral rupture intersecting a detachment and stepping to the north below it. Seismicity on this proposed detachment propagated eastward intersecting the future Duzce rupture in a burst of small events during the first few days of November. During the next ten days seismicity spread over the extreme eastern portion of the November 12 rupture. This change in the pattern of seismicity may manifest a strain event that triggered the Duzce mainshock.

The Edges of Large Earthquakes and the Epicenters of Future Earthquakes: Stress Induced Correlations in Elastodynamic Fault Models

Bruce E. Shaw
Lamont-Doherty Earth Observatory

Fault models can generate complex sequences of events from frictional instabilities, even when the material properties are completely uniform along the fault. These complex sequences arise from the heterogeneous stress and strain fields which are produced through the dynamics of repeated ruptures on the fault. Visual inspection of the patterns of events produced in these models shows a striking and ubiquitous feature: future events tend to occur near the edges of

where large events died out. In this paper, we explore this feature more deeply. First, using long catalogues generated by the model, we quantify the effect. We show, interestingly, that it is an even larger effect for future small events than it is for future large events. Then, using our ability to directly measure all aspects of the model, we find a physical explanation for our observations by looking at the stress fields associated with large events. Looking at the average stress field we see a large stress concentration left at the edge of the large events, out of which the future events emerge. Further, we see the smearing out of the stress concentration as small events occur. This shows why the epicenters of future small events are more correlated with the edges of large events than are the epicenters of future large events. Finally, we discuss how results from our simple model may be relevant to the more complicated case of the Earth.

Seismic Reflection Images and 3D Structures Model of Blind-Thrust and Strike-Slip Faults Systems in the Los Angeles Basin

John H. Shaw, Andreas Plesch, Carlos Rivero, Christiane Stidham, and M. Peter Seuss
Harvard University

We define the subsurface architecture of major fault systems in the Los Angeles basin, with an emphasis on blind thrusts, through the analysis of a regional seismic reflection transect and the development of three-dimensional structural models. With SCEC funding, we constructed a regional seismic reflection transect composed of four 2-D reflection profiles and part of a 3D seismic survey that were provided by petroleum industry sponsors. The transect, which integrates relocated earthquakes, focal mechanisms, and well control, images several large and potentially seismogenic fault systems (Palos Verdes, Newport-Inglewood, Compton, Elysian Park, Puente Hills, Whittier, etc.) that threaten the Los Angeles metropolitan region. On the south end of the transect, the Palos Verdes fault system is defined by steeply dipping (strike-slip) faults and Pliocene contractional folds above a southwest-dipping fault ramp. The deep ramp is a reactivated Neogene normal fault and is illuminated by relocated seismicity. The style of shallow deformation is suggestive of strain partitioning above a deep, oblique-slip fault ramp. In the center of the transect, the Wilmington anticline is underlain by a thrust that ramps upward from the Compton-Los Alamitos blind-thrust system. The northern basin is characterized by an imbricate thrust stack, which includes the Elysian Park, Puente Hills, Las Cienegas, and San Vincente faults. To define the three dimensional geometry of these blind thrusts, and their interactions with active strike-slip faults, we constructed three-dimensional fault models in the northern LA basin and in the Inner California Borderlands. These models illustrate the size and geometric segmentation of blind-thrust faults, which influence estimated earthquake sizes and seismic hazards.

Long-term Earthquake Forecast based on Geodetic Data for Southern California

Zheng-Kang Shen and David D. Jackson
University of California, Los Angeles

We use geodetic strain rates to estimate earthquake potential in southern California. We first compile a data set of long-term strain rates using the most recent crustal deformation model from the Southern California Earthquake Center (SCEC), results from two USGS GPS profiles, and strain rates based on triangulation and trilateration. The SCEC model covers most of southern California. The USGS profiles cross the Parkfield section of the San Andreas fault (Murray et al., 2000) and the central section of the Eastern California Shear Zone (Gan et al., 2000). The triangulation and trilateration data (Sauber et al., 1994) help to define the strain rate

prior to the Landers earthquakes. We then make corrections for transient strains following M7 and larger earthquakes using known rupture parameters and a visco-elastic earth model.

We estimate the probability of earthquake occurrence per unit area, time, and magnitude assuming that the normalized earthquake magnitude distribution is spatially invariant and the long-term earthquake rate is proportional to the maximum shear strain rate.

We then compare the estimated earthquake rate with the historical catalog. The geodetically derived earthquake potential correlates well with the historic occurrence of M5.5 and larger earthquakes. The earthquake potential estimate is correlated even better with the spatial distribution of earthquake moments, perhaps because larger events tend to occur along major faults where the strain rate is concentrated.

Our test was retrospective, and we might obtain overly optimistic results if the historic earthquakes actually caused the strain concentration and if we did not adequately correct for post-seismic strain. Only prospective tests in southern California and elsewhere can show the true predictive power of geodetic strain measurements, so we devise likelihood tests for use with future earthquake data.

Co-Seismic Static Deformation from the October 16, 1999 M7.1 Hector Mine CA Earthquake

Mark Simons, Y. Fialko, and Ji Chen
California Institute of Technology

We use interferometric data acquired by the ERS-1/2 satellites to infer slip characteristics of the Hector Mine Earthquake. We use data from both ascending and descending orbits and incorporate both the phase and the azimuth offset information derived from the amplitude image. These two components of the deformation field are by definition orthogonal. To validate the data, we calculate both the satellite line-of-sight and along track components of the displacement field measured by available GPS data. We find excellent agreement between the two data types. In many areas along the rupture, we are able to follow the line-of-sight (LOS) displacement field to very near the surface rupture zone (about 100 m). Our current inversions for fault slip assume an elastic half space with the initial fault geometry prescribed based on the geologically mapped surface rupture, and interferometric data (e.g., phase, azimuthal offsets, and decorrelation patterns). The geometry is subsequently refined through iteration in the inversions to allow for sub-vertical dip of the fault plane. To reduce the computational burden, both the phase and azimuth data are sampled using a sampling density that is proportional to the measured surface strain field. Our model parameterization incorporates an increase in subfault size with depth to alleviate problems with model resolution. We use a gradient inversion method incorporating an applied smoothing constraint and an assumption that the strike slip component is purely right-lateral. Our preferred model has fault segments that dip between 75 and 90 degrees to the west. We infer that most of the seismic moment was released within the upper 5 km in the northern section of the rupture area, with a maximum slip of about 7 m. Addition of the GPS data to the inversion helps to constrain slip on the deep portion of the fault (below 10 km). We are currently exploring the ability of seismic data to further constrain the static slip distribution, as well as the effects of a horizontally layered elastic model.

The SCEC Hector Mines Portable Deployment

Jamison Steidl, Aaron Martin, Elizabeth Cochran, and Ralph Archuleta
University of California at Santa Barbara

Two weeks after the M7.1 Hector Mines earthquake, a large-scale deployment of portable recorders took place to record the aftershock sequence in the near-source region. The entire

~40km of surface rupture was contained within the United States Marine Corps Air-ground Combat Center. One of the goals of the deployment was to record earthquakes from within and surrounding the main fault break, and use fault-crossing and fault-parallel arrays of stations to look for fault-zone guided waves. In order to gain access to the near-source zone, close coordination and logistical support was provided by the Marines. The deployment could not have taken place without the cooperative efforts of many individuals from SCEC, UCSB, UCLA, USC, USGS, UCSD, and SDSU.

The deployment consisted of two arrays, one to the north named the Bullion Mountain array (BMA), and one to the south, named the Bullion Wash array (BWA). The BMA and BWA were both set up with fault-crossing and fault-parallel arrays to examine fault-zone structure. In addition the BWA also had a 2-D dense array of 25 stations at 50 meter spacing in a 5x5-element array which had one edge in the fault zone and spread out across the alluvial wash. One of the goals of the 2-D array was to be able to examine the wavefield as it evolves with time to better understand the sources of late arriving energy.

The BMA consisted of 30 stations total and produced 7.8 Gbytes of raw data. The BWA consisted of 46 stations total and produced 14.2 Gbytes of raw data. Initial processing of the BWA and event association with earthquake catalog information shows that 73 events were recorded on 40 or more stations, and 241 events at 30 or more stations. Preliminary event associated raw data from both the BMA and BWA has been available via the PBIC web site at UCSB. At the SCEC annual meeting we will have a sign-up list for users who which a copy of the CD release of instrument and timing corrected processed event data which we plan to distribute on the 1-year anniversary of the Hector Mines earthquake.

Earthquake Source Effect on Kappa and Its Impact on the Commonly Used w^{-2} Source Model

Feng Su, Yuehua Zeng, John G. Anderson and James N. Brune
Seismological Laboratory, University of Nevada-Reno, Reno, Nevada

The earthquake high frequency spectral decay parameter kappa is commonly considered as a site effect after correction for attenuation between the source and station. In this study, however, we find there is a substantial contribution to kappa from the earthquake source. Aftershocks of the Northridge earthquake at two separated stations in Tarzana show about 20-30 msec of highly correlated variability in measurements of kappa after path attenuation correction. The correlation is most easily explained by the variability of source effect from different events. From aftershocks of the Little Skull Mountain, Nevada earthquake, we find earthquake stress drop is strongly correlated to the variations of kappa estimation. Using an inverse scheme to separate source, site and path effect on kappa, we found the earthquake stress drop is correlated to source kappa factor only. The variation of kappa measurement at a station is greatly reduced after source kappa factors have been removed. The result suggests that the commonly used w^{-2} source model is not adequate to describe the source spectra of these aftershock events. Using the kappa measurement from very small earthquakes ($M_L < 1$) by Biasi and Smith (1998) to constrain the source kappa factor, we constructed the source spectra of these aftershocks. We found these source spectra closely followed the w^{-1} model.

The Contribution of Permanent Aseismic Strain to the Strain Budget for the San Cayetano fault

Jan Vermilye, Whittier College
Leonardo Seeber, Lamont-Doherty Earth Observatory

Strain in the seismogenic layer is controlled by a regime of steady deformation below the brittle-ductile transition. Ultimately, most of the strain in the brittle layer is thought to be accommodated by fault slip in large earthquakes. During the interseismic stress rise, strain is predominantly elastic and recoverable. Some of the strain between large earthquakes, however, is permanent. In this project, we are investigating processes accounting for this permanent interseismic strain in an active setting and we are attempting to evaluate their contributions. We find that permanent aseismic strain is significant and suggest that it may be temporally and spatially related to large earthquakes.

The San Cayetano is a seismically active fault in the western Transverse Ranges. It is one of the fastest moving thrust faults in southern California. We examined pressure solution and brittle structure within the San Cayetano fault damage zone in order to evaluate the roles of distinct modes of deformation within the seismic cycle. We find that pressure-solution controlled deformation includes: 1) diffuse grain-scale deformation within the rock masses 2) shortening along cleavage planes, 3) aseismic slip on small faults and 4) cobble interpenetration. Another component of the strain between large earthquakes is contributed by mesoscopic-scale brittle faults that are thought to generate low-magnitude diffused seismicity.

We distinguish between cataclastic and solution-precipitation slip faults. The cataclastic faults are associated with gouge and may be seismogenic. These faults measure at least several meters in length and have accumulated displacements on the order of several cm to meters. Their spacing seems to correlate roughly with fault size, displacement, and gouge thickness. Strain analyses at several locations show these faults accommodate 10-20% shortening. In contrast, faults with mineral growth and no gouge are smaller, more densely spaced, and have displacements in the mm to cm range. Shortening strains of 3-10% are accommodated by these faults. Strain orientations derived from these faults are remarkably consistent; shortening directions are NE-SW for both fault sets at a number of different localities along our transect. These orientations are also consistent with pre-folding pressure solution structures and borehole breakouts. Current regional compressive strain from GPS and stress from earthquakes are directed NNE.

Pressure-solution strain detracts from the elastic strain energy budget and decreases the hazard from earthquakes. In addition to this first-order effect, pressure-solution strain is probably coupled with other deformation processes such as fault-related folding and with the stress/strain cycle associated with large seismogenic faults. Pressure solution strain rates depend on stress level and on fluid flow, both of which vary systematically during the earthquake cycle. Pressure solution strain may retard the rise in stress during the interseismic period. The ratio between permanent and elastic strain may increase as the main rupture is approached and may also be high but differently distributed in space afterwards. Understanding how pressure solution affects the coupling between stress and strain may be critical in the interpretation of geodetic deformation in terms of loading of seismogenic faults.

Earthquake Potential Models

Steven N. Ward
University of California, Santa Cruz

I am developing several maps of earthquake potential/earthquake probability in support of SCEC's Regional Earthquake Likelihood Models (RELM) program. RELM has asked its

participants to generate a range of "well documented and physically defensible" models of earthquake rate density based on inputs from geology, seismicity, geodesy, and computer simulation. One goal of the program is to assess the impact, or lack of impact, that certain assumptions inherent to earthquake potential assessment (fault segmentation or M_{max} , for instance) have on earthquake hazard. I offer two classes of earthquake potential maps -- one based purely on geodesy and one based on computer simulations of earthquakes on the fault system of southern California. The geodetic models employ GPS site velocities from SCEC Velmap2, SOPAC and the USGS. These velocities are first mapped into strain and rotation rates, and then the strain rate is translated into moment rate density using Kostrov's formula. Moment rate density then becomes earthquake rate density under the assumption of a truncated Gutenberg-Richter seismicity distribution of given b -value and M_{max} . Earthquake potential maps constructed for M_{max} equal to 8.1 and 8.5 should span the range of likely behavior. Earthquake potential models based on computer simulations follow those that I have produced for the faults of the San Francisco Bay Area. Fault-based assessments differ from geodetic-based ones in that only those locations that have a specified fault have earthquake potential. I include all southern California faults that slip at rates greater than or equal to 1 mm/y -- some 3,600 km in all. Fault traces are smoothed versions of the CDMG database. All faults with dips less than 90 degrees are replaced by vertical surfaces -- a concession to the 2-D nature of my simulations. Even with these concessions, the simulation operates with, and inverts, 1000 x 1000 matrices -- about the limit of what can be done on a low-end workstation.

Mapping b -value Heterogeneities

Joel Wedberg and Charles G. Sammis
University of Southern California

The b -value mapping technique of Wyss and Wiemer was applied to California seismicity. Two study regions were defined. One was 1.5 degrees to either side of a line extended from -123 degrees longitude, 39 degrees latitude to -120.5 degrees longitude, 35.5 degrees latitude, and this included the epicenter of the Loma Prieta event. The other study region included the epicenters of the other five events $M \sim 6.3$ in California since 1980, and extended 1.5 degrees to either side of a line from -120 degrees longitude, 36 degrees latitude to -115 degrees longitude to 32 degrees latitude. Spatial and temporal fluctuations in b -value were mapped by superimposing 2-D, 0.1 degree grids on the two study regions. At each grid point, a circle was drawn and the radius increased until it contained 200 earthquakes. For these 200 events a b -value was calculated, using the Unbiased Maximum Likelihood Method. The fixed number of events used to calculate b -value introduces a trade-off between temporal and spatial resolution. To explore this trade-off a variety of time windows between one and twelve months was used with a variety of space windows, as determined by the number of earthquakes required for a b -value calculation. A six month window, using 200 earthquakes per b -value calculation, provided the best correlation between low b -value and large events. It was found that the epicenters of all California earthquakes $\sim M6.3$ since 1980 were located at points with b -values that were within the bottom 11% of the entire study region. Five earthquakes smaller than $M6.3$ also were tested but occurred in areas with b -values that were not high or low in any systematic sense with respect to the rest of the study region.

A Preliminary Analysis of the LARSE II Data

Zhimei Yan and Robert W. Clayton
California Institute of Technology

We have begun an analysis of the explosion data recorded along the main north-south line of the LARSE II survey. This dataset consists of some 90 shots recorded by over 1000 receivers on a line 110 km in length. To date, we have converted the data to an ISIS format, which has allowed us to examine the records and to pick the first arrivals for most of the larger shots.

It is clear from the data that the upper crust has large lateral variations that are obscuring later arrivals. Based on the short-offset first-arrival picks we have constructed a simple upper crustal model that will allow us to correct this contribution out of the data in order to look for coherent lower crustal arrivals.

One aspect of the upper crustal arrivals that is intriguing is the refracted arrivals for the shots between the San Andreas and Clearwater (25 km south of the SAF) faults. These refractions all have slow arrivals that are coincident with the faults and are independent of the source location. We have used a finite-difference method to test various types of models to explain this observation. Our preferred model has an uplifted block of high velocity material.

EARTHQUAKES IN CALIFORNIA: A SURVIVOR'S GUIDE

Robert S. Yeats
Oregon State University

This book will be published by the Oregon State University Press in March, 2001, and will be available for Earthquake Awareness Month in April. Copies will be available at the GSA/AAPG and SSA meetings in April. SCEC Outreach provided me some funds for illustrations and interviews.

The book includes a history of earthquake awareness: Native American, Spanish and Mexican experiences, ignoring the problem after the 1868, 1906, and 1925 earthquakes, then, starting in 1933, enacting the most advanced earthquake protection legislation in the world (Alquist Priolo, Seismic Hazard Mapping Act, SMIP, strong building codes, etc.). Four chapters deal with earthquake sources: San Andreas, Transverse Ranges, Basin and Range, and Cascadia. Also discussed are probabilistic earthquake forecasting, including SCEC and Bay Area forecasts. Separate chapters deal with site response (strong ground motion, liquefaction, and landsliding) and tsunamis. My idea is to present an up to date picture of current thinking, and try to transmit to the general public the excitement we feel when we advance the frontiers of knowledge.

Earthquake insurance includes a discussion of the CEA. Several chapters deal with earthquake preparedness: retrofitting your house, large structures, preparing an earthquake plan, deciding about earthquake insurance, and the role of government at all levels.

The book is suitable for undergraduate courses relating science, technology, and society, and can be used by high school students for reports; it is also appropriate for emergency management personnel and for the general public. It is patterned after *Living with Earthquakes* in the Pacific Northwest, published by the OSU Press in 1998.

Recent Surface Ruptures Along the Cholame Segment of the San Andreas Fault

Jeri J. Young, Laura Colini and Ramon Arrowsmith, Arizona State University
Lisa B. Grant, University of California, Irvine

Recurrence models for earthquakes along the central San Andreas Fault (SAF) are poorly constrained due to the lack of paleoseismic data along the Cholame segment and ambiguous geomorphic offsets that are alternately interpreted as 3-4 or 6 meters from the 1857 earthquake. We have conducted a paleoseismic study along this segment of the fault to determine the dates of earthquakes and the amount of lateral offset of the last two events. The LY4 site is located approximately 37.5 km southeast of Highway 46 and comprises 3 fault perpendicular trenches, 2 parallel trenches, and several hand dug trenches, including re-excavation of the LY4-99 fault perpendicular trench investigated by Stone et al. At the surface, the fault is identified by steep fault scarps and by less pronounced geomorphic lineaments southwest and northeast of the site, respectively. The stratigraphy on the southeast side of the SAF is predominately densely bioturbated tan-gray silts.

Alternating gravels, sands and silts are well preserved on the northwest side of the fault. Truncation of fine and coarse-grained deposits in the lower halves of 2 fault perpendicular trenches, the vertical displacement and disruption of overlying silts, sands, and gravels, and fracturing of younger historic deposits are best explained by three earthquakes. Abruptly truncated sand and silt layers that are not correlative to units across the fault zone indicate the oldest earthquake, L2. Evidence for the younger earthquake, L1, consists of sand, silt and gravel layers that are vertically displaced approximately 25 to 30 cm and disrupted by filled-in fractures up to 20 cm wide. Tectonic fractures that dissect historic gray-tan silts and an overlying paleosol and fine-grained sands and silts suggests a third earthquake, L0, which occurred after 1857. We excavated a silt-filled fracture, which widens with depth and continues for 2 meters along the fault zone with right step geometry across the top surface of historic-age fine sandy silts. We interpret the fracture as a seismogenic feature caused by the youngest event, L0. This silt filled fracture belongs to a set of fractures with a N 6 W to N 38 W orientation which are correlative and parallel to the orientation of another silt filled set of fractures in an adjacent trench. Preliminary excavation of the edge of an alluvial fan deposit, composed of a coarse, poorly sorted gravel, provides the basis for estimating dextral offset of 2.75 plus or minus 0.75 meters for event L1 and/or L2. The location of piercing points is diffuse due to lateral facies changes at the eastern and southern edges of the alluvial deposit.

An Asymmetric Subevent Rupture Model for the Composite Earthquake Source

Yuehua Zeng
University of Nevada, Reno

Zeng et al. (1994) have proposed a composite source model for synthetic strong ground motion simulation. In that model, a subevent radiates a Brune's pulse or a circular rupture crack pulse (Sato and Hirasawa, 1973) as the rupture front passes through the center of the event. The method has been proved to be successful in generating realistic strong motion seismograms in comparison with observations from earthquakes in California, eastern US, Guerrero of Mexico, Turkey and India. The method has since been improved by including scattering waves from small scale heterogeneity structure of the earth, site specific ground motion prediction using weak motion site amplification, and non-linear soil response using geotechnical engineering models.

In this paper, I have introduced an asymmetric circular rupture model to improve the subevent source radiation. This asymmetric circular rupture assuming the Eshelby's (1957) static

solution for a circular crack under uniform shear stress at every successive instant of rupture. Instead of assuming a fixed central location for a symmetric growing crack by Sato and Hirasawa, I assume the center moves at a velocity less than the growing velocity of the crack. As a result, the rupture velocity at any point inside the crack becomes a vector sum of the two velocities. When the moving velocity of the center is zero, we have the Sato and Hirasawa's growing crack model. When it is equal to the growing velocity of the crack, the rupture nucleates from the edge of the crack. The source pulse from this asymmetric growing crack is given in a compact analytical form. The resulting ground motion calculated from this improved subevent ruptures gives better rupture directivity than our early study in comparison with the observation from Landers, Loma Prieta, Northridge, Imperial Valley and Kobe earthquakes. This is done by using the near-fault directivity model of Somerville et al. (1997) to test the synthetic prediction of the rupture directivity effect from those earthquake ground motions in terms of fault normal and fault parallel components.

Preliminary Results of Crustal Structure from the LARSE-II Passive Recording Experiment Using Teleseismic P-to-S Converted Waves

Lupei Zhu

University of Southern California

The 1999-2000 Los Angeles Region Seismic Experiment (LARSE-II) contained a passive recording phase in which 83 three-component broadband and short-period instruments were deployed along a 100 km long profile. The profile started near the coast of Malibu and transversed the Santa Monica Mts, the San Fernando and the Santa Clarita Valleys, the San Gabriel Mountains, the San Andreas Fault (SAF), and ended in the Antelope Valley of the Mojave Desert. This passive recording experiment lasted 6 months and has recorded numerous regional and teleseismic events. In this study, we used teleseismic P-to-S converted waves to image subsurface sedimentary basin and deep crustal structures. We first analyzed 4527 three-component P waveforms from 87 teleseismic events ranging from 30 to 95 degrees in epicentral distance. For each event, we aligned all station records at the first arrivals by cross-correlation and stacked all vertical waveforms to estimate the effective source time function for the event. We then deconvolved this common source time function from all records to compute station receiver functions. A total of 2362 receiver functions were obtained. We generated a 2-D crustal structure image along the profile by stacking and migrating the radial receiver functions using the Common Conversion Point (CCP) stacking technique. The image shows three sedimentary basins under the San Fernando, the Santa Clarita, and the Antelope Valleys. Their depths vary along the profile and reach a maximum depth of 6 to 8 kms. In the deeper part of the section, the Moho is seen clearly as a continuous flat feature at a depth of 34 km under Mojave.

It terminates near the downward extension of the SAF. The deep structure under the San Fernando Valley and the Santa Clarita Valley is very complicated. There is no detectable P- to-S conversions at a depth range of 20 to 40 km between the Santa Monica Mts. and the San Gabriel Mts. Instead, several separated conversion bands can be seen at a depth range of 40 to 50 km, which might suggest thickened crust. We also compared the Bouguer gravity anomaly and teleseismic arrival time delays along the profile with the predictions from the inferred crustal model. The preliminary modeling shows that most of the anomalies can be explained by the shallow sedimentary basins.

